TURUN
YLIOPISTO
UNIVERSITY
OF TURKU

From Biology to Mechanics: Effects of Silver Fluoride Treatments on Dentin

Merve Üçtaşlı

TURUN YLIOPISTON JULKAISUJA – ANNALES UNIVERSITATIS TURKUENSIS
SARJA – SER. D OSA – TOM. 1968 | MEDICA – ODONTOLOGICA | TURKU 2026

TURUN
YLIOPISTO
UNIVERSITY
OF TURKU

FROM BIOLOGY TO MECHANICS: EFFECTS OF SILVER FLUORIDE TREATMENTS ON DENTIN

Merve Üçtaşlı

TURUN YLIOPISTON JULKAISUJA – ANNALES UNIVERSITATIS TURKUENSIS
SARJA – SER. D OSA – TOM. 1968 | MEDICA – ODONTOLOGICA | TURKU 2026

University of Turku

Faculty of Medicine
Institute of Dentistry
Department of Cariology and Restorative Dentistry
Finnish Doctoral Programme in Oral Sciences – FINDOS Turku

Supervised by

Professor Arzu Tezvergil-Mutluay
Department of Cariology and Restorative Dentistry, Institute of Dentistry
University of Turku
Turku, Finland

Professor Mustafa Murat Mutluay
Department of Oral and Maxillofacial Surgery, Institute of Dentistry
University of Helsinki
Helsinki, Finland

Reviewed by

Professor Marja-Liisa Laitala
Research Unit of Population Health
Faculty of Medicine
University of Oulu
Oulu, Finland

Associate Professor Monica Yamauti
Department of Biomedical and Applied Sciences, School of Dentistry
Indiana University
Indianapolis, Indiana, USA

Opponent

Professor Milena Cadenaro
Department of Medicine, Surgery and Health Sciences
University of Trieste
Trieste, Italy

The originality of this publication has been checked in accordance with the University of Turku quality assurance system using the Turnitin Originality Check service.

ISBN 978-952-02-0656-7 (PRINT)
ISBN 978-952-02-0657-4 (PDF)
ISSN 0355-9483 (Print)
ISSN 2343-3213 (Online)
Painosalama, Turku, Finland 2026

To my beloved parents, for your constant love and support
Incredibly fortunate to have you in my life
Kocaman öpüyorum

UNIVERSITY OF TURKU
Faculty of Medicine
Institute of Dentistry
Department of Cariology and Restorative Dentistry
MERVE ÜÇTAŞLI: From Biology to Mechanics: Effects of Silver Fluoride Treatments on Dentin
Doctoral Dissertation, 201 pp.
Finnish Doctoral Programme in Oral Sciences – FINDOS Turku
May 2026

ABSTRACT

Silver fluoride-based treatments have gained increasing clinical and research attention as promising therapeutic agents for caries arrest, yet their interactions with dentin remain uncharacterized. The aim of the present thesis was to investigate the adhesive, enzymatic, biocompatibility, and fatigue-related behavior of dentin treated with ammonia-based silver diamine fluoride (SDF) and water-based silver fluoride (SF), with or without the application of potassium iodide (KI). Four studies were accomplished. Study I evaluated the resin-dentin bonding to SDF- and SDF + KI-treated dentin using different bonding strategies, surface treatment approaches and delayed bonding time points. Study II investigated the long-term effects of SDF and SF treatments, with or without KI, on dentin collagen matrix stability over a six-month period. Study III assessed trans-dentin and direct cytotoxicity using dentin barrier test and cell viability assays. Study IV evaluated the fracture strength and fatigue resistance of carious dentin treated with silver fluoride-based treatments using a microcosm biofilm model under quasi-static and cyclic loading conditions. Immediate self-etch bonding to SDF- or SDF + KI-treated dentin severely reduced bond strengths, whereas acid etching, rinsing, airborne-particle abrasion or delayed bonding restored bonding performance. Silver fluoride treatments reduced total enzymatic activity and partially preserved mechanical properties of dentin collagen, while KI application increased collagen degradation. SF treatment showed higher biocompatibility than SDF treatment, especially without KI application. Caries substantially reduced dentin fatigue resistance, but SF treatment without KI application improved endurance limits and resistance to crack propagation. Water-based silver fluoride without potassium iodide emerged as the most promising formulation, combining superior biocompatibility and mechanical performance. The use of potassium iodide should be reconsidered, particularly when esthetic demand is less important. These findings highlight the clinical potential of water-based silver fluoride as a better alternative to ammonia-based silver diamine fluoride and provide guidance for optimizing silver fluoride-based treatment protocols.

KEYWORDS: Aqueous silver fluoride (SF); Biocompatibility; Bond strength; Degradation; Dentin; Fatigue; Microcosm biofilm; Potassium iodide (KI); Silver diamine fluoride (SDF)

TURUN YLIOPISTO
Lääketieteellinen tiedekunta
Hammaslääketieteen laitos
Kariologia ja korjaava hammashoito
MERVE ÜÇTAŞLI: Biologiasta mekaniikkaan: hopeafluoridihoitojen vaikutukset dentiinin
Väitöskirja, 201 s.
Kansallinen suun terveystieteiden tohtoriohjelma – FINDOS Turku
Toukokuu 2026

TIIVISTELMÄ

Hopeafluoridit ovat viime vuosina saaneet kasvavaa kliinistä ja tutkimuksellista kiinnostusta lupaavina karieksen etenemistä pysäyttävinä menetelminä, mutta niiden vuorovaikutuksia dentiinin kanssa ei vielä riittävästi tunneta. Tämän väitöskirjan tarkoituksena oli tutkia dentiinin mekaanisia, entsymaattisia, bioyhteensopivia ja väsymisresistenssiin liittyviä tekijöitä sen jälkeen, kun dentiini oli käsitelty ammoniakkipohjaisella hopeadiamiini-fluoridilla (SDF) tai vesipohjaisella hopeafluoridilla (SF) joko kaliumjodidin (KI) kanssa tai ilman sitä. Väitöskirja koostui neljästä osatutkimuksesta. Tutkimus I arvioi resiini-dentiinisidoksen lujuutta SDF- ja SDF + KI-käsitellyissä dentiineissä käyttäen erilaisia sidostusmenetelmiä, pintakäsittelyitä ja sidostuksen ajankohtia SDF-käsittelyn jälkeen. Tutkimus II tarkasteli SDF:n ja SF:n pitkäaikaisvaikutuksia dentiinin kollageenimatriisin stabiilisuuteen KI:n kanssa tai ilman sitä kuuden kuukauden seuranta-aikana. Tutkimus III arvioi dentiinin läpäisevää ja suoraa sytotoksisuutta dentiinibarrieri-testillä ja solujen elinkykykokeilla. Tutkimus IV selvitti hopeafluoridilla käsitellyn karieksen heikentämän dentiinin murtolujuutta ja väsymisresistenssiä biofilmimallissa kvasistaattisissa ja syklisissä kuormitusolosuhteissa. Välitön itse-etsaava sidostus SDF- ja SDF + KI-käsiteltyyn dentiiniin heikensi sidoksen lujuutta, kun taas happoetsaus, huuhtelu, jauhepuhallus tai viivästynyt sidostus palauttivat sidoslujuuden. Hopeafluoridit vähensivät entsyymiaktiivisuutta ja säilyttivät osittain kollageenin mekaanisia ominaisuuksia, kun taas KI lisäsi kollageenin hajoamista. SF osoitti parempaa bioyhteensopivuutta kuin SDF, erityisesti ilman KI:tä. Karies heikensi dentiinin väsymisresistenssiä, mutta SF ilman KI:tä paransi kestävyysarvoja ja vähensi halkeamien etenemistä. Vesipohjainen hopeafluoridi ilman kaliumjodidia osoittautui lupaavimmaksi vaihtoehdoksi, sillä se yhdisti hyvän bioyhteensopivuuden ja hyvät mekaaniset ominaisuudet. Kaliumjodidin käyttöä tulisi harkita uudelleen erityisesti tilanteissa, joissa esteettiset vaatimukset ovat toissijaisia. Tulokset korostavat vesipohjaisen hopeafluoridin kliinistä soveltuvuutta ammoniakkipohjaista hopeafluoridia parempana vaihtoehtona ja tarjoavat samalla ohjeita hopeafluoridin käyttötapojen kehittämiseen.

AVAINSANAT: Bioyhteensopivuus; Biofilmi: Dentiini; Hopeadiamiini-fluoridi (SDF); Kaliumjodidi (KI); Materiaalin heikkeneminen; Sidoslujuus; Väsymisresistenssi; Vesipohjainen hopeafluoridi (SF)

Table of Contents

Abbreviations

ANOVA	Analysis of variance
BisEMA	Ethoxylated bisphenol A dimethacrylate
BisGMA	Bisphenol glycidyl methacrylate
BSA	Bovine serum albumin
BPA	Bisphenol A
CA	Cross-sectional area
$CaCl_2$	Calcium chloride
$CaCl_2 \cdot H_2O$	Calcium chloride monohydrate
CC	Cysteine cathepsin
CFU	Colony-forming unit
cm	Centimeter
cm^2	Centimeter square
CO_2	Carbon dioxide
CQ	Camphorquinone
CTX	C-terminal crosslinked telopeptide of type I collagen
D	Dentin
DIC	Differential interference contrast
DMSO	Dimethyl sulfoxide
DQ	Dye-quenched
E	Elastic modulus
ECM	Extracellular matrix
ELISA	Enzyme-linked immunosorbent assay
ER	Etch-and-rinse
FBS	Fetal bovine serum
FITC	Fluorescein isothiocyanate
g	Unit of mass, gram
GMA	Bisphenol glycidyl methacrylate
h	Hour
HAP	Hydroxyapatite
H_3PO_4	Phosphoric acid
HEMA	2-hydroxyethyl methacrylate

HEPES	Hydroxyethylpiperazine ethane sulfonic acid
HL	Hybrid layer
HMDS	Hexamethyldisilazane
HYP	Hydroxyproline
Hz	Hertz, cycles per second
ICTP	Crosslinked carboxyterminal telopeptide of type I collagen
ISO	International Organization for Standards
KCl	Potassium chloride
KI	Potassium iodide
kV	Kilovolt
L	Liter
Lp	Hydraulic conductance
MARC	Managing accurate resin curing
MDP	Methacryloyloxydecyl dihydrogen phosphate
min	Minute, 60 seconds
mg	Milligram
mL	Milliliter
mm	Millimeter
mM	Millimolar
MMP	Matrix metalloproteinase
MPa	Megapascal
MTT	Methylthiazolium
MW	Milliwatt
N	Newton
NaCl	Sodium chloride
NaN_3	Sodium azide
NaOCl	Sodium hypochloride
ng	Nanogram
P	Maximum load
PBS	Phosphate buffered saline
pg	Picogram
pH	Power of hydrogen
ppm	Parts per million
PTF	Pre-test failure
RIA	Radioimmunoassay
rpm	Revolutions per minute
s	Second
SD	Standard deviation
SDF	Silver diamine fluoride/Ammonia-based silver fluoride
SDI	Southern Dental Industries

SE	Self-etch
SEE	Selective-enamel-etch
SEM	Scanning electron microscope
SF	Water-based silver fluoride/Aqueous silver fluoride/Ammonia-free silver fluoride
SiC	Silicon carbide
SnF_2	Stannous fluoride
TEGDMA	Tryethylene glycol dimethacrylate
Tris-HCl	Tris(hydroxymethyl)aminomethane hydrochloride
UDMA	Urethane dimethacrylate
UK	United Kingdom
USA	United States of America
v%	Volume percentage
v/v	Volume/volume, dilution
v/v%	Volume per volume percentage
WHO	World Health Organization
wt%	Weight percentage
w/v%	Weight per volume percentage
w/w%	Weight per weight percentage
$ZnCl_2$	Zinc chloride
µTBS	Micro-tensile bond strength
µm	Micrometer
µL	Microliter
α	Alpha

List of Original Publications

This dissertation is based on the following original publications, which are referred to in the text by their Roman numerals:

I Uctasli M, Stape THS, Mutluay MM, Tezvergil-Mutluay A. Silver diamine fluoride and resin-dentin bonding: Optimization of application protocols. *International Journal of Adhesion and Adhesives*, 2023; 126: 103468. https://doi.org/10.1016/j.ijadhadh.2023.103468

II Uctasli M, Seseogullari-Dirihan R, Stape THS, Mutluay MM, Tezvergil-Mutluay A. Long-term effect of ammonia- and water-based silver fluoride on dentin collagen matrix. *Dental Materials*, 2026; 42: 533–544. https://doi.org/10.1016/j.dental.2025.10.016

III Uctasli M, Seseogullari-Dirihan R, Mutluay MM, Tezvergil-Mutluay A. Cytotoxicity of ammonia- and water-based silver fluoride treatments. *European Journal of Oral Sciences*, 2026; 134: e70055. https://doi.org/10.1111/eos.70055

IV Uctasli M, Stape THS, Seseogullari-Dirihan R, Mutluay MM, Tezvergil-Mutluay A. Fatigue resistance of human carious dentin treated with ammonia- and water-based silver fluoride. Manuscript.

1 Introduction

Dental caries remains the most prevalent non-communicable, biofilm-mediated disease worldwide and continues to represent a major global health burden [Selwitz et al., 2007; Pitts et al., 2017] and characterized by net mineral loss of dental hard tissues [MacHiulskiene et al., 2020]. Despite notable advances in preventive and restorative dentistry, untreated caries affects approximately 2.5 billion people globally [Wen et al., 2022] and remains a leading cause of pain, tooth loss and reduced oral function. This persistent prevalence underscores the urgent need for effective, evidence-based management strategies that are aligned with international oral health policies.

Caries is a multifactorial and dynamic disease resulting from interaction between dental tissues, cariogenic biofilms, dietary carbohydrates and host-related factors [Pitts et al., 2017]. In dentin, caries progression is not only characterized by mineral loss but also by degradation of the organic matrix, primarily type I collagen, which leads to progressive weakening of the tissue and structural integrity loss [Carrilho et al., 2009].

The caries management philosophy has shifted from a traditional drill and fill approach toward a more conservative and biologically oriented model [Schwendicke et al., 2021]. Contemporary caries management emphasizes early diagnosis, disease control and preservation of tooth structure through non-invasive and minimally invasive strategies. The primary objective is to arrest lesion progression, promote remineralization and protect affected dental tissues rather than relying solely on surgical removal of carious tissue [Opdam et al., 2024].

Throughout the years, fluoride-containing agents have gained attention and been used to control the progression of dentin caries process [Slayton et al., 2018; Jiang et al., 2021]. Silver fluoride formulations, both ammonia-based and water-based silver fluoride, have emerged as effective therapeutic agents for arresting caries and incorporated into contemporary caries management protocols [Rosenblatt et al., 2009; Mei et al., 2018]. These materials combine the antimicrobial properties of silver ions with the remineralizing effects of fluoride [Contreras et al., 2017].

Ammonia-based silver fluoride, commonly known as silver diamine fluoride (SDF), has been used for several decades and has demonstrated high clinical

effectiveness in arresting carious lesions, reducing dentin hypersensitivity and inhibiting cariogenic biofilms in adults [Yee et al., 2009; Contreras et al., 2017; Mei et al., 2018], children [Chu, and Lo, 2008; Duangthip et al., 2015] and elderly [Li et al., 2016; Chan et al., 2022]. Ammonia-based silver fluoride was originally formulated during the PhD studies of Dr. Misuho Nishino under the supervision of Dr. Reichi Yamaga at Osaka University, Japan, in the late 1960s [Nishino, 1969]. The first commercial 38% SDF product for dental treatment was marketed as Saforide in Japan.

Water-based, ammonia-free silver fluoride, commonly known as aqueous silver fluoride (SF), has also been used for arresting caries lesions, reducing dentin hypersensitivity and inhibiting cariogenic biofilms. Water-based silver fluoride was first introduced by Dr. Graham Craig at University of Sydney, Australia, in the late 1970s [Craig et al., 1981]. The commercial product was 40% SF, often used in conjunction with a stannous fluoride (SnF_2) paste manufactured by Creighton Pharmaceuticals in Australia.

However, silver fluoride treatments present esthetic drawbacks, the oxidation of free silver ions result in discoloration of teeth and surrounding tissues, which reduces their acceptance in clinical practice. The application of potassium iodide (KI) immediately after either ammonia- or water-based silver fluoride treatments addresses this discoloration issue and leads to the formation of a white silver iodide compound that decreases the appearance of black dentin staining [Primus, 2017; Roberts et al., 2020]. The adjunctive use of potassium iodide with silver fluoride treatments was first introduced by Dr. Geoffrey Knight at University of Adelaide, Australia, in the 2000s [Knight et al., 2005].

Subsequently, an Australian manufacturer, Southern Dental Industries (SDI), developed a two-bottle system consisting of SDF and KI, which was introduced under the product name Riva Star in 2015. In 2020, the same manufacturer introduced Riva Star Aqua, a two-bottle system consisting of SF and KI, as an alternative to SDF. Water-based formulation aimed to improve patient comfort by reducing unpleasant taste, odor and soft tissue irritation associated with ammonia-based solutions. Therefore, silver fluoride treatments can be applied either as ammonia- or water-based silver fluoride alone (SDF or SF) or in combination with potassium iodide (KI).

The widespread clinical use, together with expanding research interest highlight the importance of silver fluoride treatments in restorative and preventive dentistry. The US Food and Drug Administration approved SDF for tooth desensitization and caries treatment in 2014 and 2015, respectively [Jiang et al., 2021]. The World Health Organization has included SDF in its list of essential medicines [World Health Organization (WHO), 2022]. Moreover, SDF has emerged as a possible off-label approach to extend the longevity of resin-dentin interfaces due to its

potential inhibition of host-derived endogenous proteases [Mei et al., 2012; Mei et al., 2014], in addition to its antimicrobial and remineralizing properties and thereby reducing collagen degradation [Mei et al., 2013a].

Silver fluoride-based treatments are increasingly employed in clinical practice and have shown benefits in arresting dental caries, however, important scientific and clinical questions remain regarding their interactions with dental tissues and restorative materials. Research on water-based silver fluoride and application of potassium iodide is still limited. In addition, ammonia-based silver fluoride also requires further clarification due to inconclusive findings in the existing literature.

Therefore, this doctoral thesis investigates underlying mechanisms of action of ammonia- and water-based silver fluoride treatments, with or without the application of potassium iodide, focusing on their influence on resin-dentin bonding, host-derived enzymatic activity, cytotoxicity and long-term mechanical performance. The series of studies included in this thesis aims to support improvements in the quality and longevity of restorative dental care, especially in high-caries-risk patients, children and older adults, where caries prevalence and treatment needs continue to increase.

2 Review of the Literature

2.1 Tooth structure

2.1.1 Enamel

Enamel is a highly mineralized tissue composed of approximately 88% by volume or 96% by weight hydroxyapatite ($Ca_{10}(PO_4)_6(OH)_2$), 10% by volume or 3% by weight water, and 2% by volume or 1% by weight organic components [O´Brien, 2008] and is the hardest tissue in the human body [Mann, and Dickinson, 2005]. Hydroxyapatite crystallites are roughly rectangular in cross-section and are organized together by organic molecules, with an average size of about 50 nm in width, 25 nm in thickness, and several microns in length [Li et al., 2014b]. Being the outermost layer of the teeth, enamel forms an insulating barrier that resists multiple physical, thermal and chemical challenges, including compressive forces, abrasion, attrition, and acidic exposure from plaque and diet. In addition, prolonged exposure of the enamel surface to the oral environment leads to hypermineralization of the enamel, further enhancing its protective function. Enamel is in intimate contact with saliva and plaque fluid, and the surfaces of enamel hydroxyapatite crystals are in dynamic equilibrium with these adjacent aqueous phases. Consequently, preservation of enamel integrity is important and highly dependent on effective preventive strategies and early intervention.

2.1.1.1 Adhesion to enamel

Due to its high mineral content and relatively homogeneous structure, bonding to enamel is considered a reliable and durable procedure. The concept of bonding to enamel dates back to the 1950s [Buonocore, 1955], when resin monomers were first shown to penetrate acid-etched enamel surfaces [Perdigão et al., 2019]. Bonding to enamel is regarded as a highly reliable clinical procedure that can be performed without major technical difficulties because the biochemical structure of enamel is primarily composed of hydroxyapatite [O´Brien, 2008].

Phosphoric acid remains the standard etchant for enamel surface conditioning, with a clinically preferred concentration range of 30-40%. To achieve optimal

etching efficacy and surface morphology, phosphoric acid gel at concentrations between 32% and 37%, applied for 15 to 60 s, is recommended [Amran et al., 2025]. As alternatives to phosphoric acid, milder acidic agents such as maleic acid (10%) or polycarboxylic acid (10-20%) may also be used for enamel surface conditioning, however, organic acids generally produce shallower demineralization and do not generate the same etching pattern as phosphoric acid [Van Meerbeek et al., 2020].

Once the enamel surface is conditioned with phosphoric acid, the superficial hydroxyapatite crystals are partially dissolved, resulting in the formation of a roughened surface layer with a depth of approximately 0.5-5 µm. This demineralization process leads to characteristic etching patterns depending on prism orientation, including the dissolution of prism cores (Type I pattern) or the dissolution of prism peripheries (Type II pattern). In addition, acid etching increases the surface free energy of enamel, and the resulting capillary action facilitates the penetration of low-viscosity adhesive resin into the micro-porosities of the etched enamel surface, forming resin tags. Consequently, a strong micromechanical bond between enamel and resin is established [Fanfoni et al., 2017; Perdigão et al., 2019]. Therefore, acid etching of the prepared enamel surface with phosphoric acid is essential in adhesive restorative procedures and should not be omitted.

2.1.2 Dentin

Dentin constitutes the bulk of the tooth and acts as a stress-absorbing substrate for the overlying enamel or cementum. In contrast to enamel, dentin differs in biochemical composition and structural organization. Dentin contains approximately 45% by volume or 70% by weight hydroxyapatite, 25% by volume or 10% by weight water, and 30% by volume or 20% by weight organic matrix [O´Brien, 2008]. Organic matrix of dentin is predominantly composed of type I collagen, that forms a three dimensional network of dentin prior to the mineralization process within the maturation phase of tooth development [Tjäderhane et al., 2009] and serves as the structural scaffold for mineral deposition during dentinogenesis.

At the nanoscale, hydroxyapatite crystals are intimately associated with collagen fibrils, forming a mineral-organic framework that provides both rigidity and toughness. At the microscale, dentin is characterized by the presence of dentinal tubules embedded within an intertubular collagen matrix. Dentinal tubules extend from the dentin-pulp border toward the dentin-enamel and dentin-cementum junctions, forming a complex tubular network that plays a key role in dentin sensitivity and permeability [Pashley et al., 1987]. In addition, dentinal tubules allow communication between the pulp and the external environment. Tubule density and diameter increase toward the dentin-pulp border, with diameters ranging from approximately 0.8 µm near the dentin-enamel junction to about 3 µm close to the

pulp [Tjäderhane, and Haapasalo, 2009]. Tubule density decreases from roughly 45,000/mm² in deep dentin to around 20,000/mm² beneath the dentin-enamel junction [Pashley et al., 1987]. Dentinal fluid is primarily located inside dentinal tubules, and because deep dentin contains more tubules with larger diameters, the dentin surface becomes wetter, more permeable, and lower in mineral content closer to the pulp [Tjäderhane et al., 2009]. In addition to dentinal fluid, dentinal tubules contain odontoblastic processes that extend from the odontoblasts in the pulp toward the dentin surface. These regional variations influence dentin sensitivity, bonding performance, and susceptibility to caries progression.

2.1.2.1 Adhesion to dentin

Due to its hydrated and heterogeneous nature, characterized by the presence of dentinal tubules and a collagen-rich organic matrix, the predictability of bonding performance in dentin decreases considerably and requires distinct surface preparation strategies to achieve durable adhesion [Tjäderhane, 2015; Perdigão et al., 2019; Fronza et al., 2022]. Superficial dentin, which contains more minerals, provides more predictable bonding, whereas deep dentin presents greater challenges due to increased tubule diameter and fluid content, and the reduced available intertubular area for bonding [Breschi et al., 2018].

Currently, two main approaches are employed for dentin bonding: etch-and-rinse and self-etch [Van Meerbeek et al., 2003]. The fundamental difference between these two approaches is the etching step. In the etch-and-rinse approach, dentin is conditioned with phosphoric acid (H_3PO_4, 32–40%) prior to adhesive application. In the self-etch approach, no phosphoric acid etching is performed, instead, the bonding mechanism relies on acidic methacrylate monomers in the adhesive that simultaneously demineralize the dentin while infiltrating it [Marchesi et al., 2013]. The separate etching step in the etch-and-rinse approach removes the smear layer, demineralizes the superficial dentin and exposes the collagen network, allowing the subsequent diffusion of resin monomers into the demineralized matrix [Perdigão, 2020]. Therefore, adhesion is achieved primarily through micromechanical interlocking between the resin and the collagen fibrils. In the self-etch approach, smear layer is modified rather than removed and adhesion is based on a dual mechanism combining micromechanical interlocking with chemical bonding to the dentin structure [Cadenaro et al., 2019; Perdigão, 2020]. The chemical bonding depends on the type of functional monomers in the adhesive, such as 10-methacryloyloxydecyl dihydrogen phosphate (10-MDP), a functional monomer with strong potential for chemical bonding [Nagarkar et al., 2019; Burke, and Mackenzie, 2021]. The methacrylate group of 10-MDP participates in polymerization, while the phosphate group ionically interacts with calcium in

hydroxyapatite, forming a stable MDP-Ca salt. An additional advantage of the self-etch approach is its lower technique sensitivity, the absence of a separate etching and rinsing step eliminates the need for precise moisture control of the exposed collagen matrix [Perdigão et al., 2019].

Dental adhesive systems are continuously evolving, with advances in their composition, application protocols, and clinical indications [Cadenaro et al., 2005; Cadenaro et al., 2023]. In 2011, a new category of adhesive systems, known as universal adhesives, was introduced with the aim of simplifying clinical procedures, reducing application errors and increasing versatility [Burke, and Mackenzie, 2021; Cadenaro et al., 2023]. Universal adhesives are single-bottle, multi-mode systems that can be applied using etch-and-rinse (ER), self-etch (SE), or selective enamel-etching (SEE) approaches. Depending on cavity depth different adhesive agent application strategies can be selected based on the clinical situation:

when the preparation is on enamel surface etch-and-rinse (ER)

when the preparation is on dentin surface self-etch (SE)

when the preparation is on both enamel and dentin surfaces selective enamel-etching (SEE).

In SEE approach, the enamel surface of the cavity preparation is selectively etched, while dentin surface is subsequently bonded using the SE approach.

2.1.3 Dentin collagen matrix

The organic matrix of dentin is composed predominantly of collagen, which constitutes approximately 90% of its organic component. Type I collagen is the most abundant form, with trace amounts of type III and type V collagen also present [Tjäderhane et al., 2009]. The remaining 10% of organic matrix consists of non-collagenous proteins, including proteoglycans, phosphoproteins and γ-carboxyglutamate-containing proteins, which collectively contribute to matrix organization, mineralization and mechanical behavior [Breschi et al., 2018].

Type I collagen is composed of three polypeptide α-chains arranged into a left-handed triple-helical structure. This configuration arises from a characteristic amino acid sequence dominated by glycine, proline, and hydroxyproline, with hydroxyproline playing a critical role in stabilizing the triple-helical structure and increasing its thermal stability. Proteoglycans are one of the major non-collagenous proteins within the dentin organic matrix and play a key role in matrix organization, hydration, mineralization, and biomechanical behavior [Germann, and Heidemann, 1988]. By binding water within the interfibrillar spaces, proteoglycans contribute to the viscoelastic properties of dentin, enhance its resistance to mechanical

deformation, and influence mineralization by interacting with mineral ions and matrix proteins, thereby affecting crystal nucleation and growth. Water is present both within and between the interfibrillar spaces of collagen fibrils and is an essential component of the dentin collagen matrix, playing a central role in its structural and mechanical behavior. Hydrogen bonding between water molecules and collagen chains contributes to the stabilization of the triple-helical structure [Germann, and Heidemann, 1988].

Dentin collagen exhibits minimal turnover and is rarely replaced once formed. Instead, natural cross-linking within the collagen matrix accumulates over time, which may influence the mechanical properties of dentin with aging. The low turnover rate contributes to the long-term stability of the dentin matrix but also makes it vulnerable to irreversible degradation under pathological conditions such as caries. During caries progression, demineralization and disruption of the collagen network significantly affect dentin permeability and mechanical performance [Pashley et al., 1987]. Additionally, the formation of reparative dentin, which differs structurally from sound dentin, further alters dentin permeability and can compromise adhesive bonding. Increased hydration is associated with reduced stiffness and strength, underscoring the importance of preserving collagen integrity, proteoglycan content and water balance to maintain dentin structural stability [Tjäderhane et al., 2009].

2.1.4 Host-derived dentinal proteases

Dentin contains endogenous proteolytic enzymes that become dormant and entrapped within the mineralized extracellular matrix during tooth development. Under physiological conditions, these enzymes remain in a latent or inactive state. However, under pathological conditions such as dental caries, acidic challenges, or restorative procedures involving acid etching, these enzymes may become activated and contribute to degradation of the dentin organic matrix [Mazzoni et al., 2009; Turco et al., 2018]. Host-derived dentinal proteases are primarily matrix metalloproteinases (MMPs) and cysteine cathepsins (CCs).

Once the collagen scaffold is exposed by demineralization, degradation is mediated by the combined activity of host-derived dentinal proteases (MMPs and CCs) [Tjäderhane et al., 2013; Turco et al., 2018]. Unprotected collagen fibrils are susceptible to slow but continuous degradation, which contributes to caries progression and compromises the durability of adhesive interfaces [Pashley et al., 2004; Mazzoni et al., 2015].

2.1.4.1 Matrix metalloproteinases

Matrix metalloproteinases (MMPs), also referred to as matrixins, are a family of zinc- and calcium-dependent endopeptidases involved in both physiological and pathological remodeling of the mineralized extracellular matrix [Tezvergil-Mutluay et al., 2010]. To date, 24 different MMPs have been identified, of which 23 are present in human [Mazzoni et al., 2009], including MMP-2 (gelatinase A), MMP-3 (stromelysin), MMP-8 (collagenase), MMP-9 (gelatinase B) and MMP-20 (enamelysin). Moreover, in addition to matrix-bound MMPs, non-collagen-bound MMPs have been detected in saliva, dentinal tubules, and possibly in dentinal fluid [Mazzoni et al., 2009].

Structurally, MMPs typically consist of a propeptide domain containing a cysteine residue, a zinc-containing catalytic domain, a hinge region and a hemopexin domain. MMPs are synthesized in a latent form in which their activity is inhibited by a cysteine residue that prevents water from binding to the catalytic zinc ion [Mazzoni et al., 2015]. Displacement of this cysteine residue activates the enzyme. MMP activation can occur through several mechanisms, including exposure to low pH, heat, chemical agents, or proteolytic cleavage by other enzymes [Carrilho et al., 2009; Tezvergil-Mutluay et al., 2015b]. In dentin, MMP activation is commonly associated with initial demineralization and subsequent exposure to acidic environments, such as those created by caries processes or low pH (*i.e.* acidic resin monomers, acid etching). Once activated, MMPs degrade exposed collagen fibrils, contributing to deterioration of the dentin organic matrix [Tjäderhane et al., 2013].

2.1.4.2 Cysteine cathepsins

Cysteine cathepsins (CCs) are papain-like proteases that are present in the mineralized extracellular matrix, however, their activity increases particularly under mildly acidic pH conditions (pH 4.5-6) characteristic of caries progression [Tjäderhane et al., 2013]. In the presence of glycosaminoglycans, cathepsins can remain functional even at near-neutral pH, further extending their degradative potential within the dentin matrix. Their mechanism primarily involves intracellular proteolysis within lysosomal compartments, but they can also participate in extracellular matrix degradation [Nascimento et al., 2011; Tezvergil-Mutluay et al., 2015a]. Several cathepsins, including cathepsins B, C, L, O and K, have been identified in human dentin and among these, cathepsin K accounts for approximately 98% of the total proteolytic activity in dentin [Nascimento et al., 2011; Turk et al., 2011]. Cathepsin K is unique in its ability to cleave both the non-helical telopeptide regions and the triple-helical domain of collagen, whereas other cathepsins are limited to cleaving only the non-helical telopeptide regions [Germann, and Heidemann, 1988].

2.2 Dental caries

Caries is the most prevalent biofilm-mediated, multifactorial, sugar-driven, dynamic disease that results from disequilibrium of the demineralization and remineralization cycles in favor of demineralization and involves a bacterial shift in favor of acidogenic and aciduric bacteria [Pitts et al., 2017]. Apart from cariogenic bacteria, recent models suggest host-derived dentinal proteases (MMPs and CCs), activated under acidic conditions as a possible cause for broad surface caries progression [Mazzoni et al., 2015]. This process leads to rapid destruction of dental hard tissues that are exposed to the oral environment and following gingival recession, root surfaces becoming the primary targets of the caries process. Dentin collagen matrix in caries-affected dentin contains reduced amounts of intact type I collagen and proteoglycans compared with sound dentin yet has traditionally been considered to retain a generally preserved collagen scaffold capable of remineralization even after substantial mineral loss [Pugach et al., 2009]. In addition to dietary factors, behavioral, social and biological variables influence susceptibility to caries [Wen et al., 2022].

In the early stages, mineral loss may be reversible if biofilm is removed or the oral environment pH is restored to neutral conditions between meals. However, a prolonged imbalance favoring demineralization results in lesion progression, beginning with enamel involvement and extending from initial subsurface mineral loss to cavitated lesions affecting both enamel and dentin [Sapp et al., 2004; Pitts et al., 2017].

2.2.1 Enamel caries

Enamel caries is initiated by acid-mediated demineralization of hydroxyapatite crystals within the enamel [Vargas-Ferreira et al., 2015]. In the early stages, mineral loss occurs beneath an intact surface layer, creating a subsurface lesion clinically observed as a white-spot lesion. At this stage, the caries process may be stopped or even reversed through remineralization if the cariogenic challenge is controlled and the oral environment is improved [Sapp et al., 2004].

2.2.2 Dentin caries

Once caries progresses into dentin, the disease process involves both dissolution of the mineral phase and degradation of the collagen matrix and progress at a much faster rate than enamel caries [Sapp et al., 2004; Pitts et al., 2017]. Dual degradation mechanism results in a progressive reduction in dentin stiffness and mechanical strength by increasing porosity and inducing structural changes within the collagen matrix [Carrilho et al., 2009]. In addition, activation of host-derived proteolytic enzymes further compromises collagen integrity [Tjäderhane et al., 1998]. Due to the complex composition and ultrastructure of dentin, preventive strategies targeting

only the mineral phase are insufficient for effectively managing dentin caries progression and complicate restorative procedures [Sapp et al., 2004].

2.2.3 Root caries

Root caries is similar to dentin caries, however, they often progress more rapidly due to the lower mineral content of cementum and the underlying dentin [Zhang et al., 2020]. Root caries affects exposed root surfaces and frequently present as broad, shallow defects extending over large root surface areas rather than as localized cavities. Root caries is therefore most commonly observed in older adults, patients with xerostomia, and individuals with limited ability to maintain adequate oral hygiene. Due to increased life expectancy and improved dental care in older populations, root caries has become an increasingly relevant clinical problem [Wierichs, and Meyer-Lueckel, 2015]. Managing root caries through caries removal and restoration is challenging and far from ideal in terms of high organic content of root dentin, the close proximity to the gingiva and dental pulp and challenges related to access and moisture control [Hayes et al., 2016]. Preventive treatment strategies are therefore considered to offer a better long-term prognosis than restorative approaches. Early detection and diagnosis, together with the use of effective non-restorative interventions are crucial for managing non-cavitated root caries lesions [Paris et al., 2020].

2.3 *In vitro* dentin caries models

Well-conducted *in vivo* randomized controlled trials represent the gold standard for studying caries progression and arrest strategies, however, such studies are seldom reported because of their complexity and limited applicability across different research settings [Ferracane, 2017; Fung et al., 2018]. Therefore, *in vitro* caries models are widely used to investigate caries progression and to evaluate preventive and therapeutic strategies under controlled laboratory conditions [Clarkson et al., 1984]. *In vitro* models allow manipulation of experimental variables such as substrate, biofilm composition, pH, and exposure time, as well as the control of conditions that are difficult to regulate *in vivo*. Ideally, human teeth should be used as the substrate in dentin caries research.

Depending on the research objective, *in vitro* dentin caries models can be categorized into chemical demineralization models or bacterial demineralization models [Ferracane, 2017]. Furthermore, various *in vitro* protocols have been proposed, ranging from static to dynamic testing conditions [Ionescu, and Brambilla, 2021]. Although dynamic models offer pulsatile nutrient delivery and pH fluctuations, static models have proven sufficient to simulate dentin caries progression.

2.3.1 Chemical demineralization models

Chemical demineralization models induce mineral loss by exposing dental tissues to acidic solutions without the involvement of microorganisms (no biological component), thereby mimicking the acid challenge that occurs in the oral environment [Schwendicke et al., 2021]. These models are simple, fast, reproducible, low-cost, and suitable for testing both experimental and commercial materials [Ferracane, 2017]. pH cycling can be introduced to better replicate clinical conditions through alternating demineralization and remineralization cycles. Acidic solutions such as lactic acid, acetic acid, or buffer systems with controlled pH are applied for predetermined periods to simulate mineral dissolution [Schwendicke et al., 2019; Cifuentes-Jimenez et al., 2023].

2.3.1.1 Shallow chemical demineralization model

Shallow chemically induced lesions are typically created using mildly acidic solutions and short exposure times. These models primarily affect the superficial mineral phase and are often used to simulate early-stage caries lesions. Shallow lesions are useful for studying initial demineralization, remineralization potential, and the effects of preventive agents. However, they do not adequately reproduce the structural and biochemical complexity of dentin caries [Schwendicke et al., 2021].

2.3.1.2 Deep chemical demineralization model

Deep chemically induced lesions are generated by prolonged exposure time to acidic solutions or by using more aggressive demineralization protocols. These lesions extend further into dentin and produce greater mineral loss. While deep chemical models allow investigation of advanced demineralization and mechanical weakening of dental tissues, they also fail to replicate structural and biochemical complexity of dentin caries [Schwendicke et al., 2021].

2.3.2 Bacterial demineralization models

Bacterial demineralization models incorporate microorganisms to simulate acid production and biofilm formation, thereby better replicating the biological processes involved in caries development. Similar to chemical demineralization models, bacterial demineralization models are also simple, fast, reproducible, low-cost, and suitable for testing both experimental and commercial materials [Ferracane, 2017]. However, because there is no pH cycling, demineralization is primarily without the potential for surface remineralization.

The human oral cavity contains a highly diverse microbial consortium comprising hundreds of bacterial species [McBain, 2009; Baker et al., 2024]. Cariogenic bacteria present in oral biofilms metabolize carbohydrates to produce acids, which promote demineralization and degradation of dental tissues. These models vary in complexity depending on the bacterial species used. Microbiological models can be divided into three categories as single-species, multi-species and microcosm models [McBain, 2009].

2.3.2.1 Single-species bacterial demineralization model

Single-species models typically employ one cariogenic bacterium, such as *mutans streptococci* or *lactobacilli*. These models are useful for studying specific bacterial behaviors, acidogenicity and the effects of targeted antimicrobial agents. However, they oversimplify the caries process and do not represent the diverse microbial interactions present in natural dentin caries [McBain, 2009; Kreth et al., 2019].

2.3.2.2 Multi-species bacterial demineralization model

Although *mutans streptococci* have long been associated with caries development, it is now widely accepted that caries results from a complex interaction among microbial communities, host factors and dietary substrates rather than from a single bacterial species. Multi-species models include a defined consortium of oral bacteria selected to represent the complex nature of the biofilm [McBain, 2009]. These models provide greater biological relevance than single-species models and allow investigation of interspecies interactions. Nevertheless, they remain limited by the predefined selection of microorganisms and do not fully reflect the diversity of the oral microbiome [Mei et al., 2013b; Kreth et al., 2019].

2.3.2.3 Microcosm bacterial demineralization model

Among bacterial demineralization models, microcosm biofilm models are considered the most clinically relevant, as they better reflect the complexity of the oral environment, *in vivo* biofilm composition and behavior [McBain et al., 2005; Li et al., 2014a]. Microcosm biofilm models are derived from human saliva or dental plaque and contain a complex and heterogeneous microbial community, with saliva-derived biofilms being more commonly used due to ease of collection and standardization [McBain, 2009].

Although Brain Heart Infusion (BHI) medium is commonly used for biofilm cultivation, the newly introduced McBain medium which contains mucin, bacteriological peptone, tryptone and yeast extract can better mimic the composition

of saliva and provide essential nutrients to support multi-species biofilm growth [McBain et al., 2005]. Sucrose is added to the microcosm bacterial demineralization model as a carbohydrate source to promote cariogenic biofilm activity. Higher and more frequent sucrose concentrations may result in increased depth of dentin demineralization caused by biofilm exposure [Sissons et al., 2007].

2.4 Caries management strategies

Caries management is a personalized treatment strategy based on an accurate diagnosis and a comprehensive assessment of the individual patient. Untreated caries can compromise mastication, nutrition, quality of life and general health. Caries risk assessment is an integral part of the diagnostic phase and guides clinical decision making. Caries risk assessment involves the evaluation of multiple patient and lesion related factors, including lesion depth and proximity to the pulp, previous caries experience, oral hygiene status, salivary quantity and quality, dietary habits, socioeconomic status and access to dental care [Cheng et al., 2022]. These factors collectively influence lesion progression and treatment outcomes and should be considered when developing an individualized caries management plan [Ricketts et al., 2013].

Contemporary caries management philosophy has shifted away from the traditional drill-and-fill approach toward a minimally invasive seal-and-heal strategy, emphasizing disease control, preservation of sound tooth structure and promotion of remineralization rather than extensive surgical intervention [Ricketts et al., 2013; Schwendicke et al., 2021]. Preventing caries from developing and employing non-invasive strategies that promote remineralization in early lesions, remains a cornerstone of contemporary caries management and is essential for maintaining long-term oral health [Featherstone, 2000; Tassery et al., 2024].

The widespread use of fluoride therapy plays a central role in contemporary caries management [Featherstone, 1999; Chu et al., 2010]. Fluoride-based agents are well documented for their ability to inhibit demineralization [Chu et al., 2002], enhance remineralization [Zhao et al., 2020] and reduce caries incidence [Chu et al., 2010; Yu et al., 2018].

2.5 Silver fluoride treatments

Silver fluoride treatments have emerged as one of the most popular and effective methods among fluoride-containing materials for the prevention and management of dental caries and have demonstrated greater efficacy than fluoride use alone [Rosenblatt et al., 2009]. Silver fluoride treatments combine the remineralizing

potential of fluoride ions with the antimicrobial and anticariogenic properties of silver ions [Contreras et al., 2017; Zhao et al., 2018; Mei et al., 2018].

Silver fluoride treatments are simple, non-invasive, cost-effective, painless, rapid, lack of aerosol generation and low-cost treatments [Greenwall-Cohen et al., 2020]. According to the clinical scenario, silver fluoride treatments can either be left without subsequent restorative procedures or followed by the placement of a restoration, such as glass ionomer cement or composite resin [Sheridan et al., 2025]. Their documented clinical success has attracted increasing attention from both clinicians and researchers [Jiang et al., 2021].

2.5.1 History of silver and fluoride use

Silver ion has a long history of medical use dating back to antiquity, with documented applications across several ancient civilizations, including early medical uses in ancient China and later practices among the Greeks and Romans, who disinfected water with silver and stored it in silver vessels [Melaiye, and Youngs, 2005]. The use of silver in dentistry, specifically in the form of silver nitrate, was reported in the 1840s for caries arrest and in 1895 for the management of tooth sensitivity [Croll, and Berg, 2020]. In 1917, ammonia was added to silver nitrate to improve its stability, resulting in the formulation known as Howe`s solution [Greenwall-Cohen et al., 2020].

Fluoride ion, similar to silver, has been extensively used in various formulations to prevent and arrest dental caries, enhancing remineralization and reducing enamel and dentin solubility [Chu et al., 2010]. In early 20th century silver- and fluoride-based agents were evaluated and found to be effective in arresting dental caries. In the late 1960s, silver and fluoride ions were combined with ammonia to create the first commercially available ammonia-based silver fluoride, known as Saforide [Yamaga, 2003]. This formulation was originally developed by Dr. Misuho Nishino and Dr. Reichi Yamaga at Osaka University, Japan and subsequently approved for dental treatment in Japan [Nishino, 1969].

In parallel with the development of ammonia-based silver fluoride, water-based, ammonia-free silver fluoride formulation was introduced in the late 1970s by Dr. Graham Craig at the University of Sydney, Australia [Craig, 1981]. A 40% water-based silver fluoride along with 10% stannous fluoride (SnF_2) was produced by Creigton Pharmaceuticals (Australia) and used clinically to arrest carious lesions particularly in primary teeth. The manufacturer has since been re-established as Creigton Dental and the formulation is currently used as caries status detection solution.

To address esthetic concerns related to silver-induced discoloration, potassium iodide (KI) was later introduced by Dr. Geoffrey Knight at University of Adelaide,

Australia in the late 2000s [Knight, 2005]. In 2015, SDI (Australia) commercialized a two-bottle system consisting of ammonia-based silver fluoride (SDF) and a saturated solution of KI under the product name Riva Star. The formulation was originally developed by Dr. Graham Craig and subsequently used by Dr. Geoffrey Knight during his PhD research. Although initially introduced as desensitizing agent, Riva Star has been widely used for caries arrest. In 2020, the same manufacturer introduced Riva Star Aqua, a two-bottle system combining water-based silver fluoride (SF) and KI.

The combination of silver and fluoride into a single therapeutic agent integrates antimicrobial activity with remineralization potential, forming the basis of modern silver fluoride treatments. By 21st century, a range of *in vivo* [Zhi et al., 2012; Fung et al., 2018; Baraka et al., 2022] and *in vitro* [Mei et al., 2013b; Fung et al., 2016; Mei et al., 2018; D'Alessandro et al., 2024] studies documented the effectiveness of silver fluoride treatments in caries lesions.

Today, silver fluoride treatments have become a standard treatment option for managing and arresting dental caries, particularly in high-caries-risk populations, children and older adults [Jiang et al., 2021].

2.5.2 Mechanism of action

Although numerous studies have demonstrated the effectiveness of silver fluoride treatments in arresting dental caries, their exact mechanisms of action are multifactorial and not yet fully understood. The overall effect is thought to result from the dual action of silver ion mediated microbial inhibition and fluoride ion induced apatite formation [Zhao et al., 2018; Jamal et al., 2025].

Proposed mechanisms include the antibacterial activity of silver ions, which disrupt bacterial cell membranes and metabolic pathways, thereby inhibiting biofilm formation, as well as silver deposition within dentinal tubules that reduces dentin permeability [Yee et al., 2009; Zheng et al., 2022]. Fluoride ions promote remineralization through the formation of fluorohydroxyapatite and can also inhibit biofilm formation by binding to bacterial cellular components [Mei et al., 2017]. In addition, silver fluoride treatments attracted interest for their potential to inhibit endogenous dentin proteases, including matrix metalloproteinases and cysteine cathepsins, suggesting a possible off-label approach in enhancing the longevity of resin-dentin interfaces [Mei et al., 2012; Mei et al., 2013a; Mei et al., 2014; Muniz et al., 2024].

2.5.3 Indications for clinical use

Silver fluoride treatments are indicated to be used in various clinical applications involving both primary and permanent dentition, including enamel, dentin, and root surfaces [Fung et al., 2016; Oliveira et al., 2018; Hamdi et al., 2022]. Silver fluoride treatments have been explored not only for caries arrest and prevention but also for dentin hypersensitivity management, inhibition of endogenous enzymatic activity and as potential endodontic irrigants or inter-appointment medicaments [Greenwall-Cohen et al., 2020]. They are particularly useful in individuals with limited cooperation or special healthcare needs [Crystal et al., 2017]. The global market for silver fluoride cariostatic agents is rapidly expanding, with various formulations currently available that differ in silver concentration, solvent composition, and manufacturer [Mei et al., 2012; Fung et al., 2016; Patel et al., 2021].

Silver fluoride treatments have been used across all continents, including North America, South America, Europe, Asia, Africa and Australia. Commercially available products include Advantage Arrest (Elevate Oral Care, USA) and SilverSense SDF (Centrix, USA) in the North America, Saforide (Toyo Seiyaku Kasei, Japan), Ammdent Cariclear (Ammdent, India) and Dengen Caries (Dengen Dental, India) in Asia, Fagamin (Tedequim SRL, Argentina) and Cariesstop (Biodinamica, Brazil) in South America and Riva Star and Riva Star Aqua (SDI, Australia) in Asia, Australia and Europe [Zheng et al., 2022].

Silver fluoride treatments are currently available in two main chemical formulations depending on their solvent compositions. Complexation of silver and fluoride ions with ammonia results in ammonia-based silver fluoride, commonly known as silver diamine fluoride (SDF), whereas ammonia-free, water-based silver fluoride is referred to as aqueous silver fluoride (SF).

2.5.4 Ammonia-based silver diamine fluoride

Silver diamine fluoride (SDF), $Ag(NH_3)_2F$, is a clear, alkaline (pH ~ 13) solution composed of ammonia, silver and fluoride ions and is applied directly to active caries lesions. SDF has been shown to reduce dentin hypersensitivity, inhibit cariogenic biofilm formation and arrest caries progression [Mungur et al., 2023]. The US Food and Drug Administration officially approved SDF for tooth desensitization in 2014 and for caries treatment in 2015, and since then, both research interest and clinical use of SDF have increased [Gao et al., 2021; Jiang et al., 2021]. Reflecting its growing clinical relevance, the World Health Organization (WHO) Global Strategy Action Plan recommends the inclusion of SDF in national essential medicines lists by 2030 [World Health Organization (WHO), 2022]. In addition to international regulatory and policy guidance, national recommendations such as the Finnish Current Care Guidelines [Suomalainen Lääkäriseura Duodecim, 2023] recognize

SDF as an acceptable non-restorative caries management option, particularly when conventional restorative treatment is not feasible. Although SDF effectively arrests caries lesions, it does not restore lost tooth structure. Therefore, placement of restorative materials following SDF application is often recommended to reestablish function, although evidence regarding optimal restorative strategies remains inconclusive [Fröhlich et al., 2022].

2.5.4.1 Concentrations

Several concentrations of ammonia-based silver diamine fluoride are commercially available, most commonly 12%, 30%, and 38%. Among these, 38% SDF has demonstrated the most consistent clinical efficacy in caries arrest and is the most widely used formulation [Contreras et al., 2017; Patel et al., 2021].

2.5.5 Water-based silver fluoride

Water-based silver fluoride, also referred to as aqueous silver fluoride (SF), represents an ammonia-free alternative to SDF, is a clear, neutral (pH ~ 7) solution. In this formulation, ammonia is replaced by water, offering potential clinical advantages such as improved taste, reduced odor and decreased soft-tissue irritation [López-García et al., 2024]. However, scientific evidence regarding SF particularly its antimicrobial and biological effects, interactions with dentin collagen and its influence on bonding and mechanical properties remains limited [D'Alessandro et al., 2024; López-García et al., 2024].

2.5.6 Application of potassium iodide

Both ammonia-based and water-based silver fluoride treatments are associated with esthetic concerns due to black staining of treated dental tissues and adjacent soft tissues [Luong et al., 2022]. Discoloration results from the oxidation and precipitation of free silver ions and may limit patient acceptance, particularly in areas of high esthetic concern. To address this drawback, potassium iodide (KI) is often applied immediately after silver fluoride treatments [Primus, 2017; Roberts et al., 2020]. KI reacts with free silver ions to form a white silver iodide precipitate, thereby reducing or masking the characteristic black discoloration. Similar to water-based silver fluoride, scientific evidence regarding KI is relatively scarce [Knight et al., 2006; Turton et al., 2021] and further studies are needed to understand how KI affects the optical, chemical, mechanical and biological behavior of silver fluoride treatments.

Consequently, silver fluoride treatments may be applied either alone (SDF or SF) or in combination with KI. Currently, among commercially available systems, only Riva Star and Riva Star Aqua (SDI, Australia) are supplied with potassium iodide as a second step application.

3 Aims

The aim of this series of studies was to evaluate the adhesive, enzymatic, biocompatibility, and fatigue related effects of ammonia- and water-based silver fluoride treatments, with or without the application of potassium iodide, on dentin. The main objective was to identify the underlying mechanisms of action of ammonia- and water-based silver fluoride treatments, with or without the application of potassium iodide and to assess their impact on resin-dentin bonding, dentin matrix stability, cytotoxicity, and the fatigue resistance of carious dentin.

The specific aims of these studies were to:

I. Evaluate the optimal resin-dentin bonding protocol for ammonia-based silver fluoride (Silver Diamine Fluoride = SDF) treatment, with or without the application of potassium iodide (KI), by investigating the effects of delayed bonding and surface treatment strategies on bonding efficiency of a universal adhesive applied in both etch-and-rinse and self-etch modes. The tested null hypothesis were that SDF and SDF + KI treatments would have no effect on dentin surface morphology, hybrid layer formation, dentin permeability and micro-tensile bond strength, regardless of the adhesive application mode, delayed bonding or surface treatment strategy (Study I).

II. Evaluate the long-term effects of ammonia- and water-based silver fluoride (SDF and SF) treatments, with or without the application of potassium iodide (KI), as well as KI treatment alone, on their ability to inactivate dentin proteases and prevent degradation of dentin collagen matrix. The tested null hypothesis were that SDF and SF treatments, with or without KI, as well as KI alone, would have no effect on dentin protease activity or collagen matrix degradation when applied on demineralized dentin (Study II).

III. Evaluate the effects of ammonia- and water-based silver fluoride (SDF and SF) treatments, with or without the application of potassium iodide (KI), on trans-dentinal cell viability in simulated deep clinical cavities and direct cell

viability through treatment dilutions. The tested null hypothesis were that SDF and SF treatments, with or without KI, would have no effect on trans-dentinal and direct cell viability (Study III).

IV. Evaluate the fracture strength and fatigue resistance of carious dentin, treated with ammonia- and water-based silver fluoride treatments (SDF and SF), with or without the application of potassium iodide (KI), utilizing an *in vitro* microcosm biofilm model under quasi-static and cyclic loading conditions by four-point flexure test. The tested null hypothesis were that fracture strength and fatigue resistance of dentin would not be influenced by caries formation or by carious dentin treated with SDF and SF treatments, with or without KI (Study IV).

4 Materials and Methods

4.1 Materials

4.1.1 Sound human teeth

Nine hundred and fifty-eight extracted sound human third molars were extracted for routine dental treatments and were exempt from ethical approval according to the Finnish Act on the Medical Use of Human Organs, Tissues and Cells (101/2001) [Finland, 2001] and were used in the present thesis. Teeth were stored at 4 °C in 0.9% NaCl containing 0.02% sodium azide (NaN_3) to prevent bacterial growth and used no later than 3 months after extractions. Teeth were classified as sound based on visual examination and teeth presenting any signs consistent with ICDAS scores ≥ 3 were excluded [Pitts et al., 2013].

Sample size calculations were performed for each study. For Study I, sample size for non-trimmed micro-tensile bond strength (μTBS) testing was determined in accordance with the Academy of Dental Materials guidelines [Armstrong et al., 2017]. For Study I (dentin permeability), Study II, Study III and Study IV (quasi-static data), sample size calculations were determined using G*Power software (version 3.1.9.7, Kiel University, Germany). Unlike quasi-static testing, fatigue resistance assessment involves progressive damage accumulation under cyclic loading until failure. Therefore, conventional statistical power calculations designed for single-load tests are not directly applicable to fatigue experiments. The sample size used for fatigue testing was selected based on established protocols in the fatigue literature and in consistent with previous *in vitro* studies evaluating the fatigue resistance/strength of dental hard tissues and resin-dentin interfaces under comparable experimental conditions [Arola et al., 2010; Mutluay et al., 2013; Stape et al., 2022].

4.1.2 Preparation of mid-coronal dentin surface specimens (Study I and II)

Dentin specimens were prepared to obtain standardized mid-coronal dentin surfaces for subsequent surface treatments and bonding procedures to produce resin-dentin beams for mechanical testing (Study I) and for microscopic analyses including scanning electron microscopy (SEM) (Study I and II) and *in situ* zymography using confocal microscopy (Study II). Sound human third molars were coronally sectioned under water-cooling to expose flat mid-coronal dentin surfaces using a diamond saw (Isomet 1000 Precision Saw, Buehler Ltd, USA). Absence of remaining enamel was verified using a stereomicroscope (Leica M60, Leica Microsystems, Germany) at 40× magnification. Roots were removed 1 mm below the cervical line and discarded.

Exposed mid-coronal dentin surfaces were wet-polished with 320-grit silicon carbide (SiC) paper (CarbiMet, Buehler Ltd, USA) for 60 s at 350 rpm (MetaServ 250 Grinder-Polish, Buehler Ltd, USA) for smear layer standardization. Crown segments were then randomly allocated to their respective experimental groups according to the study design, for micro-tensile bond strength test, hybrid layer and dentin etching pattern analysis by scanning electron microscopy (SEM) and evaluation of gelatinolytic activity by *in situ* zymography.

4.1.3 Preparation of dentin beam specimens (Study II and IV)

Water-cooled saw (Isomet 1000 Precision Saw, Buehler Ltd, USA) was used to section rectangular dentin beams from mid-coronal dentin region of each tooth to obtain rectangular dentin beams with nominal cross-sections of roughly 0.3 mm thickness × 3 mm width × 7 mm length (Study II) and 0.4 mm thickness × 1.4 mm width × 6 mm length (Study IV). In all dentin beam specimens, dentinal tubules were oriented perpendicular to their longitudinal axis. Schematic diagrams of dentin beam specimen preparation are presented in **Figure 1**.

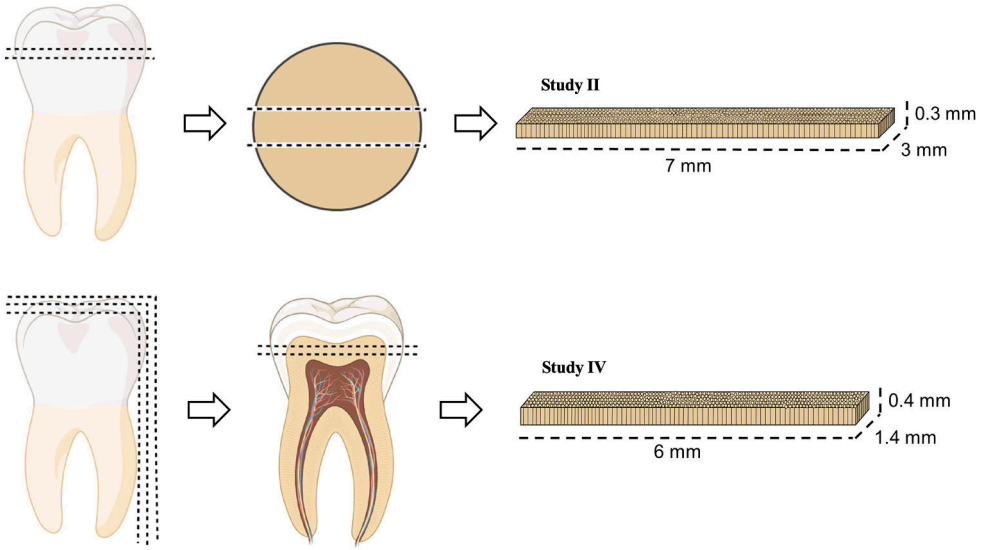

Figure 1. Schematic diagrams of dentin beam specimen preparation for Study II and Study IV. (*Modified from the supplementary data in Study IV*)

For Study II, primary sections were made perpendicular to the long axis of the tooth to obtain a single dentin disc from the mid-coronal dentin region, with a thickness of 0.3 mm. Secondary sections were subsequently performed in mesio-distal direction to produce rectangular dentin beams. To allow repeated measurements to be performed on the same surface, a small reference dimple was made at the corner of each dentin beam on the occlusal surface. Prepared dentin beams were stirred in aqueous 10 wt % H_3PO_4 (Phosphoric acid, Merck Sigma-Aldrich, Germany) for 40 min at 25 °C for complete demineralization and subsequently rinsed in distilled water at 4 °C for 1 h under constant stirring at 60 rpm (Loopster digital, IKA, Germany). Digital radiographs were taken to verify the absence of residual minerals. Initial modulus of elasticity of each beam was determined by three point bending test using universal testing machine (Autograph AGS-X Series, Shimadzu, Japan), then beams were dried in vacuum desiccator containing dry silica beads for 72 h and initial dry mass of each beam was weighted. After initial baseline measurements of modulus of elasticity and dry mass, demineralized dentin beams ($n = 10$ dentin beam/group) were assigned into 6 balanced groups, so that their mean modulus of elasticity and dry mass values were statistically similar.

For Study IV, primary sections were made parallel to the tooth long axis to obtain tooth slices with a thickness of 1.4 mm. Secondary sections were then performed perpendicular to the tooth long axis, within the mid-coronal region of each slice to produce rectangular dentin beams. Smear layer standardization was achieved by wet-

polishing the occlusal side of dentin beams with 600-grit silicon carbide (SiC) paper (CarbiMet, Buehler Ltd, USA) for 5 s. Prepared dentin beams were disinfected with 70% ethanol for 5 min, after which a microcosm biofilm model was formed and dentin beam specimens were randomly allocated to further experimental and control groups.

After both demineralization processes (phosphoric acid or microcosm biofilm model), digital images were obtained using a stereomicroscope (Leica M60, Leica Microsystems, Germany) and thickness and width dimension of the demineralized beams were precisely measured using an open-source image software (ImageJ, National Institute of Health, USA).

4.1.4 Preparation of dentin disc specimens (Study I, III and IV)

Deep coronal dentin discs of 0.4 mm thickness were prepared to evaluate the dentin permeability (Study III). Mid-coronal dentin discs measuring 1 mm (Study I) and 2 mm (Study IV) in thicknesses were prepared to measure dentin permeability and occlusal surface and cross-sectional microhardness, respectively.

Sound human third molars were sectioned perpendicularly to their long axis under water-cooling using a diamond saw (Isomet 1000 Precision Saw, Buehler Ltd, USA). In Study III, teeth were sectioned directly above the pulp chamber to obtain deep dentin discs measuring approximately 0.5 mm in thickness and 10 mm in diameter. In Study I and IV, teeth were sectioned above the pulp chamber at the mid-coronal dentin to produce dentin discs measuring approximately 1 and 2 mm in thickness, respectively.

A digital micrometer was used to determine the thickness and diameter of each disc (Mitutoyo, Japan). Absence of residual enamel, pulp horns and perforations were verified with a stereo microscope (Leica M60, Leica Microsystems, Germany) at 40× magnification. Dentin discs presenting enamel, perforations or pulpal exposures were discarded and replaced.

One dentin disc was obtained from each tooth in Study I, III and IV. In Study I, exposed mid coronal dentin surfaces were wet-polished with 320-grit silicon carbide (SiC) paper (CarbiMet, Buehler Ltd, USA) for 60 s at 350 rpm (MetaServ 250 Grinder-Polish, Buehler Ltd, USA) to standardize the smear layer. In study III, to obtain dentin discs with a final thickness of 0.4 (± 0.02) mm, discs were wet-polished from the occlusal surfaces with 320-grit SiC paper [ISO 7405, 2018]. In study IV, smear layer standardization was achieved with 600 and 1200-grit SiC paper to obtain scratch-free, smooth surfaces. The occlusal surface of each dentin disc was determined based on the conical geometry of dentinal tubules and was marked.

4.1.5 Treatment of dentin with silver fluoride treatments (Study I, II, III and IV)

Ammonia-based (Study I, II, III and IV) and water-based (Study II, III and IV) silver fluoride treatments, with or without the application of potassium iodide (KI) (Study I, II, III and IV) were applied to prepared dentin surfaces, dentin beams or dentin discs using a standardized experimental protocol developed based on the manufacturers' recommendations. Classifications, materials, compositions and pH values of the materials are presented in **Table 1**.

The ammonia-based silver fluoride treatment employed in this study was Riva Star (SDI, Australia). Riva Star is a two-bottle system consisting of an ammonia-based silver diamine fluoride (SDF) solution as the first step and a potassium iodide (KI) solution as the second step. In all studies, silver fluoride treatments were applied to dentin specimens using a microbrush.

For Study I and III, one drop of SDF was dispensed into a dappen dish and actively applied to the prepared dentin surfaces or dentin disc surfaces for 60 s, respectively. When KI was included in the protocol, the second step was performed immediately after SDF application. Two drops of KI were dispensed into a dappen dish and actively applied to the dentin surface for a total of 60 s. During the first 30 s, KI was actively applied to dentin, followed by replacement of the microbrush and reapplication of fresh solution for an additional 30 s. The initially creamy white precipitate was observed to turn clear during application. In Studies II and IV, 2 µL of SDF and 4 µL of KI was actively applied to each prepared dentin beam surface following the same protocol. In Study II, KI treatment alone was applied on each prepared dentin beam surface as a separate KI treatment alone group.

The water-based silver fluoride treatment employed in this study was Riva Star Aqua (SDI, Australia). Riva Star Aqua is also a two-bottle system consisting of a water-based silver fluoride (SF) solution as the first step and a potassium iodide (KI) solution as the second step. In Study I, the water-based silver fluoride treatment was not included, as it was not available on the market at the time of the experiment. In Study II, III and IV, the water-based silver fluoride treatment, was applied to dentin specimens using the same protocol as described for the ammonia-based silver fluoride treatment.

Table 1. Classification, material (manufacturer), composition and pH value of materials used in the present thesis.

Classification	Material	Composition	pH
Ammonia-based silver fluoride	Riva Star (SDI, Australia) Step1: Silver Diamine Fluoride = SDF	silver (32.6% w/v), fluoride (5.7% w/v), ammonia (15–20%w/v), water (40–60% w/v)	12.05*
	Step 2: Potassium Iodide = KI	potassium iodide (58% w/w)	8.63*
Water-based silver fluoride	Riva Star Aqua (SDI, Australia) Step 1: Aqueous Silver Fluoride = SF	silver (32.6% w/v), fluoride (5.7% w/v), water (50–70% w/v)	7.73*
	Step 2: Potassium Iodide = KI	potassium iodide (58% w/w)	7.94*
Airborne particle abrasion	Cojet System and Sand (Solventum, USA)	30 µm aluminum oxide, crystalline free fumed amorphous silica particles	-
Universal etchant	Scotchbond Universal Etchant (Solventum, USA)	32% phosphoric acid, water, synthetic amorphous silica, polyethylene glycol and aluminum oxide	0.1
Universal adhesive	Scotchbond Universal Plus Adhesive (Solventum, USA)	MDP phosphate monomer, dimethacrylate resins contain a BPA derivative–free, crosslinking radiopaque monomer, HEMA, methacrylate modified polyalkenoic acid copolymer, filler, ethanol, water, initiators and silane	2.7
Composite resin	Filtek Ultimate Universal Restorative (Solventum, USA)	bisGMA, UDMA, TEGDMA, bisEMA, PEGDMA, 20nm silica particles, 4–11 nm zirconium particles (78.5 wt% and 63.3 v%)	-

* The pH values of ammonia- and water-based silver fluoride treatments were determined at Adhesive Dentistry Research Laboratory, Institute of Dentistry, University of Turku, Turku, Finland. *Abbreviations:* MDP = methacryloyloxydecyl dihydrogen phosphate; BPA = Bisphenol A; HEMA = 2-hydroxyethyl methacrylate; bis-GMA = bisphenol glycidyl methacrylate; UDMA = urethane dimethacrylate; TEGDMA = tryethylene glycol dimethacrylate; bisEMA = ethoxylated bisphenol-A dimethacrylate; PEGDMA = poly(ethylene glycol) dimethacrylate. (*Modified from the supplementary data published in Study I*)

4.1.6 Bonding protocols (Study I and II)

4.1.6.1 Delayed bonding (Study I)

Delayed bonding, defined as storing the prepared dentin specimens in artificial saliva for designated time points, was applied prior to restorative procedures for micro-tensile bond strength (μTBS) testing and hybrid layer analysis and prior to dentin permeability assessment (Study I).

Following the ammonia-based silver diamine fluoride (SDF) treatment, with or without the application of potassium iodide (KI), treated dentin surfaces were either subjected immediately to further surface treatment approaches (airborne particle abrasion or water rinsing for 15 s) and subsequent restoration with a mild universal adhesive in both etch-and-rinse or self-etch mode, or they were stored in artificial saliva (pH 7.4) [Tezvergil-Mutluay et al., 2010] for 7, 15 or 30 days prior further surface treatments or restorations. Similarly, prepared dentin discs (1 mm thickness) treated with ammonia-based silver diamine fluoride (SDF), with or without the application of potassium iodide (KI), were first subjected to immediate dentin permeability measurements and subsequently stored in artificial saliva [Tezvergil-Mutluay et al., 2010] for 7, 15 and 30 days, after which permeability measurements were repeated.

For the delayed bonding groups, each treated dentin specimen was placed in a test tube containing 15 mL of artificial saliva and stored at 37 °C in a shaking water bath at 60 cycles/min. Each prepared dentin disc was placed inside each well in 24 well-plates containing 2 mL or artificial saliva and stored at 37 °C on a plate shaker at 400 rpm. Artificial saliva was replaced daily. Artificial saliva (pH 7.4) used in all experiments contained 5 mM hydroxyethylpiperazine ethane sulfonic acid (HEPES), 2.5 mM calcium chloride monohydrate ($CaCl_2 \cdot H_2O$), 0.05 mM zinc chloride ($ZnCl_2$), and 0.3 mM sodium azide (NaN_3) [Tezvergil-Mutluay et al., 2010].

4.1.6.2 Airborne particle abrasion (Study I)

Airborne particle abrasion was applied to evaluate the micro-tensile bond strength, hybrid layer analysis and dentin etching pattern test methods (Study I).

Following the ammonia-based silver diamine fluoride (SDF) treatment, with or without the application of potassium iodide (KI), either immediately or after storage in artificial saliva for 7, 15 or 30 days, airborne particle abrasion (Cojet System, Solventum, USA) was performed. Dentin surfaces without ammonia-based silver fluoride treatments served as control groups. The nozzle tip was positioned perpendicular to the prepared dentin surface at a distance of approximately 1 mm and airborne particle abrasion was performed for 30 s at 3 bar using 30 μm alumina

silica particles (CoJet-Sand, Solventum, USA). The treated surfaces were then rinsed with water stream for 30 s, after that, a mild universal adhesive was applied in either etch-and-rinse or self-etch mode.

Similarly, to prepare specimens for dentin etching pattern analysis, prepared dentin surfaces that were treated with ammonia-based silver diamine fluoride (SDF) treatment, with or without the application of potassium iodide (KI) were subjected to airborne particle abrasion following the same protocol and subsequently either rinsed or left unrinsed depending on the experimental group. Dentin surfaces without ammonia-based silver fluoride treatments served as control groups. Airborne particle abrasion composition and material is presented in **Table 1**.

4.1.6.3 Composite resin restoration (Study I and II)

Resin restorations were carried out to evaluate the micro-tensile bond strength, hybrid layer analysis, dentin etching pattern (Study I) and gelatinase activity by *in situ* zymography (Study II). All bonding procedures were carried out by a single operator.

Following the ammonia-based silver diamine fluoride (SDF) treatment, with or without the application of potassium iodide (KI), either immediately or after storage in artificial saliva for 7, 15 or 30 days, and subsequent surface treatment approaches (airborne-particle abrasion or water rinsing for 15 s), a mild universal adhesive (Scotchbond Universal Plus, Solventum, USA) was applied onto the dentin surface using either etch-and-rinse or self-etch mode. Bonding in etch-and-rinse mode consisted of etching dentin surfaces with 32% phosphoric acid gel (Scotchbond Universal Etchant, Solventum, USA) for 15 s, rinsed with water for 15 s and blot-dried with absorbent paper. The adhesive was actively applied for 20 s with light manual pressure (approximately 4 g, corresponding to slight rubbing pressure), followed by gentle solvent evaporation for 10 s and light cured for 10 s using multiwave LED light curing unit (Valo Corded, Ultradent, USA) with an irradiance of 1800 mW/cm². Light irradiance of the light curing unit was measured using MARC Light Collector (MARC-LC, Bluelight Analytics, Canada). Bonding in self-etch mode consisted of the same application steps, except for phosphoric acid etching and rinsing. Composite blocks were built using a nanofilled composite resin (Filtek Ultimate Universal Restorative, A2B shade, Solventum, USA) in two 2-mm increments, each increment was light cured for 20 s.

For dentin etching pattern analysis, the application protocols were performed as described above, with the exception that the bonding agent was not light cured but instead thoroughly rinsed off with water for 30 s to expose the underlying dentin surface. Composite resin was not applied.

To evaluate gelatinase activity, prepared dentin surfaces were bonded following the etch-and-rinse mode. Dentin surfaces were etched with 32% phosphoric acid gel (Scotchbond Universal Etchant, Solventum, USA) for 5 s, rinsed with water for 15 s, and blot-dried with absorbent paper. In this protocol, ammonia- and water-based silver fluoride treatments (SDF and SF), with or without the application of potassium iodide (KI), were applied after the etching step, prior to adhesive application. Etched dentin without silver fluoride treatments served as the control group. Adhesive application and light curing were performed as described above. Composite blocks were built using a nanofilled composite resin in a single 2-mm increment and light cured for 20 s.

Material, composition and pH values of universal etchant, universal adhesive and composite resin are presented in **Table 1**.

4.1.7 Preparation of silver fluoride treatment dilutions (Study III)

Three different dilutions as 10^{-3}, 10^{-4} and 10^{-5} were prepared in cell media for both ammonia- and water-based silver fluoride solution (SDF and SF), either alone or combined with potassium iodide (KI). The dilution groups were as follows: (*i*) SDF, (*ii*) SDF + KI, (*iii*) SF and (*iv*) SF + KI. For the SDF and SF groups, stock solutions were directly diluted in cell media to achieve final concentrations of 10^{-3}, 10^{-4} and 10^{-5}. For the SDF + KI and SF + KI groups, equal volumes of SDF or SF solution were first mixed with KI, after which the mixture was further diluted in cell media to reach the final concentrations.

4.2 Research methods

A total of 20 research methods were employed in the present thesis. The adhesive, enzymatic, biocompatibility, and fatigue-related behavior of dentin treated with ammonia- and water-based silver fluoride (SDF and SF) treatments, with or without the application of potassium iodide (KI), were evaluated. In addition, the microcosm biofilm model used in Study IV was characterized utilizing colony-forming unit counts, dentin surface and cross-sectional microhardness, lactic acid production and biofilm viability. Imaging techniques, including scanning electron microscopy and *in situ* zymography using confocal microscopy, were used for morphological and enzymatic assessments.

4.2.1 Micro-tensile bond strength (Study I)

The micro-tensile bond strength (μTBS) evaluation consisted of the following experimental groups. The two main groups were treated with ammonia-based silver diamine fluoride (SDF), with or without the application of potassium iodide (KI). Teeth within each treatment group were then randomly assigned into subgroups (n = 5 teeth/group) according to delayed bonding time points (immediate, 7, 15, or 30 days), surface treatment approach (with or without airborne particle abrasion and with or without water rinsing for 15 s), and the application mode of a mild universal adhesive (etch-and-rinse or self-etch). Control groups consisted of untreated dentin surfaces (with or without airborne particle abrasion) that were immediately bonded using the same mild universal adhesive applied in either etch-and-rinse or self-etch mode. A summary of the experimental design is presented in **Figure 2**.

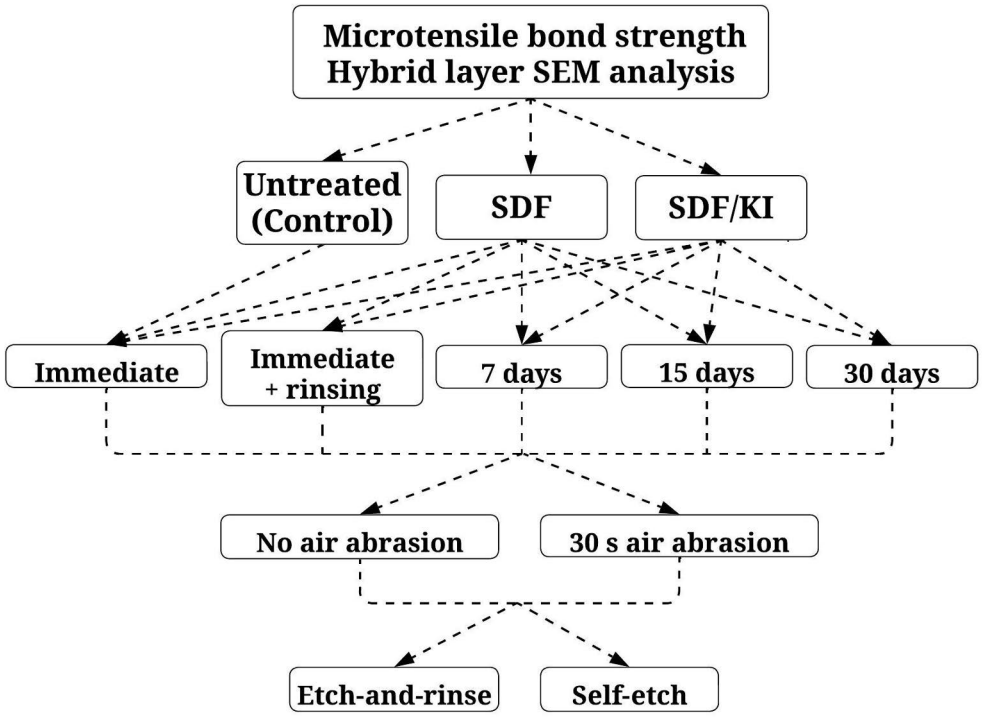

Figure 2. Flowchart of the experimental design of micro-tensile bond strength and hybrid layer analysis test methods. Each experimental subgroup consisted of n = 5 teeth. (*Modified from the supplementary data published in Study I*)

Restored crown segments were stored in distilled water at 37 °C for 24 h. Then, restored crowns were sectioned longitudinally in mesio-distal and bucco-lingual directions perpendicular to the bonded interface with a diamond saw (Isomet 1000 Precision Saw, Buehler Ltd, USA). Resin-dentin beams were produced with a cross-sectional area of approximately 0.9 mm^2. Micro-tensile bond strength evaluation was performed according to the Academy of Dental Materials guidelines for non-trimmed μTBS testing [Armstrong et al., 2017]. A minimum of 8 beams per tooth (n = 5 teeth/group) were tested for each experimental condition. Each beam was individually attached to a custom-made micro-tensile testing jig using a cyanoacrylate adhesive (Loctite 416, Henkel Corp, Ireland) and tested under tensile stress in a universal testing machine (Autograph AGS-X Series, Shimadzu, Japan) at a crosshead speed of 0.5 mm/min until failure to obtain the maximum load (P) in newtons (N). The cross-sectional area (CA) of each beam in mm^2 was measured using a digital caliper. Micro-tensile bond strength (μTBS) values were calculated in megapascals (MPa) using the formula μTBS = P/CA (Trapezium X Software, Shimadzu, Japan). All specimens were tested by a blinded operator. Tooth was considered as the statistical unit, bond strengths of resin-dentin beams from each tooth were averaged to represent the bond strength of each tooth. Bond strength of each tooth belonging the same group were averaged to represent the bond strength of each experimental group. Pre-test failures (PTFs) were included in the calculations as 0 MP in accordance with the Academy of Dental Materials recommendations [Armstrong et al., 2017].

4.2.1.1 Failure mode analysis (Study I)

Both surfaces of fractured resin-dentin beams were observed using a stereomicroscope (Leica M60, Leica Microsystems, Germany) with 40 × magnification to determine failure modes. When failure modes could not be clearly identified especially between adhesive and mixed failure types, specimens were examined using scanning electron microscopy (SEM) (Phenom ProX, Phenom-World, Netherlands). Failure modes were classified as adhesive failure (failure at resin/dentin interface), mixed failure (failure at resin/dentin interface with cohesive failure of the neighboring substrates) and cohesive failure (failure exclusive within dentin or composite resin).

4.2.2 Hybrid layer SEM analysis (Study I)

Two randomly selected resin-dentin beams for each tooth (n = 5 teeth/group) were prepared according to the previously described experimental groups for the micro-tensile bond strength test, were used for hybrid layer characterization using scanning

electron microscopy (SEM). A summary of the experimental design is presented in **Figure 2**.

Selected resin-dentin beams were embedded in epoxy resin and wet-polished with silicon carbide (SiC) papers of decreasing grit sizes, 320-grit for 4 min, 600-grit for 6 min, 1200-grit for 8 min, and 4000-grit for 10 min. Final polishing was performed using a 0.05 μm aluminum oxide polishing paste (Buehler Ltd, USA) for 5 min. After each polishing step, the epoxy embedded beams were ultrasonically cleaned in distilled water [Perdigao et al., 1995]. Bonded interfaces were treated with 50% phosphoric acid (H_3PO_4) for 5 s and 3% sodium hypochlorite (NaOCl) for 10 min, dried in silica overnight, mounted on aluminum stubs, sputtered with gold/palladium and analyzed on mapping mode at 10 kV by SEM (Phenom ProX, Phenom-World, Netherlands). A series of sequential micrographs of the bonded interfaces (5500× magnification) were obtained from each resin-dentin beam by an experienced blinded operator. Three randomly selected areas on each micrograph located between adjacent resin tags were analyzed by a single-blinded experienced examiner for hybrid layer thickness using an open-source image software (ImageJ, National Institute of Health, USA). Measurements obtained from each tooth were averaged to determine the hybrid layer thickness for each experimental group.

4.2.3 Etching pattern SEM analysis (Study I)

Prepared and wet polished flat mid-coronal dentin surfaces were randomly assigned to 21 groups (n = 2 teeth/group) according to the experimental design presented in **Figure 3**.

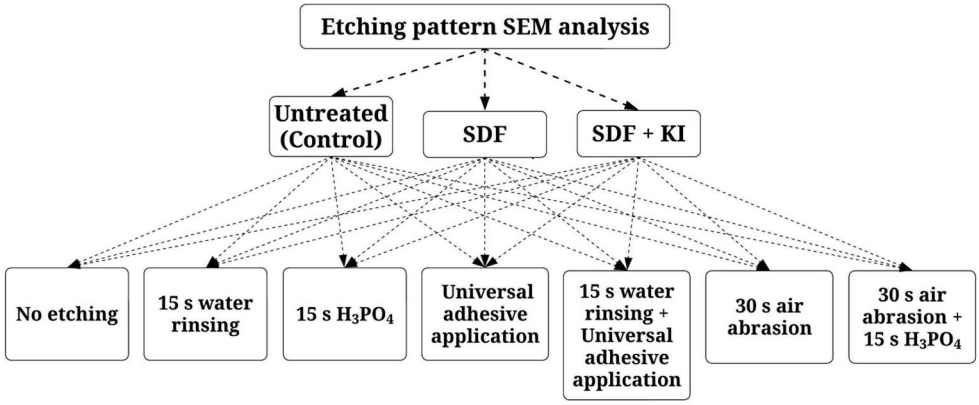

Figure 3. Flowchart of the experimental design of etching pattern analysis test method. Each experimental subgroup consisted of n = 2 teeth. (*Modified from the supplementary data published in Study I*)

Application protocols were performed as described in Section 4.1.6 Bonding protocols. Specimens were dehydrated in ascending ethanol concentrations (25%, 50%, 60%, 70%, 80%, 90% and 100%) for 30 min at each concentration, followed by immersion in 100% ethanol for 1 h. Subsequently, specimens were transferred to a 1:1 solution of hezamethyldisilazane (HMDS) and ethanol for 1 h and then fixed in HMDS (Sigma Aldrich, USA) [Perdigao et al., 1995]. Specimens were mounted on aluminum stubs, sputter coated with gold-palladium and analyzed by SEM (Phenom ProX, Phenom-World, Netherlands) on backscattering mode at 10 kV (5000× magnification). All specimens were examined by an experienced-blinded operator.

4.2.4 Dentin permeability (Study I and III)

To evaluate the passage of ions through the dentin tubules, dentin permeability was evaluated using a flow-measurement infiltration apparatus (SLI-1000 Liquid Flow Meter, Sensirion, Switzerland) in a modified split-chamber unit, which was linked to a deionized water container at a simulated hydrostatic pressure of 20 cm [Zhang et al., 2018]. Hydraulic conductance (Lp) was calculated by dividing fluid flow ($\mu L \cdot min^{-1}$), under simulated hydrostatic pressure (20 cm H_2O), by the available dentin surface area (cm^2). Maximum dentin permeability was defined by the hydraulic conductance calculated after etching dentin discs with 50% citric acid for 30 s to remove smear layer and smear plugs and to reopen dentinal tubules (Study I and III).

In Study I, after maximum permeability measurements, dentin discs (n = 12 dentin disc/group) were randomly allocated into two groups according to ammonia-based silver fluoride treatment (SDF), either with or without the application of potassium iodide (KI). Hydraulic conductance values were recorded immediately after SDF or SDF + KI treatments and after storage in artificial saliva for 7, 15 or 30 days. An isolated control group consisting of SDF and SDF + KI treatment followed by water rinsing for 15 s was included. Dentin permeability was expressed as a percentage reduction in hydraulic conductance (Lp%) considering the maximum permeability as the baseline values. Each dentin disc served as its own dentin permeability control.

In Study III, dentin permeability measurements were recorded prior to dentin barrier cytotoxicity test setup in order to obtain dentin discs with similar permeability values. Dentin discs (n = 30 dentin disc/group) were homogeneously allocated into groups based on their maximum permeability measurements and eight dentin discs with similar permeability values were used in each dentin barrier cytotoxicity test setup [ISO 7405, 2018]. After permeability measurements, dentin discs were rinsed

with distilled water and sterilized by autoclaving in 0.9% sodium chloride (NaCl) at 121 °C for 25 min.

4.2.5 Loss of dry mass (Study II)

Loss of dry dentin mass was used as an indirect method to evaluate the enzymatic degradation of the demineralized dentin collagen matrix, allowing estimation of the amount of solubilized collagen over time [Carrilho et al., 2009; Mazzoni et al., 2014]. To measure the initial dry mass of completely demineralized dentin beam specimens (0.3 × 3 × 7 mm), dentin beams were stored in a vacuum desiccator for 72 h after demineralization and rinsing as described in Section 4.1.3. Preparation of dentin beam specimens. Dry mass of each beam was then measured using an analytical microbalance (XP6 Microbalance, Mettler Toledo, USA). Following the initial measurements, dentin beams were rehydrated in distilled water at 4 °C for 1 h. Dentin beam specimens were distributed into 6 balanced experimental groups according to the mean dry mass of each group which was statistically similar. Ammonia- and water-based silver fluoride (SDF and SF) treatments, with or without application of potassium iodide (KI), as well as KI application alone, were applied on dentin beams. Untreated demineralized dentin beams were served as control group. After treatments, beams were rinsed with distilled water inside 96-well plate at a microplate shaker at 300 rpm and subsequently blot dried with absorbent paper. Dry mass measurements were repeated immediately after treatments following the same protocol. Then, each dentin beam was placed into an individually labeled O-ring polypropylene tube containing 500 µl zinc- and calcium-containing artificial saliva (pH 7.4) [Tezvergil-Mutluay et al., 2010] and incubated in a shaking water bath (60 cycles/min) at 37 °C, for designated incubation periods of 1-week, 1-month, 3-month or 6-month to facilitate artificial saliva diffusion within collagen fibrils. After each incubation period, dentin beams were rinsed at 4 °C for 24 h in distilled water to remove media salts before dry mass measurements. Measurement of the dry mass was reassessed after dehydration in desiccator under same conditions. The loss of dry mass was calculated as the percentage change of dry mass loss referring to the dry mass recorded for each beam after corresponding silver fluoride treatments [Tezvergil-Mutluay et al., 2012]. Demineralized dentin beams without any treatment served as control group.

The incubation medium was stored frozen at -80 °C. Those media were analyzed for solubilized telopeptides of collagen (ICTP & CTX), hydroxyproline (HYP) release and total extractable protein (Bradford assay).

4.2.6 Modulus of elasticity (Study II)

Three-point bending configuration was used under controlled strain to measure the modulus of elasticity, which allows repeated measurements to be performed on the same specimen [Bedran-Russo et al., 2008]. Demineralized dentin beam specimens were placed on a three-point bending jig (Instron, Instron Inc., USA) with a span length of 5 mm between supports, fully immersed in distilled water, and subjected to flexural testing up to 3% strain at a displacement rate of 0.5 mm/min using a 5 N load cell (SMT1-5N, Interface, USA) mounted on a universal testing machine (Autograph AGS-X, Shimadzu, Japan). After reaching maximum displacement, the load was immediately returned to 0% stress within 15 s to prevent creep of the demineralized collagen matrix [Tezvergil-Mutluay et al., 2012]. Apparent modulus of elasticity (E) was calculated using the equation $E = mL^3/4bh^3$ where m is the slope of the linear portion of the load-displacement curve (N/mm), L is the span length (5 mm), b is the width, and h is the thickness of the demineralized dentin beam (mm) and expressed in MPa. Each demineralized dentin beam was tested in duplicate and the mean value was used as the E value for each demineralized dentin beam. E were evaluated initially on demineralized dentin beams which served as baseline measurements. Based on baseline measurements, dentin beam specimens were distributed into six balanced experimental groups according to the mean modulus of elasticity of each group which was statistically similar. E was remeasured, after the application of ammonia- and water-based silver fluoride (SDF and SF) treatments, with or without application of potassium iodide (KI), as well as KI application alone, and after each designated incubation period (1-week, 1-month, 3-month or 6-month) in zinc- and calcium-containing artificial saliva (pH 7.4) [Tezvergil-Mutluay et al., 2010]. Demineralized dentin beams without any treatment served as control group.

4.2.7 Total enzymatic activity (Study II)

A commercially available colorimetric matrix metalloproteinase (MMP) assay kit (SensoLyte Generic MMP Assay Kit, AnaSpec, USA) was used to quantify total matrix-bound MMP activity [Seseogullari-Dirihan et al., 2016]. This assay enables the detection of the combined activity of multiple MMPs, including MMP-1, -2, -3, -7, -8, -9, -12, -13, and -14, and offers direct information regarding the effectiveness of MMP activation or inactivation [Mazzoni et al., 2015]. The assay can detect nanogram levels of active MMPs in dentin. Demineralized dentin beams served as the source of endogenous MMPs [Tezvergil-Mutluay et al., 2012]. Following the application of ammonia- and water-based silver fluoride (SDF and SF) treatments, with or without application of potassium iodide (KI), as well as KI application alone, dentin beam specimens were rinsed, blot-dried with absorbent paper and incubated in 200 µL of substrate and assay buffer in the 96-well plate for 2 h at 25 ºC to assess

the MMP activity. Demineralized dentin beams without any treatment served as control group. Every 30 min, dentin beams were removed from the wells and MMP activity was measured using a spectrophotometer (Synergy HT, BioTek Instruments, USA) at a wavelength of 412 nm. Data were recorded until enzymatic activity reached a peak value. Subsequently, the beams were rinsed in distilled water to remove residual MMP substrate and incubated for designated periods of 1-week, 1--month, 3-month or 6-month in zinc- and calcium-containing artificial saliva (pH 7.4) [Tezvergil-Mutluay et al., 2010]. Demineralized dentin beams without any treatment served as control group. After each incubation period, beams were rinsed. The total enzymatic activity was reassessed following the same protocol. The percentage inhibition of MMPs were calculated by subtracting the mean values of the control group from that of the treatment groups, then dividing the result by the control mean.

4.2.8 Solubilized telopeptides of collagen (Study II)

Different C-telopeptide fragments released into the incubation media (zinc- and calcium-containing artificial saliva (pH 7.4) [Tezvergil-Mutluay et al., 2010]) were analyzed after each predefined media after each incubation period (1-week, 1-month, 3-month or 6-month) to evaluate the specific role of matrix metalloproteinases (MMPs) and cysteine cathepsins (CCs) in type I collagen degradation MMPs and CCs are responsible for cleaving the distinct telopeptide regions of type I collagen. Matrix degradation mediated by MMPs were determined by measuring the amount of solubilized type I collagen C-terminal cross-linked telopeptides [Garnero et al., 2003], cathepsin K-induced degradation of type I collagen was evaluated by the amount of solubilized C-terminal peptide. Cathepsin K is the only known source of CTX [Tezvergil-Mutluay et al., 2015a]. The quantification of ICTP and CTX fragments was carried out using commercially available kits for MMPs (UniQ ICTP RIA, Aidian Diagnostics, Finland) and CCs (Serum CrossLaps ELISA, IDS, Denmark), respectively. Following each incubation period (1-week, 1-month, 3-month or 6-month) in zinc- and calcium-containing artificial saliva (pH 7.4) [Tezvergil-Mutluay et al., 2010], aliquots of 20-25 µL of incubation media were taken from each tube to quantify solubilized ICTP and CTX fragments following the manufacturers` protocol. ICTP measurements were obtained using a gamma counter (Wallac Wizard, Turku, Finland) at 1000 counts and CTX measurements were performed using a spectrophotometer (Synergy HT, Bio Tek Inst, USA) at 450 nm absorbance. The amount of collagen degradation as ICTP release was calculated using a 5-point fitting curve with known concentration standards from 1 to 50 ng/mL, with the limit of 0.6 ng/mL by a gamma counter. The amount of collagen degradation

as CTX release was calculated with a standard curve using standards with known concentrations provided by the manufacturer.

4.2.9 Hydroxyproline quantification (Study II)

The amount of collagen solubilization was evaluated from the incubation media (zinc- and calcium-containing artificial saliva (pH 7.4) [Tezvergil-Mutluay et al., 2010]) after each designated incubation period (1-week, 1-month, 3-month or 6-month) in zinc- and calcium-containing artificial saliva (pH 7.4) [Tezvergil-Mutluay et al., 2010]. by quantification of hydroxyproline (HYP). Type I collagen contains approximately 9.6% hydroxyproline in its amino acid composition. Solubilized collagen peptide fragments were quantified following a previously described hydroxyproline assay protocol [Reddy, and Enwemeka, 1996] Briefly, aliquots of HYP standards (2–20 µg) prepared from stock solutions and 25 µL of incubation media were mixed with 25 µL of 4 N sodium hydroxide (NaOH) (final concentration 2 N) in a total volume of 50 µL in 2 mL Nalgene O-ring tubes. Specimens were hydrolyzed by autoclaving at 120 °C for 20 min. Subsequently, 450 µL of chloramine-T solution was added to each hydrolyzed specimen and gently mixed to allow oxidation for 20 min at room temperature. Then, 500 µL of Ehrlich's aldehyde reagent was added to each specimen for chromophore formation, followed by incubation at 65 °C for 20 min. Absorbance was measured using a spectrophotometer (Model UV-A180, Shimadzu, Japan) at 550 nm. HYP release were calculated by plotting absorbance values against the standard HYP curves.

4.2.10 Total extractable protein (Study II)

Extracted dentin proteins released into the incubation media (zinc- and calcium-containing artificial saliva (pH 7.4) [Tezvergil-Mutluay et al., 2010]) from demineralized dentin were used for the quantification of extractable protein level after each designated incubation period (1-week, 1-month, 3-month or 6-month) using the Bradford protein assay. Bradford protein assay, originally introduced by Bradford (1976), is a widely used colorimetric method for determining protein concentrations in biological specimens and cell fractions [Bradford, 1976]. The assay is based on the proportional binding of Coomassie Brilliant Blue dye to proteins, resulting in a color change that is directly related to protein concentration. Extracted proteins from each dentin beam into the incubation media were tested according to the manufacturer's instructions using a commercial kit based on the Bradford assay (Bio-Rad, Hercules, USA) [Bradford, 1976]. Briefly, 1 to 50 µg/mL series of bovine serum albumin (BSA) standards (50 µL) and 50 µL aliquots of

incubation media were prepared in parallel. After 5 min of incubation to allow color development, absorbance was measured using a spectrophotometer (Synergy HT, BioTek Instruments, USA) at a wavelength of 595 nm. A linear standard curve was prepared by plotting the average reading for each BSA standard against its concentration in μg/mL and the standard curve was used to determine the total extractable protein concentration.

4.2.11 Dentin surface and cross-section SEM analysis (Study II)

Additional demineralized dentin beams were treated with ammonia- and water-based silver fluoride (SDF and SF) treatments, with or without application of potassium iodide (KI). Demineralized dentin beams without any silver fluoride treatment served as control group (n = 4 dentin beam/group). The group that was treated with KI alone, was not prepared for SEM analysis, as KI application alone is not used in clinical practice. Half of the specimens were evaluated for surface morphology, whereas the remaining specimens were fractured in liquid nitrogen to obtain cross-sectional views. The specimens were dehydrated in ascending ethanol concentrations (25%, 50%, 60%, 70%, 80%, 90%, and 100%) for 30 min at each concentration, followed by immersion in 100% ethanol for 1 h. Subsequently, specimens were transferred to a 1:1 solution of hexamethyldisilazane (HMDS) and ethanol for 1 h and then fixed in HMDS (Sigma-Aldrich, USA) [Perdigao et al., 1995]. Dentin beams were mounted on aluminum stubs, sputter coated with gold-palladium and analyzed by SEM (Phenom ProX, Phenom-World, Netherlands) on backscattering mode at an accelerating voltage of 10 kV and magnifications up to 2500×.

4.2.12 Gelatinase activity by *in situ* zymography (Study II)

In situ zymography was first described by Galis et al [Galis et al., 1994] to analyze the gelatinolytic activity in tissue sections. This technique enables localization of enzyme activity and visualization of its spatial distribution without the need for specific antibodies. It is based on a fluorescence substrate that can be applied to both tissue sections and cell cultures. The technique was later modified by introducing dye-quenched (DQ) gelatin to detect the localization of gelatinolytic activity within tissue sections. Gelatin is labeled with fluorescein isothiocyanate (FITC), which can be visualized as fluorescence produced at sites of gelatinolytic activity after cleavage of DQ-gelatin. The distribution of gelatinolysis within the hybrid layer using *in situ* zymography was first described by Mazzoni et al. [Mazzoni et al., 2012] and the same protocol was followed in Study II.

Prepared dentin surfaces were bonded according to the procedures described in Section 4.1.6.3 Composite resin restoration. The bonded specimens (n = 2 teeth/group) were then sectioned vertically into 0.3 mm-thick slabs to expose the resin-dentin interfaces, wet-polished with 600-, 1200-, and 2000-grit silicon carbide (SiC) papers, and ultrasonically cleaned for 5 min after polishing. The four central slabs from each specimen were selected for evaluation. The 0.3 mm-thick sections were demineralized with 10% phosphoric acid for 10 s, rinsed with distilled water for 20 s, and blot-dried with absorbent paper. A self-quenched fluorescein-conjugated gelatin substrate (DQ-gelatin; E-12055, Molecular Probes, Eugene, USA) was prepared from a stock solution and diluted 1:8 in dilution buffer (150 mM NaCl, 5 mM $CaCl_2$, 50 mM Tris-HCl, pH 8.0). Specimens were wetted with 30 µL of gelatin solution, with and without fluorescent gelatin to prevent false readings, and then covered with a coverslip. The slides were protected from light and incubated in a humidified chamber at 37 °C for 24 h. Interfacial endogenous gelatinase activity was observed using a confocal laser scanning microscope (Zeiss LSM 880, Carl Zeiss, Germany) with an excitation wavelength of 488 nm. The entire resin-dentin interface was examined, and sequential images (z-stacks) were recorded from each dentin slice. Images were quantitatively analyzed using open-source image analysis software (ImageJ, National Institutes of Health, USA) by a single-blinded examiner. Readings obtained from specimens treated with gelatin solution without fluorescent were used as background readings. Gelatinolytic activity was expressed as the percentage of the fluorescent area.

4.2.13 pH measurement (Study II and III)

The pH values of each bottle of commercially available ammonia- and water-based silver fluoride solution (Riva Star and Riva Star Aqua, SDI, Australia) as well as the prepared dilutions (10^{-3}, 10^{-4} and 10^{-5}) were measured using a calibrated electrode pH meter (PHM210; Radiometer Analytical, France) with an accuracy of ± 0.01. After each measurement, the electrode was washed with distilled water to prevent contamination. The pH values of commercially available silver fluoride treatments are presented in **Table 1**. The pH of each prepared dilution (10^{-3}, 10^{-4} and 10^{-5}) was measured 5 times, mean values and standard deviations were calculated.

4.2.14 Preparation of pulp-derived three-dimensional cell culture (Study III)

Immortalized clonal large T-antigen transfected bovine pulp-derived cells (SV40), originally derived from calf dental papilla [Thonemann, and Schmalz, 2000; ISO 7405, 2018], of which the clonal subline “SVNeo3B cells”, were provided as a kind

donation from Regensburg University and stored in liquid nitrogen until use. Cells were passaged and maintained in growth medium consisting of α-modified Eagle's minimum essential medium (α-MEM; M8042, Merck Sigma-Aldrich, Germany) supplemented with 20% fetal bovine serum (FBS) (Gibco, Thermo Fisher, USA), 150 IU/mL penicillin, 150 mg/mL streptomycin, 0.125 mg/mL amphotericin B, and 0.1 mg/mL geneticin (Merck Sigma-Aldrich, Germany) at 37 °C in a humidified atmosphere of 5% CO_2. Cells between passages 19 and 24 were used. Polyamide nylon meshes (pore size 150 µm, diameter 8 mm) were cleaned with 0.1 M acetic acid for 30 min at room temperature, rinsed three times with distilled water, and coated with 0.03 mg/mL bovine plasma fibronectin (Merck Sigma-Aldrich, Germany). A six-well tissue culture plate was filled with 1.25 mL of α-MEM supplemented with 20% FBS and Millicell inserts (Merck Sigma-Aldrich, Germany) were placed in each well to support initial cell growth on the polyamide nylon meshes. Four meshes were placed into each insert. Cell numbers were calculated using an automated cell counter (TC20, Bio-Rad, USA) after mixing 15 µL of cell suspension with 0.4% trypan blue and loading 10 µL of the mixture into the counting chamber. Cell suspensions were adjusted to 80.000 cells per 20 µL for each polyamide nylon mesh. Cultures were incubated for 48 h at 37 °C, 5% CO_2, and 100% humidity to allow cell attachment and growth. After incubation, the polyamide nylon meshes were transferred to a 24-well plate and placed individually into wells containing 1 mL of α-MEM supplemented with 20% FBS. The culture medium was changed three times per week for 14 days to generate three-dimensional pulp-derived cell cultures on the meshes. Additional meshes were prepared for each test to ensure an adequate number of cells on membranes. To select eight polyamide nylon meshes with comparable three-dimensional cell viability for each dentin barrier test setup, the cultures were transferred to a new 24-well plate on the day of the experiment. Each well contained 400 µL of α-MEM and 20 µL of cell proliferation reagent (WST-1, Roche, Switzerland). After 1 h of incubation, optical density was measured at 440 nm using a spectrophotometer (Synergy HT, BioTek Inst., USA). Meshes exhibiting similar cell viability values (n = 8 mesh/test setup) were selected for use in each dentin barrier cytotoxicity test setup.

4.2.15 Dentin barrier cytotoxicity test (Study III)

Dentin barrier cytotoxicity test, also referred as trans-dentinal cytotoxicity test was carried out according to ISO 7405 [ISO 7405, 2018]. In this method, tested materials are applied over dentin discs and allowed to pass through dentinal tubules to evaluate cell response inside split-chamber compartments [Salim Al-Ani et al., 2021]. Polyamide nylon meshes containing pulp-derived three-dimensional cell cultures were placed in the lower compartment of commercially available individual

perfusion split chambers (Minucells and Minutissue, Bad Abbach, Germany) in direct contact with the pulpal side of the prepared dentin discs and secured using a stainless-steel holder. The pulpal compartment was perfused with assay medium supplemented with 5.96 g/L hydroxyethylpiperazine ethane sulfonic acid (HEPES) at a flow rate of 0.3 mL/h for 24 h using a precision pump (Minucells and Minutissue, Bad Abbach, Germany). After 24 h, perfusion was briefly interrupted and the dentin surfaces were gently rinsed with distilled water for 30 s. Ammonia- and water-based silver fluoride (SDF and SF) treatments, with or without the application of potassium iodide (KI), were applied to the upper chamber in direct contact with the occlusal surface of the dentin discs and allowed to dry. According to ISO 7405 B.3 [ISO 7405, 2018], a light-curing glass ionomer cement, which is known to cause toxic effects, was prepared and served as the positive control (50% cell viability). A polyvinylsiloxane impression material (Express VPS, Solventum, USA) was used as the negative control (100% cell viability).

After closing the split chambers, cells were perfused at a rate of 0.2 mL/h for 24 h. Cell meshes were gently sectioned by the metallic inserts into 4 mm^2 circular pieces, retrieved from the stainless-steel holder and placed into 24-well plates containing 0.5 mL of methylthiazolium (MTT) solution. The 24-well plates were incubated for 2 h at 37 °C, 5% CO_2, and 100% humidity. Following incubation, polyamide nylon meshes were washed with phosphate buffered saline and transferred to a 48-well plate containing 0.25 mL dimethyl sulfoxide. The blue formazan precipitate was extracted from the mitochondria using 0.25 mL dimethyl sulfoxide on a shaker at room temperature for 15 min. About 200 µL of this solution were transferred to a 96-well plate. Cell viability were assessed by the MTT assay and read by a spectrophotometer (Synergy HT, BioTek Instruments, USA) at 540 nm.

MTT assay is one of the most commonly used tests to evaluate cytotoxicity precisely and quickly. It is based on a quantitative measurement of cell viability from cells metabolic activity, through the reduction of yellow tetrazolium salt (3-(4,5-dimethylthiazol-2-yl)-2,5-diphenyltetrazolium bromide), which reflects the number of viable cells and can be analyzed spectrophotometrically.

In each dentin barrier test setup, eight dentin discs with similar permeabilities and eight polyamide nylon meshes with similar cell viability were used. Each experiment consisted of eight perfusion split chambers and the dentin barrier test was repeated until 30 readings were obtained for each material tested. Positive and negative controls were included in each test setup and all components of the test setup were sterilized after each experiment. The mean absorption values of the negative and positive controls were set to represent 100% and 50% cell viability, respectively. Results were calculated as percentages based on the plotted curve generated from the negative and positive control specimens.

4.2.16 Direct cell viability assay to evaluate the cytotoxicity of dilutions (Study III)

Direct cell viability assay test was conducted according to ISO 10993-5 [ISO 10993-5, 2009]. The same cell line (SV40) was used to test the effect of dilutions of ammonia- and water-based silver fluoride (SDF and SF) treatments, with or without the addition of potassium iodide (KI). Cells were seeded into 96-well plates at a density of 1×10^4 cells per well in complete culture medium. After 24 h of incubation in a humidified atmosphere at 37 °C with 5% CO_2, the culture medium was replaced and the cells were exposed to the test dilutions (100 µL per well). Fresh medium was served as the negative control. After 24 h of exposure, the plates were examined under a light microscope to assess morphological changes. The culture medium was then removed from each well and 50 µL of 0.5 mg/mL MTT solution was added. The plates were incubated for 3 h at 37 °C in a humidified atmosphere with 5% CO_2. Subsequently, the MTT solution was removed and 100 µL of dimethyl sulfoxide (DMSO) was added to each well to dissolve the formazan crystals. The optical density was quantified using a spectrophotometer (Synergy HT, BioTek Instruments, USA) at 570 nm. Three independent experiments were performed in triplicates. The percent cell viability was calculated using the optical density of negative control specimens set to 100%.

4.2.17 Microcosm biofilm model (Study IV)

Prepared dentin beam specimens were subjected to a revised *in vitro* microcosm biofilm model [Exterkate et al., 2010; Li et al., 2014a] to promote cariogenic biofilm growth and to replicate more realistically *in vivo* conditions for caries formation. Briefly, dentin pellicle was formed on the occlusal sides of dentin beams for 2 h using sterile protein-containing human saliva. Then, a biofilm inoculum composed of saliva from human donors, McBain medium and 0.2% (v/v) sucrose supplement was prepared. The microcosm biofilm model was formed on occlusal sides of dentin beams at three incubation periods (2, 7 or 14 days) to determine the optimal length of the microcosm biofilm model for caries formation. Biofilm efficacy was assessed using colony-forming unit (CFU) counts, dentin microhardness (surface & cross-section), lactic acid production and MTT metabolic activity. Based on the result, 2-day microcosm biofilm model was selected.

4.2.17.1 Human saliva collection (Study IV)

Human saliva used in this study was collected solely for the methodological purposes from volunteers, pooled and used in an anonymized form. Human saliva was collected from 10 healthy donors with natural dentition, without active caries or

periodontal disease and no antibiotic use within the preceding 3 months [Li et al., 2014a]. Verbal informed consent was obtained from all volunteer donors and no identifiable information was recorded. Donors did not brush their teeth for 24 h and abstained from food/drink intake for at least 2 h before saliva donation. Saliva was collected in the morning under chewing stimulation with parafilm for 10 min and kept on ice. Equal amounts of saliva from each of 10 donors were then combined and mixed. The experiments were performed from the same batch of frozen saliva. Half of the saliva was filtered through sterilized gauze swabs (SteriluxEs, Hartmann, Germany) to remove any solid (food) debris, diluted in sterile glycerol (70% saliva and 30% glycerol) and 1-2 mL aliquots were stored at -80 ^{o}C to be used in the biofilm inoculum. Protein was removed from the other half of the saliva, centrifuged for 40 min at 9500 g at 4 ^{o}C to remove debris, annealed for 30 min at 60 ^{o}C, for sterilization to avoid protein denaturation and centrifuged again for 40 min at 9500 g at 4 ^{o}C. The sterile protein-containing saliva was frozen at -80 ^{o}C to be used for salivary pellicle formation.

4.2.17.2 Pellicle and biofilm formation (Study IV)

Each disinfected dentin beam was placed into a well of sterile 24-well plates, with the coronal surface facing up. In order to allow salivary pellicles to cover the coronal surface of dentin beams, 300 µL of sterile protein-containing saliva was added to each well and incubated for 2 h at 37 °C in a standard non-CO_2 incubator. Subsequently, beams were transferred to new 24-well plates and 500 µL of biofilm inoculum was added to each well and incubated for 8 h in 5% CO_2 at 37 ^{o}C. The biofilm inoculum was composed of saliva from human donors, McBain medium and 0.2% (v/v) sucrose supplement. The saliva-glycerol stock was added with 1:50 final dilution in McBain medium and 0.2% (v/v) sucrose was then added to the biofilm inoculum [Exterkate et al., 2010]. McBain medium was composed of mucin (type II, porcine, gastric) at a concentration of 2.5 g/L; bacteriological peptone, 2.0 g/L; tryptone, 2.0 g/L; yeast extract, 1.0 g/L; NaCl, 0.35 g/L, KCl, 0.2 g/L; $CaCl_2$, 0.2 g/L; cysteine hydrochloride, 0.1 g/L; haemin, 0.001 g/L; vitamin K1, 0.0002 g/L, at pH 7 [McBain et al., 2005] and used within a month of preparation. All chemicals were obtained from Merck Sigma-Aldrich (Germany), unless otherwise specified. After 8 h, beams were transferred into fresh biofilm inoculum and incubated for 16 h, completing the initial 24 h [Li et al., 2014a]. Following the initial incubation, beams were further incubated with daily biofilm inoculum changed at 24 h intervals for a total duration of 2, 7 or 14 days. The whole process allowed bacterial attachment and colonization forming cariogenic biofilm. After each incubation period, dentin beams were rinsed three times with phosphate buffered saline (PBS) to remove loosely attached bacteria. Digital images of each beam were captured

using a stereo microscope (Leica M60, Leica Microsystems, Germany) and dimensions of the beams were measured using an open-source image software (ImageJ, National Institute of Health, USA).

4.2.17.3 Microcosm biofilm viability assay (CFU-based) (Study IV)

Dentin beams subjected to microcosm biofilm model for 2, 7 or 14 days (n = 10 dentin beam/group) were analyzed for colony-forming unit (CFU) counts. Dentin beams without microcosm biofilm formation served as control (0 day). Biofilms were harvested in PBS by sonication and vortexing. Three types of agar plates were prepared and used: (*i*) tryptic soy blood plates to determine total aerobic and anaerobic microorganisms; (*ii*) mitis salivarius agar (MSA) containing 15% sucrose to determine total *streptococci*; and (*iii*) MSA plus 0.2 units of bacitracin/mL to determine *mutans streptococci*. The bacterial suspensions were serially diluted and spread onto agar plates for CFU analysis. After 72 h of incubation at 37 °C either in 5% CO_2 or under aerobic conditions, the number of colonies were counted. Results are presented as the logarithm (base 10) of CFU values ($\log_{10}$ CFU). Moreover, the presence of cariogenic *mutans streptococci* bacteria as *Streptococcus mutans* and *Streptococcus sobrinus* species were confirmed using the polymerase chain reaction (PCR) method [Oho et al., 2000].

4.2.17.4 Dentin surface microhardness (Study IV)

To evaluate the microhardness of occlusal dentin surfaces, 2 mm-thick dentin discs were prepared (n = 10 dentin disc/group). Discs were mounted into acrylic resin (DuraLay, Reliance Dental, USA) using silicon molds, leaving the occlusal dentin surfaces exposed and serially polished with 600- and 1200-grit SiC paper under water-cooling to obtain scratch-free, smooth surfaces. Initial measurements of sound (0 day) dentin were recorded. Occlusal surfaces were subjected to the *in vitro* microcosm biofilm model for 2, 7 and 14 days. Microhardness measurements were performed after each incubation period using a microhardness tester (HMV-G21, Shimadzu, Kyoto, Japan) equipped with a Vickers indenter (10 g load, 15 s dwell time). Five readings were obtained from the occlusal surface of each dentin disc and the mean value was calculated to determine Vickers hardness number (VHN) for each dentin disc. The average VHN values of ten dentin discs were used to represent each incubation period.

4.2.17.5 Dentin cross-section microhardness (Study IV)

To evaluate the microhardness of occlusal-cervical cross-sections, 2 mm-thick dentin discs were prepared (n = 10 dentin disc/group). Discs were mounted into acrylic resin (DuraLay, Reliance Dental, USA) using silicon molds, leaving the occlusal dentin surfaces exposed and serially polished with 600- and 1200-grit SiC paper under water-cooling to obtain scratch-free, smooth surfaces. Mounted-polished discs were sectioned occluso-cervically in half parallelly to their long-axis. The exposed cross-sections were also polished with 600- and 1200-grit SiC paper under water-cooling. One half originated from each disc was randomly selected for cross-sectional measurements (n = 10 dentin disc/group). Initial measurements of sound (0 day) dentin were recorded. The exposed cross-sections were then protected with two layers of nail varnish. Occlusal surfaces were subjected to the in vitro microcosm biofilm model for 2, 7 and 14 days. The nail varnish was removed from cross-sections though polishing with 1200-grit SiC paper and reapplied before each incubation period. Microhardness measurements were performed after each incubation period using a microhardness tester (HMV-G21, Shimadzu, Kyoto, Japan) equipped with a Vickers indenter (10 g load, 15 s dwell time). Indentations for cross-sections were made occluso-cervically at 10, 20, 30, 40, 50, 100, 150, 200, 250, 300, 400 and 500 μm depths. Three readings were obtained at each depth and averaged to determine VHN. The average VHN values of ten dentin specimens were used to represent each incubation period.

4.2.17.6 Lactic acid production (Study IV)

Dentin beams subjected to microcosm biofilm model for 2, 7 or 14 days (n = 6 dentin beam/group) were measured for lactic acid production. Dentin beams were transferred into 24-well plates and immersed in 1 mL buffered peptone water (BPW) supplemented with 0.2% sucrose and incubated for 3 h at 37 °C in 5% CO_2 to allow bacteria to produce acid. The relatively high buffer capacity of BPW prevented the pH from becoming significantly acidic, as low pH would hinder bacterial acid production. Lactate concentrations in the BPW solutions were determined using an enzymatic (lactate dehydrogenase) method [Bergmeyer Hans-Uirich, 1974]. Absorbance values were obtained using a spectrophotometer (Model UV-A180, Shimadzu, Japan) at 340 nm and plotted against lactic acid standard curves.

4.2.17.7 Microcosm biofilm viability (MTT assay) (Study IV)

Dentin beams subjected to microcosm biofilm model for 2, 7 or 14 days (n = 6 dentin beam/group) were evaluated by MTT colorimetric assay which reflects the metabolic activity of the biofilms. Dentin beams were transferred to a new 24-well plate and 1 mL MTT dye (Merck Sigma-Aldrich, Germany) (0.5 mg/mL MTT in PBS) was added into each well and incubated for 1 h at 37 °C in 5% CO_2. Subsequently, beams were transferred into a new 24-well plate with 0.5 mL dimethyl sulfoxide (DMSO) (Merck Sigma-Aldrich, Germany) in each well and incubated in dark at room temperature for 20 min to dissolve the formazan crystals. 200 µL DMSO solution was then transferred into 96-well plate and the absorbance at 540 nm was measured using a spectrometer (Synergy HT, BioTek Inst, USA).

4.2.18 Characterization of the fatigue behavior (Study IV)

Dentin beams were loaded to failure under quasi-static 4-point flexure (n = 15 dentin beam/group) and 4-point fatigue under cyclic loading (n = 25 dentin beam/group) using a universal testing machine (Electropuls E1000, Instron, UK) with load capacity of 250 N and sensitivity of 0.025% [Arola et al., 2010]. The specimen geometry and flexure apparatus conform to a scaled version of ASTM D6272 for flexural testing of materials [ASTM D6272, 2017] consistent with a previous study [Arola, and Reprogel, 2006]. Testing was performed with specimens fully immersed in distilled water at room temperature to maintain hydration. 2-day microcosm biofilm model formed dentin beams were treated with ammonia- and water-based silver fluoride (SDF and SF) treatments, with or without the application of potassium iodide (KI). Untreated carious dentin formed beams and sound dentin beams served as negative and positive control, respectively. After treatments, dentin beam specimens were allowed to dry for 3 min and all groups were incubated in 500 µL artificial saliva (pH 7.4) at 37 °C in a shaking water bath at 60 cycles/min for 3 days prior to testing. Then, dentin beams were placed on a 4-point flexural fixture with the occlusal surface (tension side) facing downward. Flexure loading configuration for both quasi-static and cyclic loading were determined using a metal jig with 1.0 mm loading span and 4.0 mm supporting span (**Figure 4**), in accordance with a previous study [Arola, and Reprogel, 2006].

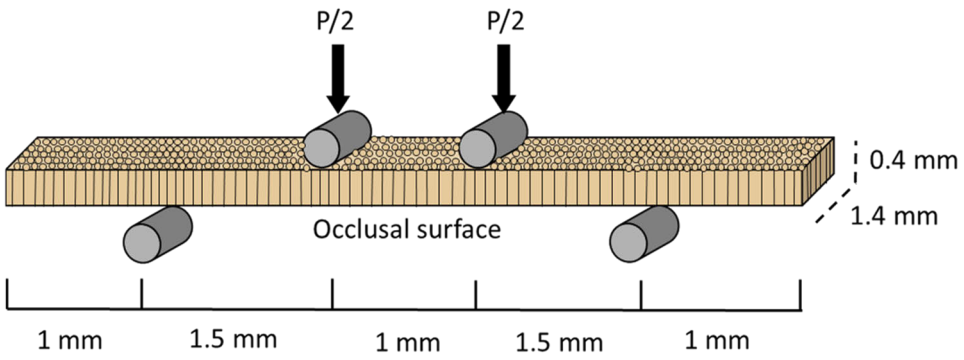

Figure 4. Schematic diagram of nominal specimen geometry and flexure loading configuration for both 4-point quasi-static and cycling loading conditions. (*Modified from the supplementary data in Study IV*)

4.2.18.1 Quasi-static 4-point flexural strength (Study IV)

Quasi-static loading was applied at a crosshead rate of 0.001 mm/s. The instantaneous load and load-line displacement were monitored at a frequency of 5 kHz through the load cycle. Flexural strength (FS) was calculated using conventional beam theory for 4-point bending in terms of the maximum measured load (P) in N, the support span (L), the loading span (*a*) and beam geometry (width b, thickness h in mm) according to $FS = 3P(L-a)/2bh^2$.

4.2.18.2 Fatigue resistance under cyclic loading (Study IV)

Cyclic loading of dentin beams was conducted using the same flexure configuration under load control with frequency of 4 Hz and stress ratio (R = ratio of minimum to maximum cyclic load) of 0.1. The cyclic loading experiments followed the staircase fatigue method beginning at approximately 90% of the determined 4-point flexural strength. Such values were identified from the quasi-static loading and followed sequential reductions in the order of 10% until failure. The process continued until reaching stress amplitudes (MPa) at which specimens did not fail within 1.0×10^6 cycles. The cyclic fatigue resistance was plotted in terms of the number of cycles to failure in log-base format. The data was fit through a non-linear regression with a Basquin-type model, according to the equation $\sigma = A(N)^B$, where A and B are the fatigue-life coefficient and fatigue-life exponent, respectively. The apparent endurance limit was estimated from the models for a fatigue limit defined at 10^7 cycles [Arola, and Reprogel, 2006].

4.2.19 Dentin surface SEM characterization (Study IV)

Tension sides of the fractured dentin beams from each experimental group were selected and evaluated by scanning electron microscopy (SEM) (n = 5 dentin beam/group) to examine the fracture surfaces. Dentin beams were ultrasonically cleaned in distilled water for 2 min, dehydrated in ascending ethanol concentrations (25%, 50%, 60%, 70%, 80%, 90%, and 100%) for 30 min at each concentration, followed by immersion in 100% ethanol for 1 h. Subsequently, specimens were transferred to a 1:1 solution of hexamethyldisilazane (HMDS) and ethanol for 1 h and then fixed in HMDS (Sigma-Aldrich, USA) [Perdigao et al., 1995]. Dentin beams were mounted on aluminum stubs and sputter coated with gold/palladium. Fractured dentin beams were analyzed on backscattering mode at 10 kV (Phenom ProX, Phenom-World, Netherlands) up to 5000× magnification. An experienced-blinded operator performed SEM examinations.

4.2.20 Statistical analyses

All results were subjected to the statistical analysis using IBM SPSS Statistics for Windows, version 28 (IBM Corporation, USA). Significance level (α) of 0.05 was used for all statistical tests. All data were subjected to the Shapiro-Wilk test to confirm the normality of data distribution and modified Levene's test to confirm the homoscedasticity.

In Study I, data regarding micro-tensile bond strength (μTBS), hybrid layer thickness and dentin permeability test methods were analyzed separately. Tooth was considered as the statistical unit for the micro-tensile bond strength data. Data on micro-tensile bond strength and dentin permeability was normally distributed and homoscedastic, therefore, micro-tensile bond strength values were subjected to three-way ANOVA followed by Tukey test and dentin permeability data were subjected to repeated measures ANOVA followed by Tukey test. Hybrid layer thickness data did not pass the normality and homoscedasticity test, therefore, data was analyzed by Kruskal-Wallis test.

In Study II, data passed normality and homoscedasticity test. Percent loss of dry mass, modulus of elasticity, total enzymatic activity, total endogenous activity, hydroxyproline quantification and total extractable protein data were analyzed using two-way repeated measures of ANOVA. *In situ* zymography data were analyzed using one-way ANOVA. Post-hoc multiple comparisons were performed with Tukey test.

In Study III, trans-dentinal cytotoxicity test data were not normally distributed, therefore, data were analyzed by the Kruskal-Wallis test followed by Dunn's test. Cell damage was further categorized as noncytotoxic, moderately cytotoxic and severely cytotoxic according to ISO 7405 criteria [ISO 7405, 2018]. Data obtained

from direct cell viability assay were normally distributed and homoscedastic, therefore, data were analyzed with one-way ANOVA followed by Tukey test.

In Study IV, normality and homoscedasticity of colony-forming unit (CFU) counts, microhardness (surface and cross-section), lactic acid production, biofilm viability and quasi-static flexure strength data were confirmed. Colony-forming unit counts, lactic acid production, biofilm viability and quasi-static flexure strength data were analyzed using one-way ANOVA followed by Tukey test. Microhardness (surface and cross-section) data were analyzed using one-way repeated measures ANOVA followed by Tukey test. Fatigue life distribution data were analyzed using Kruskal-Wallis test.

5 Results

5.1 Micro-tensile bond strength (Study I)

Micro-tensile bond strength (μTBS) data statistical analysis three-way ANOVA revealed that "surface treatment", "bonding protocol", "delayed bonding" and the interactions between "surface treatment * bonding protocol" and "bonding protocol * delayed bonding" had significant effect on micro-tensile resin-dentin bond strengths ($p < 0.0001$). Micro-tensile bond strength mean values for all groups and standard deviations are shown in **Figure 5**.

No significant differences were observed between etch-and-rinse or self-etch mode for untreated dentin control groups ($p > 0.05$). Airborne particle abrasion of untreated dentin did not significantly influence micro-tensile bond strengths regardless of the bonding mode applied ($p > 0.05$).

Under etch-and-rinse mode, neither ammonia-based silver diamine fluoride (SDF) treatment nor SDF treatment with potassium iodide (KI) application affected dentin bond strength ($p > 0.05$).

Under self-etch mode, SDF and SDF + KI treatments reduced dentin bond strength (approximately 95%) when bonding was achieved immediately after silver fluoride treatments ($p < 0.05$). However, immediate water rinsing ($p < 0.05$) or airborne particle abrasion ($p < 0.05$) of SDF- and SDF + KI-treated dentin restored micro-tensile bond strength values comparable with untreated dentin.

Delayed bonding for 7, 15 or 30 days after SDF and SDF + KI treatment resulted in bond strengths comparable to untreated dentin, with no significant differences between the delayed bonding time points ($p > 0.05$). Airborne particle abrasion performed after 7, 15 or 30 days did not significantly affect bond strength of SDF- and SDF/KI-treated dentin under self-etch mode ($p > 0.05$).

Overall, no significant differences were observed between corresponding etch-and-rinse and self-etch application modes of a universal adhesive. The only exception was, immediate self-etch mode following SDF and SDF + KI treatment, which resulted in an approximately 95% reduction in bond strength, and SDF + KI treatment followed by airborne particle abrasion at all delayed bonding time points, which resulted in a 35-40% reduction in bond strength under self-etch mode ($p < 0.05$).

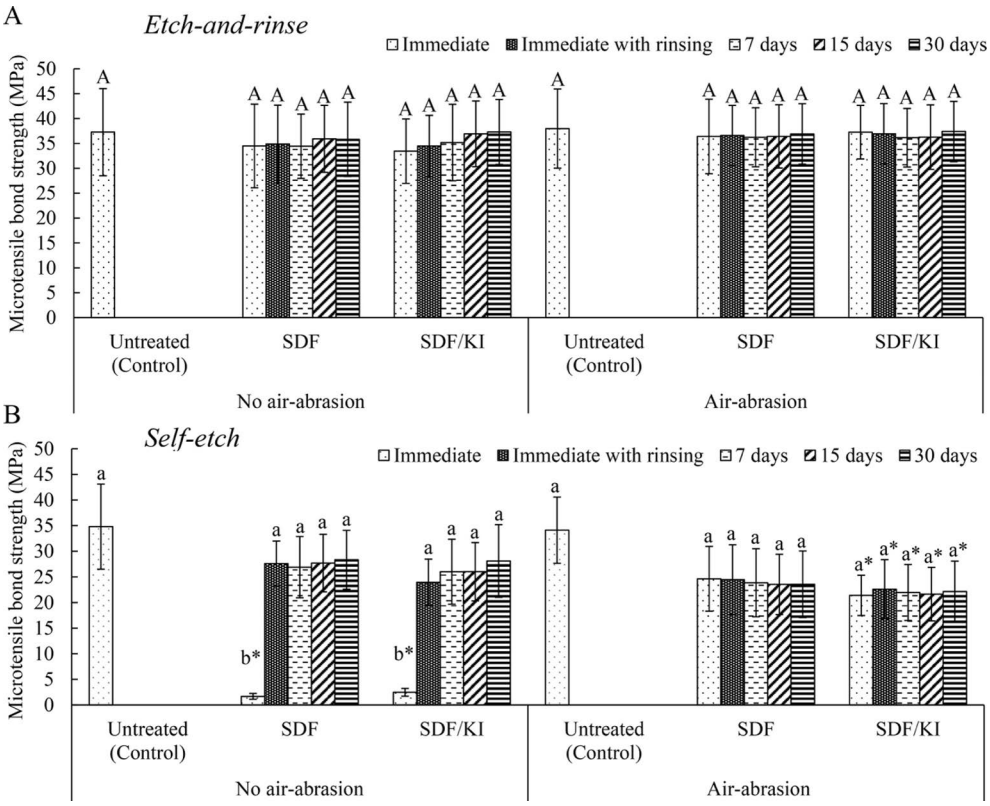

Figure 5. Micro-tensile bond strength (μTBS) means (MPa) and standard deviations of tested groups. Control groups indicate untreated dentin (with or without airborne particle abrasion) surfaces immediately bonded in either etch-and-rinse or self-etch mode. Different capital letters indicate significant differences between treatments, dentin abrasion and storage periods within etch-and-rinse groups according to Tukey test ($p < 0.05$). Different lowercase letters indicate significant differences between treatments, dentin abrasion and storage periods within self-etch groups according to Tukey test ($p < 0.05$). * indicates significant differences between application modes according to Tukey test ($p < 0.05$). *Abbreviations*: SDF = Silver Diamine Fluoride; KI = Potassium Iodide. (*From the supplementary data published in Study I*)

5.1.1 Failure mode analysis (Study I)

Failure mode distributions are shown in **Figure 6**. For all groups, the predominant mode of failure was characterized by adhesive failures (roughly 50%) followed by mixed failures (roughly 40%). Specimens bonded in self-etch mode immediately after SDF or SDF + KI treatments presented mostly pre-test failures.

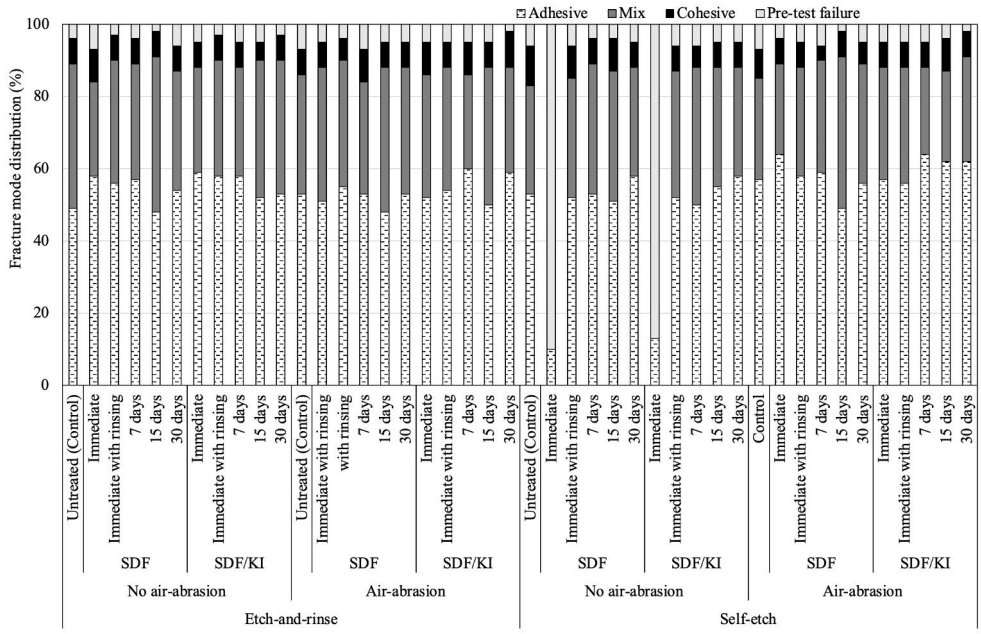

Figure 6. Failure modes of tested groups. *Abbreviations:* SDF = Silver Diamine Fluoride; KI = Potassium Iodide. (*From the supplementary data published in Study I*)

5.2 Hybrid layer SEM analysis (Study I)

Representative scanning electron microscopy (SEM) micrographs of the hybrid layer are presented in **Figure 7**. Kruskal-Wallis test demonstrated that the bonding protocol (etch-and-rinse or self-etch mode) had a significant effect on hybrid layer thickness, whereas airborne particle abrasion, SDF and SDF + KI treatments and delayed bonding time points had no significant influence on hybrid layer thickness ($p > 0.05$).

Under etch-and-rinse mode, hybrid layer thicknesses obtained with or without airborne particle abrasion were 3.54–3.35 μm for untreated dentin, 3.33–3.04 μm for SDF-treated dentin and 3.50–3.06 μm for SDF + KI-treated dentin and did not differ significantly from each other ($p > 0.05$). Etch-and-rinse bonding produced uniform and homogeneous hybrid layers with well-defined resin tags (**Figure 7 A1-A11**; **C1-C11**). Resin tags penetrated deeply into the dentinal tubules (approximately 15–30 μm) and exhibited pronounced lateral branching.

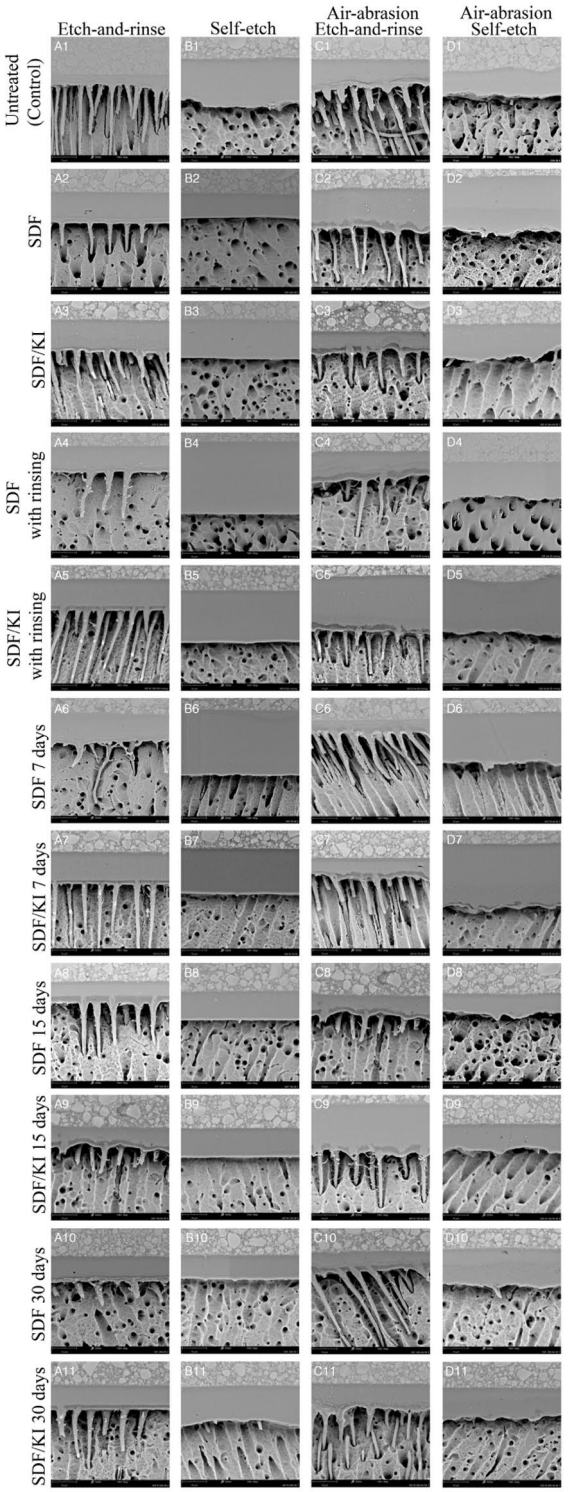

Figure 7. Representative SEM images of hybrid layer characterization. *Abbreviations*: SDF = Silver Diamine Fluoride; KI = Potassium Iodide. (Modified *from the supplementary data published in Study I*)

Under self-etch mode, significantly thinner hybrid layers ranging from 0.64 to 0.98 μm ($p < 0.05$), with shorter resin tags measuring approximately 2–10 μm (**Figure 7 B1**-**B11**; **D1**-**D11**) were achieved. Hybrid layer thicknesses obtained under self-etch mode with or without airborne particle abrasion were 0.98–0.96 μm for untreated dentin, 0.81–0.73 μm for SDF-treated dentin and 0.78–0.77 μm for SDF + KI-treated dentin and did not differ significantly from each other ($p > 0.05$). Hybrid layers produced following airborne particle abrasion appeared less homogeneous than those produced without airborne particle abrasion.

5.3 Etching pattern SEM analysis (Study I)

Representative scanning electron microscopy (SEM) micrographs of mid-coronal dentin surface morphology are presented in **Figure 8**.

Unetched specimens exhibited a dense smear layer covering the entire dentin surface (**Figure 8 A**-**C**). Self-etch mode partially dissolved the smear layer, resulting in limited tubule disobliteration (**Figure 8 J**-**M**). Airborne particle abrasion produced superficial surface irregularities and aluminum particles were observed embedded within a more porous smear layer (**Figure 8 P**).

SDF treatment and SDF with the application of potassium iodide (KI) treatment did not expose dentinal tubules or collagen fibrils (**Figure 8 B**; **K**; **Q**; **F**; **L**; **R**) and silver precipitates were observed covering most of the smear layer (**Figure 8 B**; **C**). SDF + KI treatment produced precipitates with larger dimensions that were more densely packed in localized areas (**Figure 8 C**). Airborne particle abrasion of SDF- and SDF + KI-treated specimens removed silver precipitates from the smear layer and generated irregular dentin surfaces (**Figure 8 Q**; **R**). However, self-etch mode was unable to completely remove silver precipitates from SDF- and SDF + KI-treated dentin (**Figure 8 K**; **L**).

Immediate water rinsing reduced residual silver particles on the dentin surface (**Figure 8 E**; **F**). Subsequent self-etch mode followed by rinsing further reduced silver particle content (**Figure 8 N**; **O**), revealing a small number of open dentinal tubules (**Figure 8 O**).

H_3PO_4 etching for 15 s exposed a thick layer of demineralized collagen in both untreated and SDF- and SDF + KI-treated dentin specimens (**Figure 8 G**; **H**; **I**; **S**; **T**; **U**). Smear layer free dentin surfaces with open dentinal tubules and no residual silver precipitates were observed after phosphoric acid etching (**Figure 8 G**; **H**; **I**). Airborne particle abrasion followed by phosphoric acid etching produced similar smear layer free dentin surfaces with a thick layer of exposed collagen and no detectable silver precipitates (**Figure 8 S**; **T**; **U**).

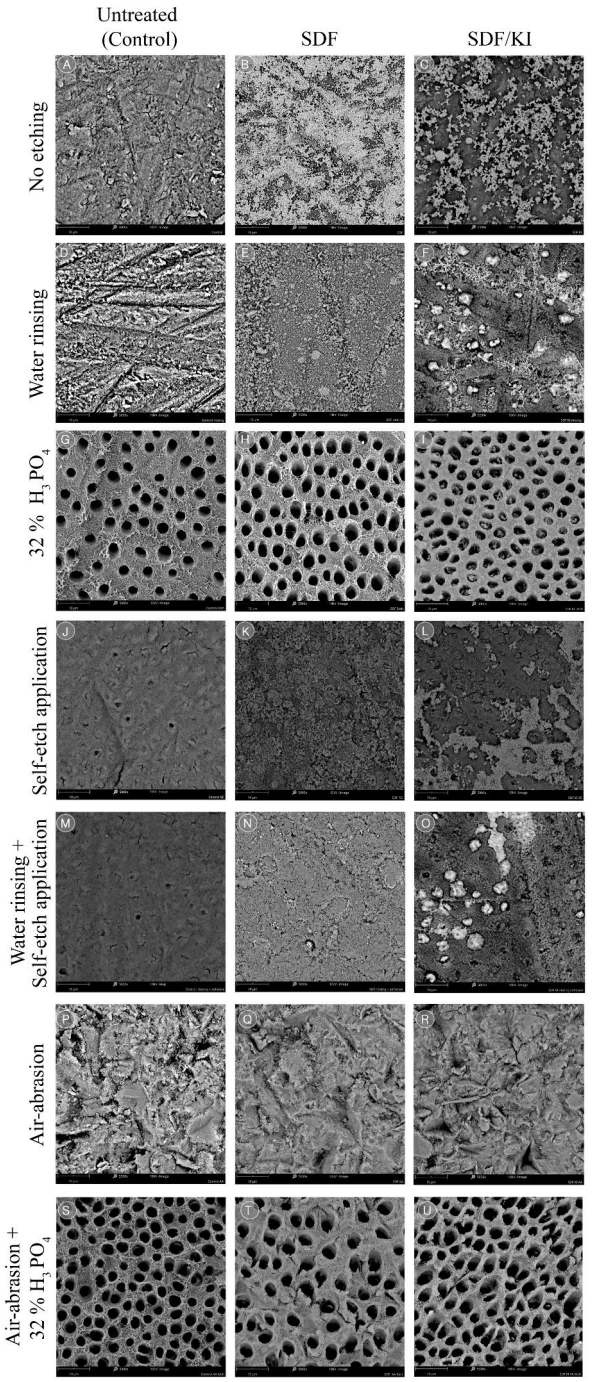

Figure 8. Representative SEM micrographs showing etching patterns of SDF-treated dentin following different bonding protocols. *Abbreviations*: SDF = Silver Diamine Fluoride; KI = Potassium Iodide.(*From the supplementary data published in Study I)*

5.4 Dentin permeability (Study I)

The mean dentin permeability values (%) and standard deviations for all experimental groups are presented in **Table 2**. Repeated-measures ANOVA revealed that delayed bonding had a significant effect on the permeability of SDF- and SDF + KI-treated dentin ($p < 0.0001$). No significant differences were detected between SDF and SDF + KI treatments at delayed bonding time points of 7, 15 or 30 days ($p > 0.05$).

Both SDF and SDF + KI treatments significantly reduced dentin permeability, resulting in an approximate 30% reduction in hydraulic conductance immediately after application ($p < 0.05$) and an approximately 20% reduction after immediate water rinsing ($p < 0.05$). Immediate and immediate with rinsing groups revealed significant differences ($p < 0.05$). Delayed bonding for 7 days did not significantly affect hydraulic conductance compared with immediate measurements without water rinsing ($p > 0.05$). However, delayed bonding for 15 and 30 days resulted in significantly lower permeability values compared with immediate measurements ($p < 0.05$).

Table 2. Dentin permeability results in percentage (%) after SDF treatments following different storage periods in artificial saliva at 37 °C.

Storage period	SDF	SDF + KI
Immediate with rinsing	80.19 ± 6.53 ^{*a}	81.66 ± 7.02 ^{*a}
Immediate	69.46 ± 8.43 ^{Aa}	70.28 ± 7.22 ^{Aa}
7 days	58.96 ± 9.62 ^{ABa}	60.28 ± 9.72 ^{ABa}
15 days	49.08 ± 10.62 ^{Ba}	54.55 ± 9.12 ^{Ba}
30 days	48.44 ± 10.41 ^{Ba}	53.25 ± 7.34 ^{Ba}

Dentin permeability was reported as percentage (Lp%) and shown as means and standard deviations (±). The Lp% value after phosphoric acid application was set as 100% (n = 12 dentin disc/group). Different capital letters indicate significant differences within columns, different lowercase letters indicate significant differences within rows and * indicate significant differences between immediate and immediate with rinsing (isolated control) according to Tukey test ($p < 0.05$). *Abbreviations:* SDF = Silver Diamine Fluoride; KI = Potassium Iodide. (*From the supplementary data published in Study I*)

5.5 Loss of dry mass (Study II)

The cumulative loss of dry mass of demineralized dentin beams across all experimental groups and incubation periods were illustrated in **Figure 9**. Untreated demineralized dentin beams served as the control group and demonstrated a significant increase in dry mass loss after 3-month incubation ($p < 0.05$).

Ammonia-based silver fluoride (SDF) treatment alone resulted in significantly lower dry mass loss at all incubation periods compared with the control group ($p < 0.05$), with no significant differences observed among the incubation time points within SDF group ($p > 0.05$).

Water-based silver fluoride (SF) treatment did not differ significantly from the control at 1-week incubation period ($p > 0.05$), however, beyond 1-week, SF-treated specimens exhibited significantly lower dry mass loss compared with the control ($p < 0.05$). No significant differences were detected among the different incubation periods within the SF group ($p > 0.05$).

In contrast, the application of potassium iodide (KI) following either SDF or SF significantly increased dry mass loss compared with their respective single-treatment groups and the control group ($p < 0.05$). The SDF + KI group exhibited a significantly higher dry mass loss (23.8 ± 4.9%) compared with the SF + KI group (11.1 ± 2.2%) ($p < 0.05$). Both groups showed a significant increase in dry mass loss from 1-week to 6-month of incubation ($p < 0.05$). The SF + KI group demonstrated dry mass loss values comparable to the control group at 3- and 6-month of incubation ($p > 0.05$).

KI application alone, resulted in the highest dry mass loss among all experimental groups ($p < 0.05$), however, no significant changes were observed across the different incubation periods within this group ($p > 0.05$).

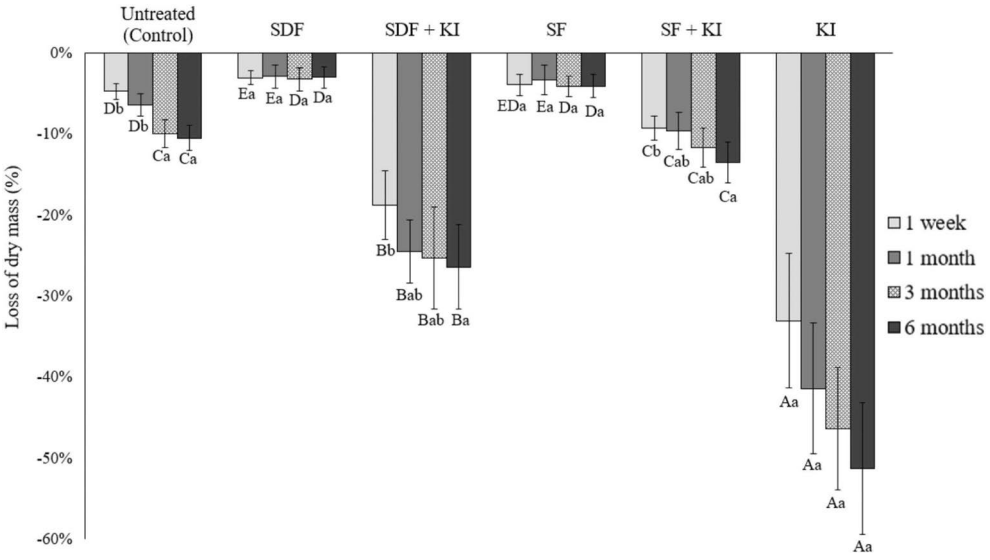

Figure 9. Cumulative loss of dry mass of demineralized dentin beams submitted to different silver fluoride treatments up to 6 months incubation. Untreated demineralized dentin beams served as control. The chart columns represent the mean values and the error bars represent standard deviations (n = 10 dentin beam/group). Different capital letters indicate significant differences between treatments within incubation periods, according to Tukey test ($p < 0.05$). Different lowercase letters indicate significant differences between incubation periods within treatment groups, according to Tukey test ($p < 0.05$). *Abbreviations*: SDF = Silver Diamine Fluoride; KI = Potassium Iodide; SF = Aqueous Silver Fluoride. (*From the supplementary data published in Study II*)

5.6 Modulus of elasticity (Study II)

The mean elastic modulus of demineralized dentin collagen at baseline for all dentin beam specimens (n = 60 dentin beams) was 7.28 ± 1.23 MPa. Changes in elastic modulus across all experimental groups and incubation periods are presented in **Figure 10**. Untreated demineralized dentin beams served as control group and did not exhibit any significant changes in elastic modulus throughout the incubation periods ($p > 0.05$).

Immediately after ammonia- and water-based silver fluoride (SDF and SF) treatments, with or without the application of potassium iodide (KI), all treatment groups except for the KI application alone group demonstrated a significant increase in elastic modulus compared with both their baseline values and the control group ($p < 0.05$). The elastic modulus values of the SDF and SF groups remained significantly higher than those of the control group throughout all incubation periods ($p < 0.05$), with no significant differences observed among the different incubation time points within each group ($p > 0.05$).

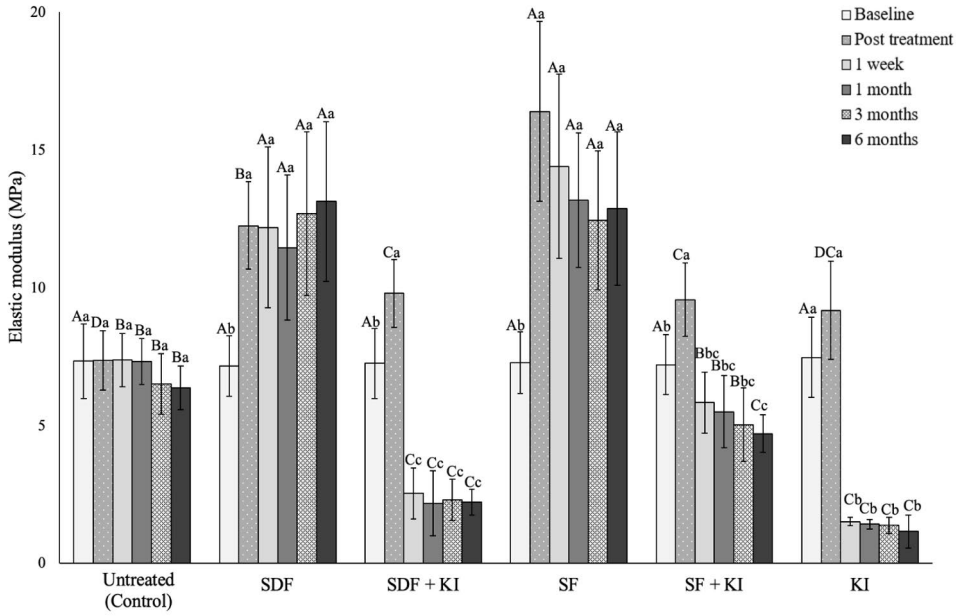

Figure 10. Elastic modulus means (MPa) and standard deviations of demineralized dentin beams submitted to different silver fluoride treatments up to 6 months incubation. Untreated demineralized dentin beams served as control. The chart columns represent the mean values and the error bars represent standard deviations (n = 10 dentin beam/group). Different capital letters indicate significant differences between treatments, within incubation periods, according to Tukey test ($p < 0.05$). Different lowercase letters indicate significant differences between incubation periods within treatment groups, according to Tukey test ($p < 0.05$). *Abbreviations*: SDF = Silver Diamine Fluoride; KI = Potassium Iodide; SF = Aqueous Silver Fluoride. (*From the supplementary data published in Study II*)

The addition of KI significantly reduced the elastic modulus after 1-week of incubation. The SDF group exhibited a 3.2-fold higher elastic modulus compared with the SDF + KI group, while the SF group demonstrated a 2.7-fold higher elastic modulus compared with the SF + KI group. The SF + KI group showed elastic modulus values comparable to the control group up to 3-month of incubation ($p > 0.05$), however, at 6-month, this group exhibited a significantly lower elastic modulus compared with the control group ($p < 0.05$).

Both the SDF + KI and KI application alone groups presented significantly lower elastic modulus values than the control group starting from the 1-week incubation period ($p < 0.05$).

5.7 Total enzymatic activity (Study II)

The results of the generic total matrix metalloproteinase (MMP) activity screening assay are presented in **Figure 11** as the percentage of total enzymatic activity inactivation. Untreated demineralized dentin beams served as the control group and exhibited no MMP inactivation. All treatment groups demonstrated a significant reduction in total MMP activity compared with the untreated control group across all incubation periods ($p < 0.05$).

Immediate after treatment and at 1-week incubation period, the ammonia-based silver fluoride (SDF) treatment, with or without the application of potassium iodide (KI) (SDF and SDF + KI) exhibited significantly greater MMP inactivation than the water-based silver fluoride (SF) treatment, with or without the application of KI (SF and SF + KI) ($p < 0.05$). Treatment with KI alone resulted in the lowest MMP inactivation values at all incubation periods ($p < 0.05$). At the 1-month incubation period, the SF group showed significantly lower MMP inactivation compared with the SF + KI, SDF and SDF + KI groups ($p < 0.05$), no statistically significant differences were observed among the latter three groups ($p > 0.05$). After 3-month of incubation, all treatment groups, with the exception of the KI application alone group, exhibited substantial MMP inactivation of approximately 95 ± 5% ($p < 0.05$).

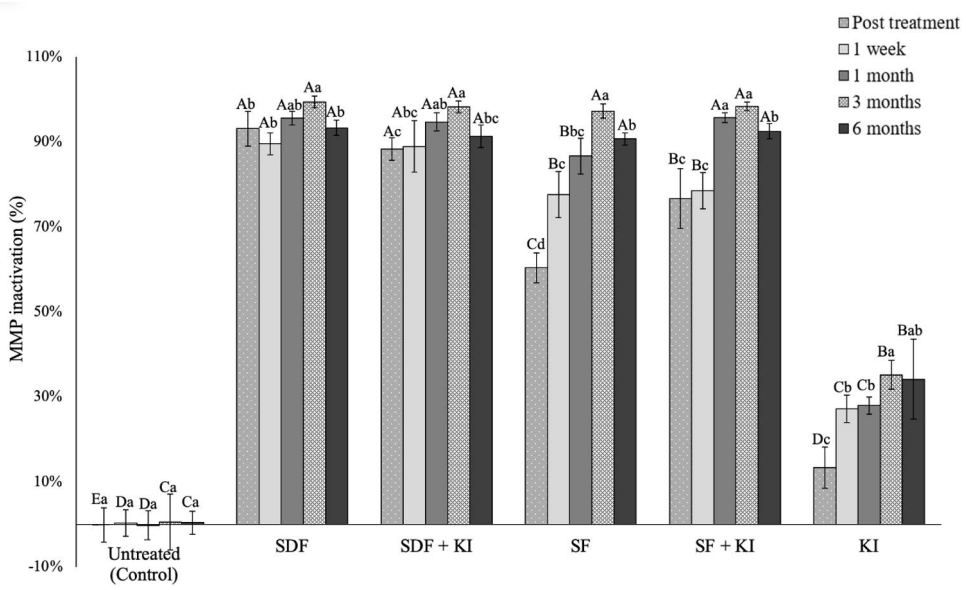

Figure 11. Total enzymatic activity of dentin MMPs shown as the mean values of percentage inactivation of MMPs of all treatment groups up to 6 months of incubation. Untreated demineralized dentin beams served as control, 0% MMP inactivation. The chart columns represent the mean values and the error bars represent standard deviations (n = 10 dentin beam/group). Different capital letters indicate significant differences between treatments within incubation periods, according to Tukey test ($p < 0.05$). Different lowercase letters indicate significant differences between incubation periods within treatment groups, according to Tukey test ($p < 0.05$). *Abbreviations*: SDF = Silver Diamine Fluoride; KI = Potassium Iodide; SF = Aqueous Silver Fluoride. (*From the supplementary data published in Study II*)

5.8 Solubilized telopeptides of collagen (Study II)

The release of the telopeptide ICTP mediated by endogenous matrix metalloproteinases (MMPs) from demineralized dentin beams is summarized in **Figure 12**. Untreated demineralized dentin beams served as the control group and exhibited the lowest MMP-mediated ICTP release, with no statistically significant difference compared with the potassium iodide (KI) application alone treatment group ($p > 0.05$).

In ammonia- and water-based silver fluoride (SDF and SF) treatment groups, ICTP release decreased significantly over time ($p < 0.05$). In contrast, MMP-mediated ICTP release progressively increased in the SDF + KI and SF + KI groups over the incubation periods ($p < 0.05$). Up to the 1-month incubation period, the SDF and SF groups demonstrated significantly higher MMP-mediated ICTP release compared with the control group ($p < 0.05$). However, at 3- and 6-month incubation periods, the groups receiving combined KI treatment (SDF + KI and SF + KI) exhibited significantly higher MMP-mediated ICTP release compared with all other groups ($p < 0.05$).

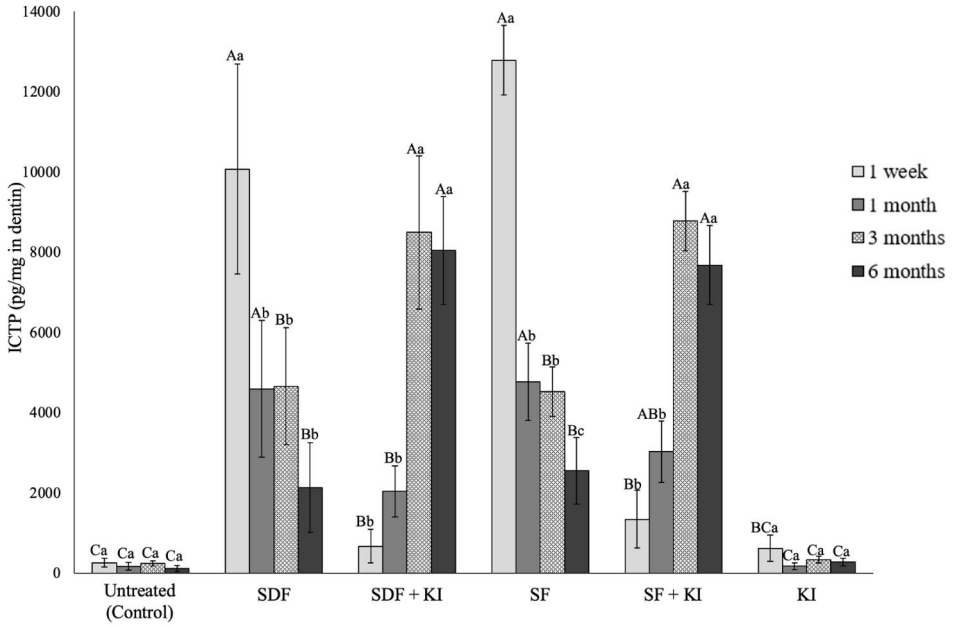

Figure 12. The rate of release of ICTP fragment from demineralized dentin beams submitted to different silver fluoride treatments. Untreated demineralized dentin beams served as control. Aliquots of calcium- and zinc- containing media were analyzed after each incubation period. Values are pg telopeptide/mg dry dentin per unit time. The chart columns represent the mean values and the error bars represent standard deviations (n = 10 dentin beam/group). Different capital letters indicate significant differences between treatments, within incubation periods, according to Tukey test ($p < 0.05$). Different lowercase letters indicate significant differences between incubation periods within treatment groups, according to Tukey test ($p < 0.05$). *Abbreviations*: SDF = Silver Diamine Fluoride; KI = Potassium Iodide; SF = Aqueous Silver Fluoride. (*From the supplementary data published in Study II*)

The release of the telopeptide CTX mediated by cathepsin K activity from demineralized dentin beams is summarized in **Figure 13**. Untreated demineralized dentin beams served as the control group. All treatment groups exhibited significantly higher CTX release compared with the control group at all incubation periods ($p < 0.05$). Although a gradual decrease in CTX release over time was observed in all treatment groups, the untreated control group still demonstrated a cumulative CTX release that was 2.7-fold lower than that of the SDF group, which showed the second lowest cumulative CTX release among the treatment groups ($p < 0.05$). After 1-week of incubation, cathepsin K-mediated CTX release was significantly higher in the SDF + KI, SF + KI, and KI application alone groups ($p < 0.05$). At the 1-month incubation period, CTX release remained significantly elevated in the SDF + KI and KI-alone groups ($p < 0.05$), whereas the SF + KI group exhibited CTX release values comparable to those of the SF group ($p > 0.05$).

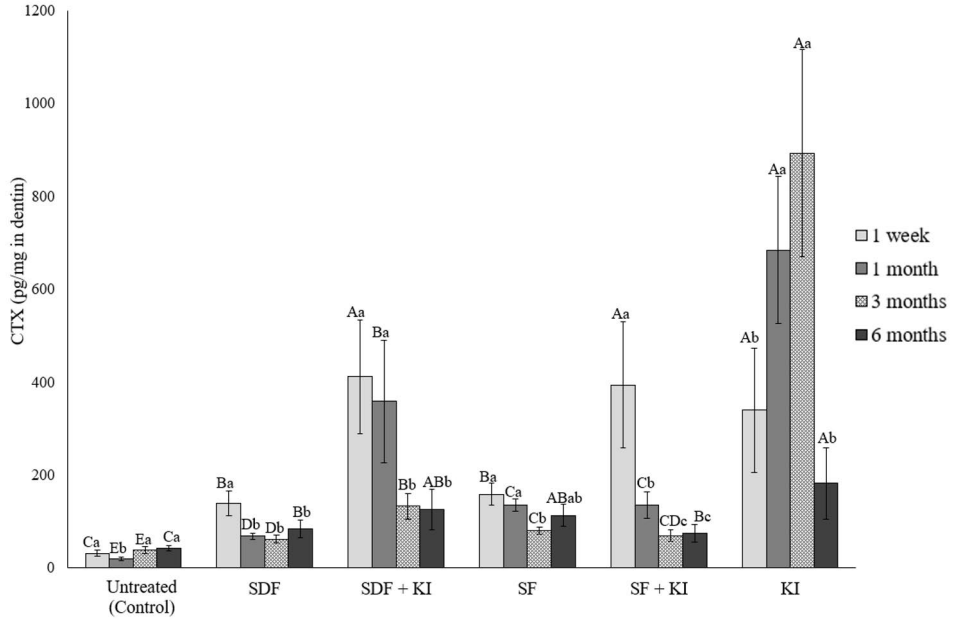

Figure 13. The rate of release of CTX fragment from demineralized dentin beams submitted to different silver fluoride treatments. Untreated demineralized dentin beams served as control. Aliquots of calcium- and zinc- containing media were analyzed after each incubation period. Values are pg telopeptide/mg dry dentin per unit time. The chart columns represent the mean values and the error bars represent standard deviations (n = 10 dentin beam/group). Different capital letters indicate significant differences between treatments, within incubation periods, according to Tukey test ($p < 0.05$). Different lowercase letters indicate significant differences between incubation periods within treatment groups, according to Tukey test ($p < 0.05$). *Abbreviations*: SDF = Silver Diamine Fluoride; KI = Potassium Iodide; SF = Aqueous Silver Fluoride. (*From the supplementary data published in Study II*)

5.9 Hydroxyproline quantification (Study II)

Hydroxyproline (HYP) release from demineralized dentin beams across all experimental groups and incubation periods is presented in **Figure 14**. Untreated demineralized dentin beams served as the control group.

Analysis of HYP, as an indicator of total collagen degradation, demonstrated that both ammonia- and water-based silver fluoride (SDF and SF) treatments, with the application of potassium iodide (KI) and KI application alone groups exhibited a 10-20-fold increase in collagen degradation at the 1-week incubation period compared with the untreated control group ($p < 0.05$). In contrast, the ammonia- and water-based silver fluoride (SDF and SF) treatments, without the application of KI showed an approximately 2-fold increase in collagen degradation at 1-week incubation, compared with the control group ($p < 0.05$). After 1 month of incubation, the SDF, SF, and KI-alone groups did not significantly differ from the control group with

respect to collagen degradation ($p > 0.05$). In comparison, the SDF + KI and SF + KI groups consistently demonstrated significantly higher collagen degradation than the SDF, SF and untreated control groups across all incubation periods ($p < 0.05$). Furthermore, at 1- and 3-month incubation periods, the SF + KI group exhibited significantly greater total collagen degradation than the SDF + KI group ($p < 0.05$).

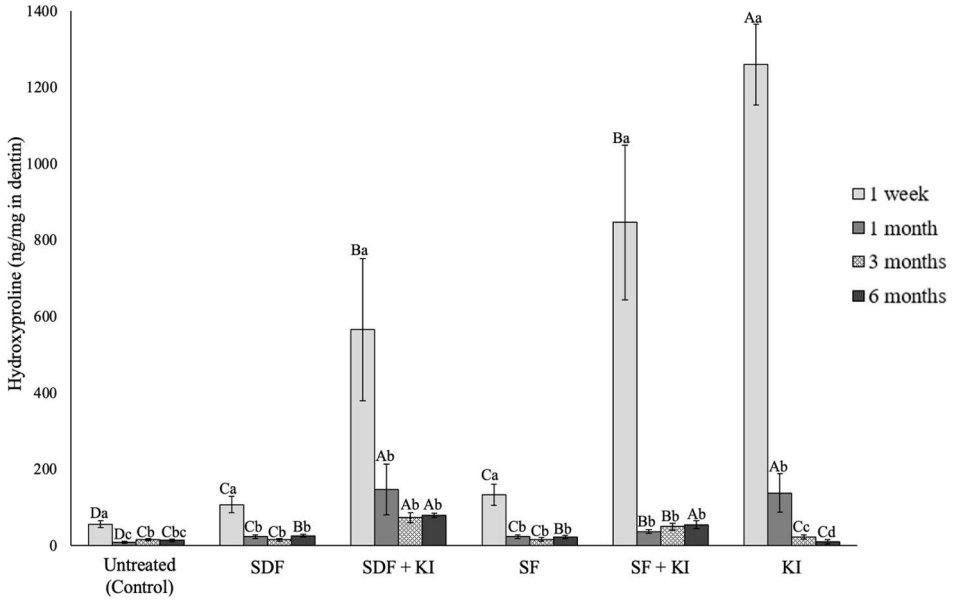

Figure 14. Hydroxyproline (HYP) levels of demineralized dentin beams submitted to different silver fluoride treatments. Untreated demineralized dentin beams served as control. Aliquots of calcium- and zinc- containing media were analyzed after each incubation period. Values are ng HYP/mg dry dentin per unit time. The chart columns represent the mean values and the error bars represent standard deviations (n = 10 dentin beam/group). Different capital letters indicate significant differences between treatments, within incubation periods, according to Tukey test ($p < 0.05$). Different lowercase letters indicate significant differences between incubation periods within treatment groups, according to Tukey test ($p < 0.05$). *Abbreviations*: SDF = Silver Diamine Fluoride; KI = Potassium Iodide; SF = Aqueous Silver Fluoride. (*From the supplementary data published in Study II*)

5.10 Total extractable protein (Study II)

Total extractable protein levels from demineralized dentin beams across all experimental groups and incubation periods are presented in **Figure 15**. Untreated demineralized dentin beams served as the control group. At the 1-week incubation period, all groups receiving potassium iodide (KI) application exhibited significantly higher extractable protein levels compared with the ammonia- and water-based silver fluoride (SDF and SF) treatment groups and untreated control groups ($p < 0.05$).

There were no significant differences in extractable protein levels between the SDF group and the untreated control group ($p > 0.05$) and between the SF group and the untreated control group. All three groups exhibiting protein levels ranging between 2400 and 3000 ng protein per mg of dry dentin ($p > 0.05$). However, a significant difference was detected between the SDF and SF groups, the SF group demonstrating higher protein levels than the SDF group ($p < 0.05$).

Across all experimental groups, protein loss decreased from 1-week to 1-month of incubation and subsequently increased from 3- to 6- month of incubation ($p < 0.05$). After 1-month incubation period, SDF, SDF + KI, SF and SF + KI groups resulted in lower protein loss compared with the untreated control group ($p < 0.05$). In contrast, the KI-alone group consistently exhibited significantly higher protein loss than the corresponding control groups at all incubation periods ($p < 0.05$).

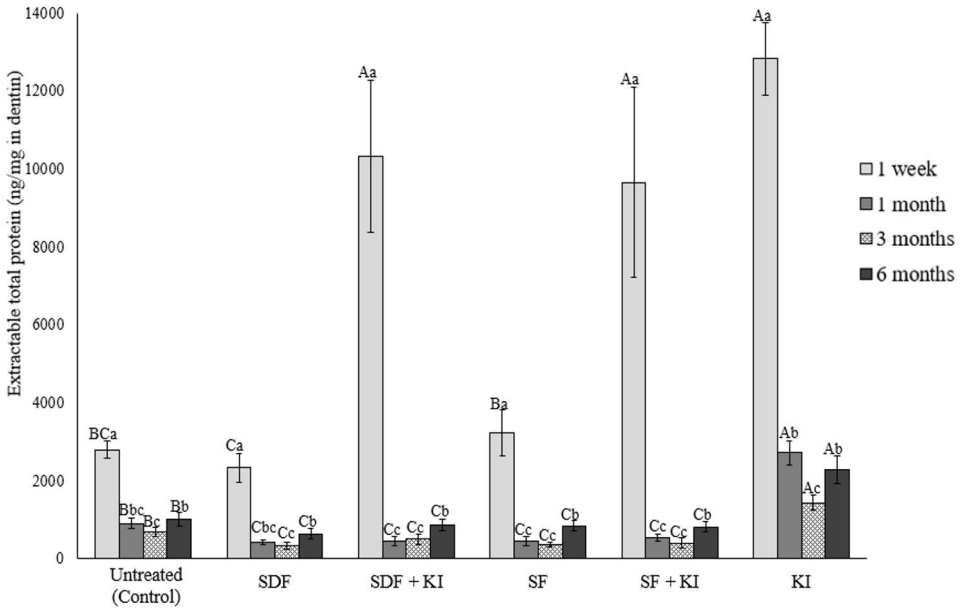

Figure 15. Extractable protein levels from demineralized dentin beams submitted to different silver fluoride treatments. Untreated demineralized dentin beams served as control. Aliquots of calcium- and zinc- containing media were analyzed after each incubation period. Values are ng total protein/mg dry dentin per unit time. The chart columns represent the mean values and the error bars represent standard deviations (n = 10/group). Different capital letters indicate significant differences between treatments, within incubation periods, according to Tukey test ($p < 0.05$). Different lowercase letters indicate significant differences between incubation periods within treatment groups, according to Tukey test ($p < 0.05$). *Abbreviations*: SDF = Silver Diamine Fluoride; KI = Potassium Iodide; SF = Aqueous Silver Fluoride. (*From the supplementary data published in Study II*)

5.11 Dentin surface and cross-section SEM analysis (Study II)

Representative scanning electron microscopy (SEM) micrographs of demineralized dentin surfaces following ammonia- and water-based silver fluoride (SDF and SF) treatments, with or without the application of potassium iodide (KI), illustrating both surface and cross-sectional views, are presented in **Figure 16**.

Phosphoric acid (H_3PO_4) etching revealed a thick layer of demineralized collagen in both untreated (control) and treated specimens (SDF, SDF + KI, SF and SF + KI) (**Figure 16**). Untreated demineralized dentin beams exhibited complete removal of the smear layer, resulting in clear tubule disobliteration without any detectable precipitates (**Figure 16 A**; **B**).

Silver precipitates were observed covering most of the dentin surface and within the dentinal tubules following both ammonia-based (SDF and SDF + KI) and water-based (SF and SF + KI) silver fluoride treatments (**Figure 16 C**; **D**; **E**; **F**; **G**; **H**; **I**; **J**). Dentin beams treated with KI demonstrated precipitates that were more densely packed and extended deeper into the dentinal tubules (**Figure 16 E**; **F**; **I**; **J**), indicating a more pronounced deposition pattern compared with treatments without KI.

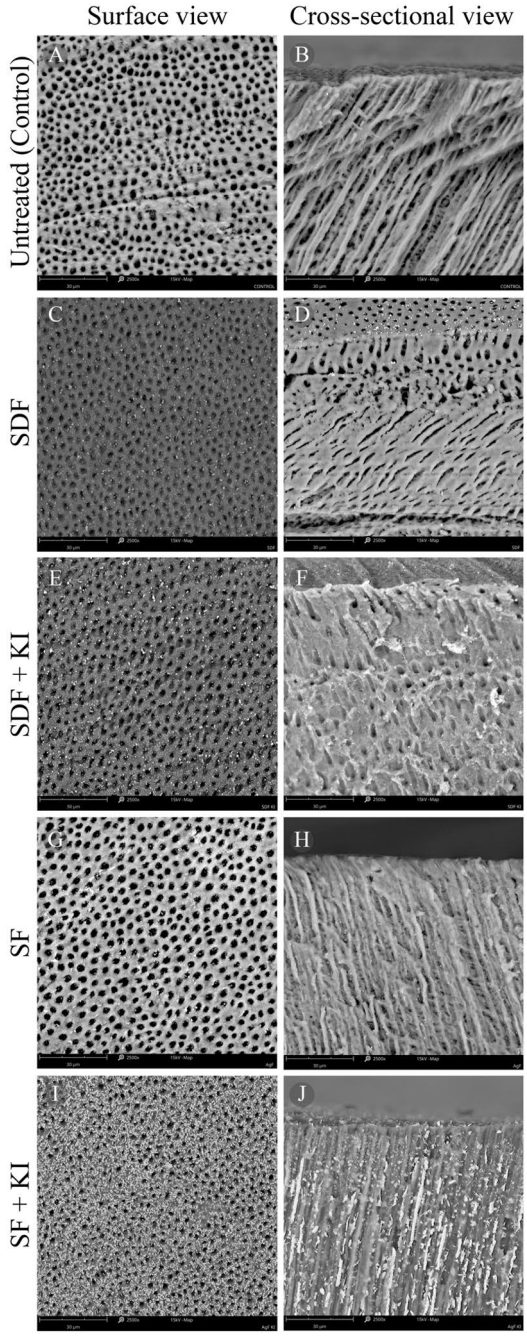

Figure 16. Representative SEM micrographs showing the surface and cross-sectional views of ammonia- (SDF and SDF + KI) and water- (SF and SF + KI) based silver fluoride treatments. *Abbreviations*: SDF = Silver Diamine Fluoride; KI = Potassium Iodide; SF = Aqueous Silver Fluoride. (*From the supplementary data published in Study II*)

5.12 Gelatinase activity by *in situ* zymography (Study II)

Representative confocal laser scanning microscopy images and the mean gelatinolytic activity values, expressed as the intensity of green fluorescence within the hybrid layer (HL), are presented in **Figure 17**. The 5 s H_3PO_4 etched untreated group served as the control.

In all experimental groups, green fluorescence was detected within the hybrid layer as well as in the underlying dentinal tubules. *In situ* zymography analysis revealed a significant reduction in gelatinase activity in both ammonia- and water-based silver fluoride (SDF and SF) treatment groups, without the application of potassium iodide (KI) compared with the untreated control group ($p < 0.05$).

In contrast, KI treatment when applied after SDF and SF resulted in a significant increase in gelatinolytic activity ($p < 0.05$). Among the treatment groups, the SF + KI group exhibited the highest gelatinolytic activity ($p < 0.05$).

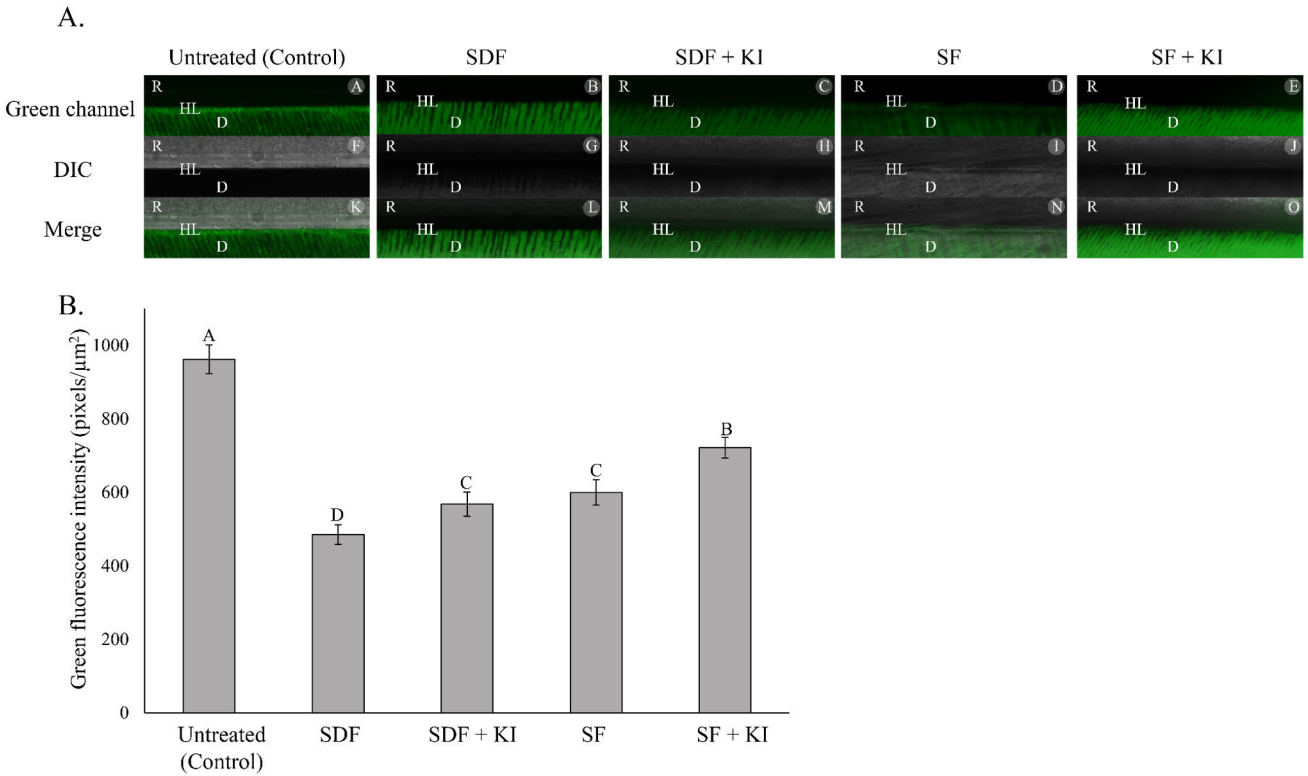

Figure 17. A. Representative *in situ* zymography images acquired at green channel (A;B;C;D;E), differential interference contrast (DIC) (F;G;H;I;J) and merged channels (K;L;M;N;O) of ammonia- (SDF and SDF + KI) and water- (SF and SF + KI) based silver fluoride treatments. B. Gelatinolytic activity expressed as intensity of green fluorescence (pixels/µm^2) within the hybrid layer. Chart columns represent the mean values and the error bars represent standard deviations of gelatinolytic activity. The untreated group served as control. Different capital letters indicate significant differences between treatments according to Tukey test ($p < 0.05$). *Abbreviations*: SDF = Silver Diamine Fluoride; KI = Potassium Iodide; SF = Aqueous Silver Fluoride; R = Resin composite; HL = Hybrid layer; D = Dentin. (*From the supplementary data published in Study II*)

5.13 Dentin barrier cytotoxicity test cell viability (Study III)

The percentage cell viability values, together with the median, mean, and standard deviation of ammonia and water-based silver fluoride (SDF and SF) treatments, with or without the application of potassium iodide (KI), after 24 h of exposure, are presented in **Figure 18**. According to Kruskal-Wallis test, dentin barrier cytotoxicity test, also referred as trans-dentinal cytotoxicity test, demonstrated that ammonia- and water-based silver fluoride treatments significantly affected cell viability ($p < 0.001$).

All treatment groups exhibited significantly lower cell viability compared with the negative control (polyvinylsiloxane impression material) (100% cell viability) ($p < 0.05$). Among the treatment groups, the water-based silver fluoride treatment (SF), without the application of potassium iodide (KI), showed the highest cell viability (79%) ($p < 0.05$). No significant differences were observed between the positive control (light-curing glass ionomer cement), SDF and SF + KI groups that exhibited approximately 50% cell viability ($p > 0.05$).

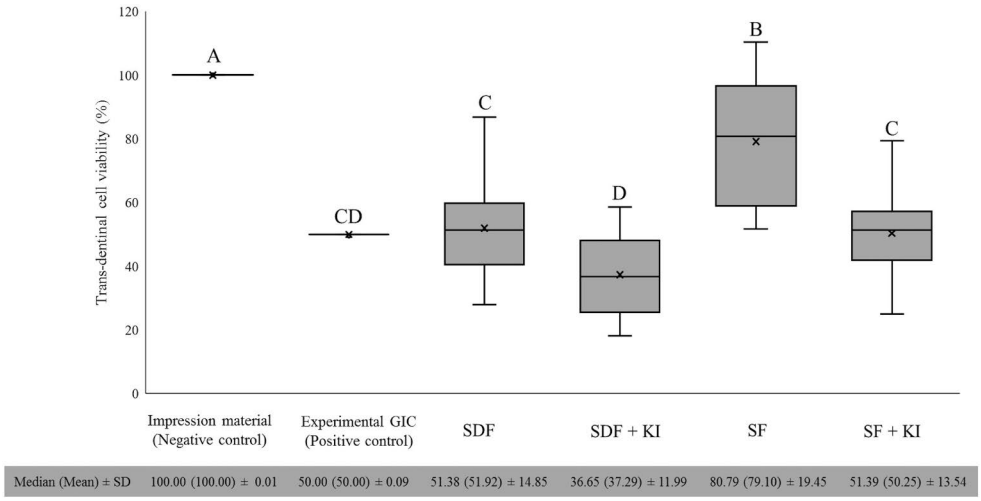

Figure 18. Box-plot diagram representing the percentage trans-dentinal cell viability (%) of SV40 pulp-derived cells exposed to ammonia- and water-based silver fluoride treatments ($n = 30$ cell viability value/group). The horizontal line inside each box represents the group median, while the "x" inside each box represents the group mean. Different upper-case letters indicate statistically significant differences between the groups according to Dunn`s test ($p < 0.05$). The median, mean and standard deviation of all groups are given below the figure. *Abbreviations*: GIC = glass ionomer cement; SDF = Silver Diamine Fluoride; KI = Potassium Iodide; SF = Aqueous Silver Fluoride; SD = Standard deviation (*From the supplementary data published in Study III*)

The addition of KI as a second step significantly reduced cell viability compared with the respective ammonia- and water-based silver fluoride treatments alone ($p < 0.05$). Specifically, SDF + KI resulted in lower cell viability (37%) compared with SDF alone (52%), and SF + KI showed lower viability (50%) compared with SF alone (79%) ($p < 0.05$). Among the treatment groups, SDF + KI group demonstrated the lowest cell viability (37%) ($p < 0.05$).

5.14 Dentin barrier cytotoxicity test assessment of cell damage (Study III)

Grading of cell damage as non-cytotoxic, moderately cytotoxic and severely cytotoxic according to ISO 7405 [ISO 7405, 2018] is presented in **Table 3** and pairwise comparisons are illustrated in **Figure 18**. Statistically significant differences were observed between the negative control (polyvinylsiloxane impression material) and the positive control (light-curing glass ionomer cement) groups ($p < 0.001$). According to the ISO-based cytotoxicity grading criteria [ISO 7405, 2018], the water-based silver fluoride treatment (SF), without the application of potassium iodide (KI) was classified as moderately cytotoxic and showed statistically significant differences compared with both the negative and positive control groups ($p < 0.05$). All other treatment groups, including SDF, SDF + KI, and SF + KI, were classified as severely cytotoxic. Those groups showed significantly lower cell viability than the negative control group ($p < 0.05$) and no significant differences compared with the positive control group ($p > 0.05$).

Table 3. Assessment of cell damage (SV40 pulp-derived cells) according to ISO 7405 after ammonia- and water-based silver fluoride treatments.

Material	Cell damage
Ammonia-based silver fluoride	
SDF	Severely cytotoxic
SDF + KI	Severely cytotoxic
Water-based silver fluoride	
SF	Moderately cytotoxic
SF + KI	Severely cytotoxic

Abbreviations: SDF = Silver Diamine Fluoride; KI = Potassium Iodide; SF = Aqueous Silver Fluoride. (*From supplementary data published in Study III*)

5.15 pH assessment of dilutions used for direct cell viability assay (Study III)

The mean pH values of ammonia and water-based silver fluoride (SDF and SF) solutions, with or without the addition of potassium iodide (KI) are presented in **Table 4**. Ammonia-based silver fluoride (SDF) solution, with or without the addition of KI, exhibited alkaline pH values up to 10^{-5} dilutions. Water-based silver fluoride (SF) solution, with or without the addition of KI, demonstrated neutral pH values at all measured dilutions. At the 10^{-5} dilution, similar neutral pH values were obtained for both ammonia- and water-based silver fluoride solutions. The additional application of KI did not influence the pH values.

Table 4. pH values mean and standard deviation (±) of the diluted ammonia- and water-based silver fluoride treatments.

Material \ Dilutions	10^{-2}	10^{-3}	10^{-4}	10^{-5}
Ammonia-based silver fluoride				
SDF	9.47 (±0.06)	8.30 (±0.07)	8.05 (±0.06)	7.87 (±0.04)
SDF + KI	9.46 (±0.05)	8.30 (±0.05)	8.03 (±0.06)	7.85 (±0.05)
Water-based silver fluoride				
SF	7.73 (±0.05)	7.78 (±0.08)	7.71 (±0.07)	7.70 (±0.07)
SF + KI	7.79 (±0.07)	7.73 (±0.05)	7.70 (±0.06)	7.69 (±0.05)

Abbreviations: SDF = Silver diamine fluoride; KI = Potassium iodide; SF = Aqueous silver fluoride. (*From supplementary data published in Study III*)

5.16 Direct cell viability assay cytotoxicity of dilutions (Study III)

Ammonia and water-based silver fluoride (SDF and SF) treatments, with or without the application of potassium iodide (KI) significantly affected cell viability according to one-way ANOVA ($p < 0.001$). The percentage of viable cells obtained from the direct cell viability assay are presented in **Figure 19**. According to ISO 10993-5 [ISO 10993-5, 2009], materials exhibiting cell viability values of 70% or higher are classified as non-cytotoxic. 70% cell viability was indicated by the dotted reference line in **Figure 19**.

At 10^{-3} dilutions, all silver fluoride treatment groups exhibited cytotoxic effects, with cell viability values around approximately 30%. The values were significantly lower than negative control (plain culture medium) ($p < 0.05$).

At 10^{-4} dilutions, cells exposed to SDF and SF demonstrated cell viability values of 70% or higher, which meant non-cytotoxicity according to ISO. SF group

exhibited significantly higher cell viability compared with SDF group ($p < 0.05$). Treatment groups including KI application showed cell viability values of approximately 40%, indicating cytotoxic effects.

At 10^{-5} dilutions, all treatment groups were classified as non-cytotoxic, by exceeding the 70% viability threshold. No statistically significant differences were observed between the SF group and the negative control ($p > 0.05$).

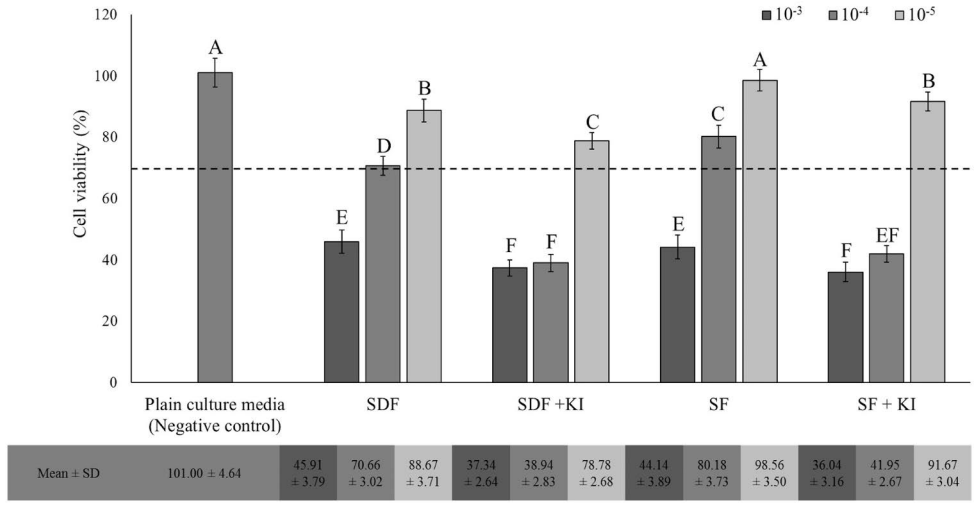

Figure 19. Cell viability (%) of SV40 pulp-derived cells exposed to prepared dilutions (10^{-3}, 10^{-4}, and 10^{-5}) of ammonia- and water-based silver fluoride treatments. Fresh culture media served as negative control and set to 100% cell viability. The dashed line represents ISO 10993 cut-off level (70%), bars below the dashed line represent cytotoxicity and bars above the dashed line represent no cytotoxicity. Different upper-case letters indicate significant differences between the groups according to Tukey test ($p < 0.05$). *Abbreviations*: SDF = Silver Diamine Fluoride; KI = Potassium Iodide; SF = Aqueous Silver Fluoride. (*From the supplementary data published in Study III*)

5.17 Microcosm biofilm viability assay (CFU-based) (Study IV)

Colony-forming unit (CFU) counts of the microcosm biofilm model formed on dentin beams after 2, 7 or 14 days are summarized in **Figure 20 A**. Sound dentin beams expressed as 0-day microcosm biofilm model revealed the lowest CFU counts for all types of microorganisms ($p < 0.05$). Total aerobic microorganisms, total anaerobic microorganisms and total *streptococci* showed similar CFU counts across 2-, 7- or 14-day incubation periods ($p > 0.05$). However, total *mutans streptococci* CFU counts decreased significantly from 2- to14-day incubation periods ($p < 0.05$). No significant differences were observed between 2 and 7 days, or between 7 and 14 days for total *mutans streptococci* CFU counts ($p > 0.05$).

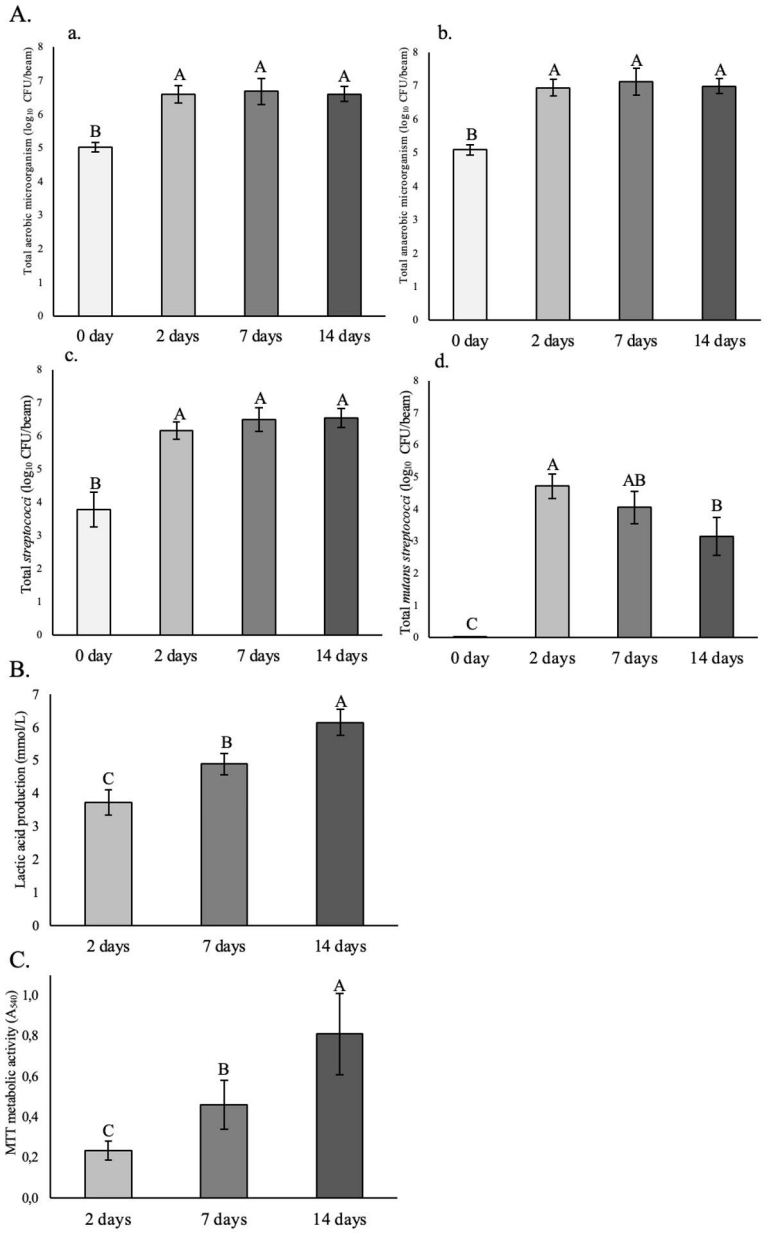

Figure 20. (A) Colony-forming unit (CFU) counts of microcosm biofilm model formed for 2, 7 or 14 days. Sound dentin beams without the microcosm biofilm model served as control group and presented as 0-day. Four types of agar plates were tested: (a) total aerobic microorganism; (b) total anaerobic microorganism; (c) total *streptococci*¸ (d) total *mutans streptococci*. (B) Lactic acid production of microcosm biofilm model formed for 2, 7 or 14 days. (C) MTT metabolic activity of microcosm biofilm model formed for 2, 7 or 14 days. Different upper-case letters indicate significant differences between the groups according to Tukey test ($p < 0.05$). (*From the supplementary data of Study IV*)

5.18 Dentin surface microhardness (Study IV)

Occlusal surface microhardness measurements of sound dentin (0-day) and after the 2-, 7- or 14-day incubation periods of microcosm biofilm formation are presented in **Figure 21 A**. Occlusal surface microhardness significantly decreased with longer incubation periods of the microcosm biofilm model ($p < 0.05$). Sound dentin expressed as 0 day exhibited the highest surface microhardness (66.73 VHN ± 2.62), followed by 2 days (16.96 VHN ± 2.69), 7 days (5.55 VHN ± 2.35) and 14 days (1.72 VHN ± 1.05) microcosm biofilm model ($p < 0.05$).

5.19 Dentin cross-section microhardness (Study IV)

Cross-sectional microhardness measurements of sound dentin (0-day) and after the 2-, 7- or 14-day incubation periods of microcosm biofilm formation are presented in **Figure 21 B**. For the 0 day, sound dentin cross-sectional microhardness measurements, no significant differences were observed among the different depths ($p > 0.05$), indicating that sound dentin maintained consistent hardness values throughout the 500-µm depth ($p > 0.05$). Sound dentin presented significantly higher hardness values than carious dentin at depths up to 250 µm. For both 2-day and 7-day incubation periods of microcosm biofilm model, microhardness values did not differ significantly between 10 and 20 µm depths ($p > 0.05$). At 14 days microcosm biofilm model, demineralization was severe enough to prevent hardness measurements at 10 µm depth, which was therefore recorded as zero. Microhardness values increased with greater depth for 2-, 7- and 14-day incubation periods. Based on 0 day, sound dentin measurements, the 2 days microcosm biofilm model exhibited a caries lesion depth of approximately 250–300 µm, the 7 days around 400 µm and the 14 days greater than 500 µm.

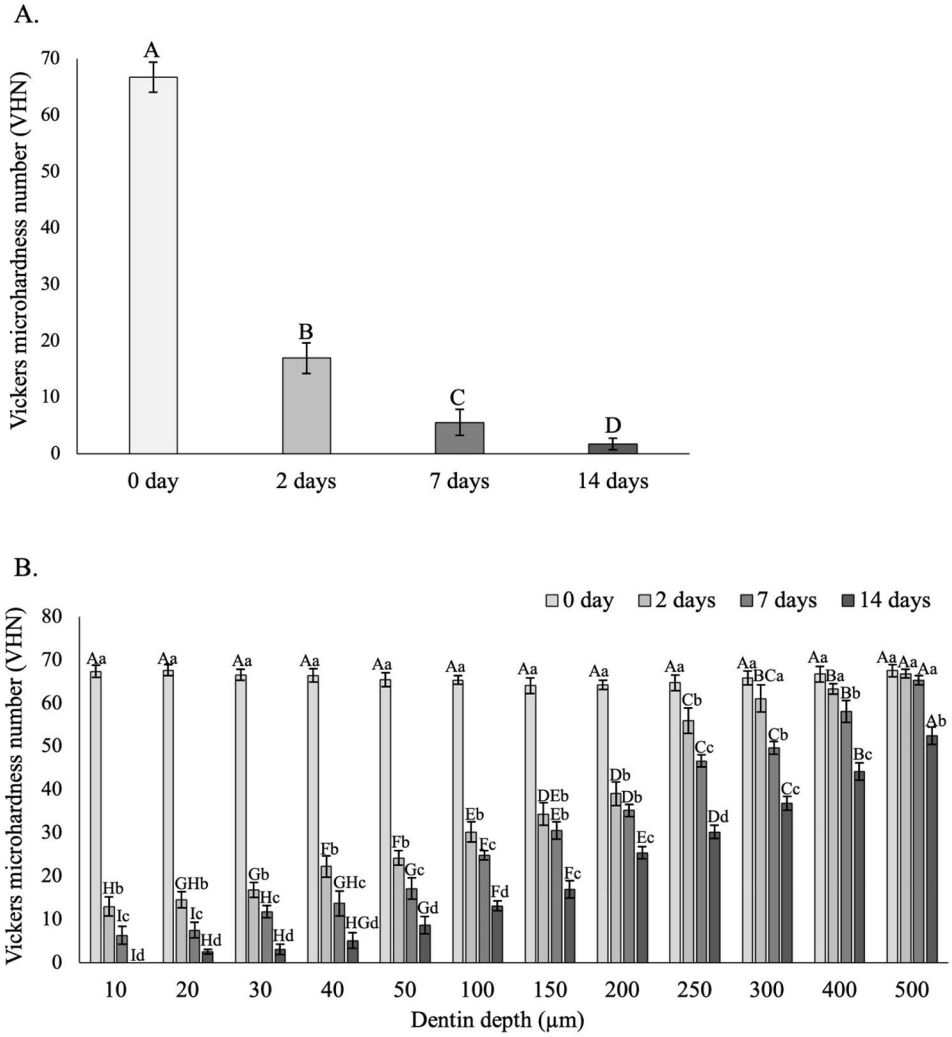

Figure 21. Dentin microhardness measurements on the (A) occlusal and (B) cross-section of dentin beams after 2, 7 or 14 days microcosm biofilm formation. Sound dentin beams not subjected to the microcosm biofilm model served as control group and presented as 0 day. Cross-sectional microhardness values (VHN) were serially measured at varying depths (10–500 µm) occluso-cervically. Different upper-case letters indicate significant differences among depths within the same microcosm biofilm incubation period, according to the Tukey test ($p < 0.05$). Different lower-case letters indicate significant differences between incubation periods at the same depth, according to the Tukey test ($p < 0.05$). Due to extensive demineralization at the 14 days incubation period, microhardness at the 10 µm depth could not be measured and were recorded as zero. (*From the supplementary data of Study IV*)

5.20 Lactic acid production (Study IV)

Lactic acid production by the microcosm biofilms for 2, 7 or 14 days are shown in **Figure 20 B**. The incubation period significantly affected lactic acid production, which increased with longer incubation periods ($p < 0.05$). The 2 days and 14 days microcosm biofilm model revealed the lowest and the highest lactic acid production, respectively ($p < 0.05$). Lactic acid production increased by approximately 31% from the 2 days to 7 days microcosm biofilm model and 26% from the 7 days to14 days model.

5.21 Microcosm biofilm viability (MTT assay) (Study IV)

Biofilm viability assessed by the MTT assay, reflecting the metabolic activity of the microcosm biofilm model formed over incubation periods of 2, 7 or 14 days are presented in **Figure 20 C**. Metabolic activity significantly increased with longer incubation periods ($p < 0.05$). Among three incubation periods, 14 days microcosm biofilm model demonstrated the highest MTT absorbance ($p < 0.05$), followed by 7 and 2 days. The 2 days microcosm biofilm model exhibited the lowest metabolic activity ($p < 0.05$). MTT metabolic activity increased by approximately 92% from the 2 days to 7 days microcosm biofilm model and by 76% from the 7 days to14 days model.

5.22 Quasi-static 4-point flexural strength (Study IV)

The 4-point flexural strength values of sound dentin, carious dentin and carious dentin treated with ammonia- and water-based silver fluoride (SDF and SF) treatments, with or without the application of potassium iodide (KI) are presented in **Table 5**. Bar-shaped dentin beams presented no significant differences regarding cross-sectional areas 0.55 mm^2 (± 0.10) between groups. Flexural strength was significantly higher in sound dentin ($p < 0.05$). Carious dentin presented significant reductions (roughly 50%) in flexural strength compared to sound dentin ($p < 0.05$). No significant differences were detected between ammonia- and water-based silver fluoride treatments (SDF and SF), with or without potassium iodide (KI) compared to untreated carious dentin ($p > 0.05$).

Table 5. Four-point flexural strength, estimated endurance limits and pairwise comparisons for ammonia-and water-based silver fluoride treatments applied on carious dentin. Sound dentin and untreated carious dentin served as positive and negative control group, respectively.

Groups		4-point flexural strength (MPa)*	Endurance limit (MPa)	Fatigue life distributions pairwise comparison**
Treatment	Dentin			
No treatment (Control)	Sound	161.56 ± 29.15[a]	44.45	A
No treatment (Control)	Carious	80.40 ± 13.48[b]	24.36	D
SDF	Carious	93.70 ± 23.25[b]	27.04	C
SDF + KI	Carious	86.86 ± 22.92[b]	25.74	CD
SF	Carious	91.69 ± 12.91[b]	33.65	B
SF +KI	Carious	89.80 ± 17.09[b]	25.79	CD

*Different lower-case letters indicate significant differences for 4-point flexural strength according to Tukey test ($p < 0.05$). Endurance limits were calculated at 1×10^7 cycles. **Different upper-case letters indicate significant differences in fatigue life distributions according to Kruskal-Wallis test ($p < 0.05$). Abbreviations: SDF = Silver Diamine Fluoride; KI = Potassium Iodide; SF = Aqueous Silver Fluoride. (*From the supplementary data in Study IV*)

5.23 Fatigue resistance under cyclic loading (Study IV)

Fatigue life diagrams (S-N curves) of sound dentin, carious dentin and carious dentin treated with ammonia- and water-based silver fluoride (SDF and SF) treatments, with or without the application of potassium iodide (KI) are shown in **Figure 22**. Regression analyses with basquin-type power law models were listed for all groups to describe the mean fatigue resistance distribution. Kruskal-Wallis test revealed significant differences in fatigue resistance between groups ($p < 0.05$). Sound dentin presented significantly higher fatigue resistance (MPa) than untreated or treated carious dentin ($p < 0.05$). SF-treated carious dentin revealed fatigue resistance significantly higher than remaining treated groups (SDF, SDF+KI, SF+KI) and untreated carious dentin ($p < 0.05$). Fatigue resistance of SDF-treated carious dentin was significantly higher than untreated carious dentin ($p < 0.05$), however, comparable to SDF+KI and SF+KI ($p > 0.05$). There were no significant differences between fatigue resistance of untreated carious dentin, SDF+KI and SF+KI.

The stress-life fatigue constants were used to estimate the apparent endurance limit for all groups at 1×10^7 cycles and are presented in **Table 5.** Sound dentin showed the highest endurance limits. Carious dentin produced 45% lower endurance limits than sound dentin. Silver treatments had no effect on the endurance limits of carious dentin, except for the water-based silver fluoride (SF) treatment, without the application of potassium iodide (KI). SF increased endurance limits of carious dentin roughly by 40%. While KI had no effects on the endurance limit of SDF-treated dentin, it reduced the endurance limits of SF-treated dentin. KI applied treatments produced endurance limits comparable to untreated carious dentin.

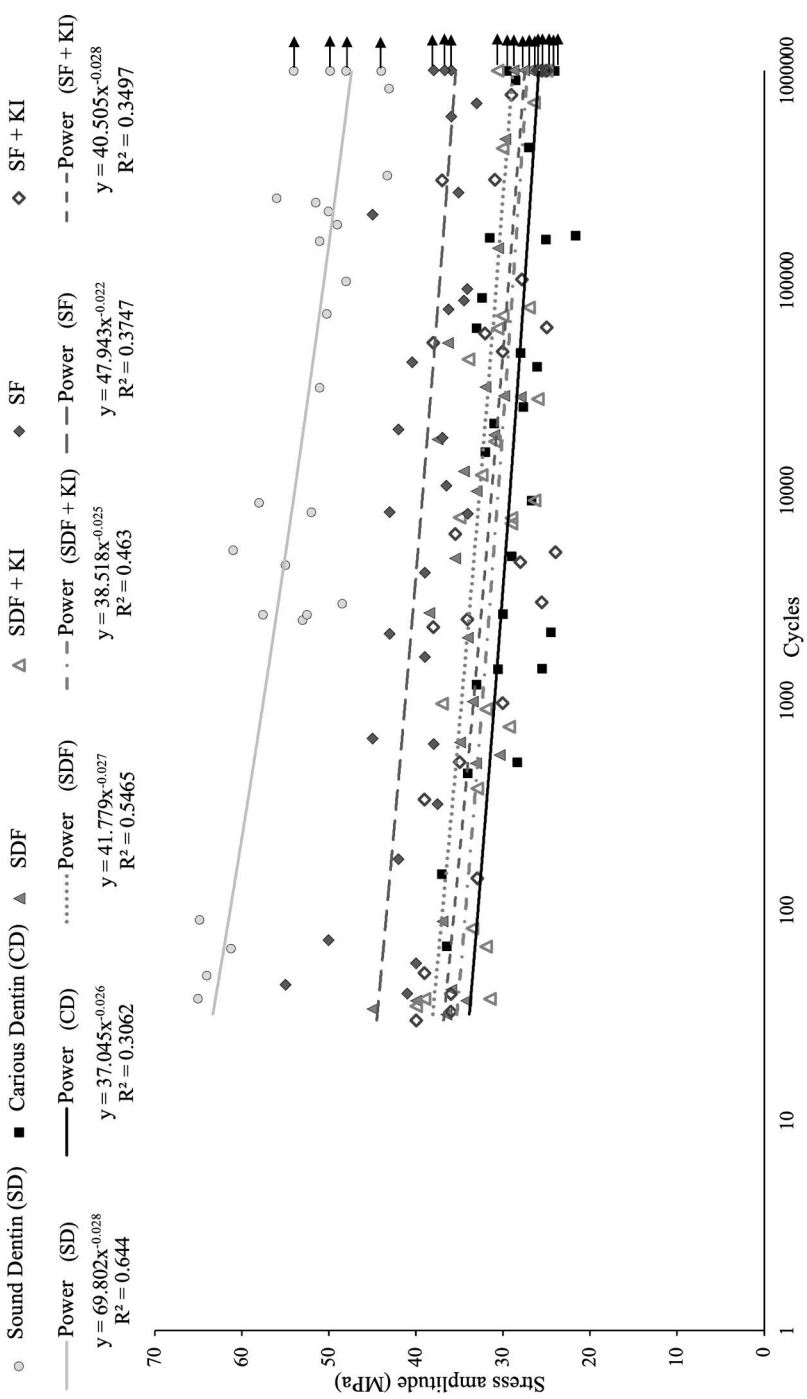

Figure 22. Stress life diagrams (S-N curves) for ammonia- and water-based silver fluoride treatments applied on carious dentin. Sound dentin and untreated carious dentin served as positive and negative control group, respectively. Note that data points with arrows represent specimens that reached 1.2×10^6 cycles and the test was discontinued. R^2 values represent the coefficient of determination. *Abbreviations*: SDF = Silver Diamine Fluoride; KI = Potassium Iodide; SF = Aqueous Silver Fluoride. *(From the supplementary data of Study IV)*

5.24 Dentin surface SEM characterization (Study IV)

Representative SEM micrographs of the tension side of fractured dentin beams (submitted to at least 500,000 cycles) of areas adjacent to fracture lines are shown in **Figure 23**. SEM analysis of fractured beams visually confirmed the presence of silver particles on dentin surfaces in ammonia- and water-based silver fluoride (SDF and SF) treatments, with or without the application of potassium iodide (KI), after cyclic loading (**Figure 23 C**; **D**; **E**; **F**). Sound dentin presented densely mineralized peritubular dentin (**Figure 23 A**). For untreated carious dentin, dissolution of both intratubular and peritubular dentin exposed collagen fibrils, indicated substantial demineralization caused by the microcosm biofilm model (**Figure 23 B**). Comparable demineralization patterns were observed for carious dentin treated with the different ammonia- and water-based silver fluoride (SDF and SF) treatments, with or without the application of potassium iodide (KI) (**Figure 23 C**; **D**; **E**; **F**). SF-treated carious dentin exhibited denser deposition of silver particles, mostly inside dentinal tubules (**Figure 23 E**). Carious dentin treated with SDF, SDF+KI or SF+KI, displayed comparable silver deposition mostly located inside the dentinal tubules (**Figure 23 C**; **D**; **F**).

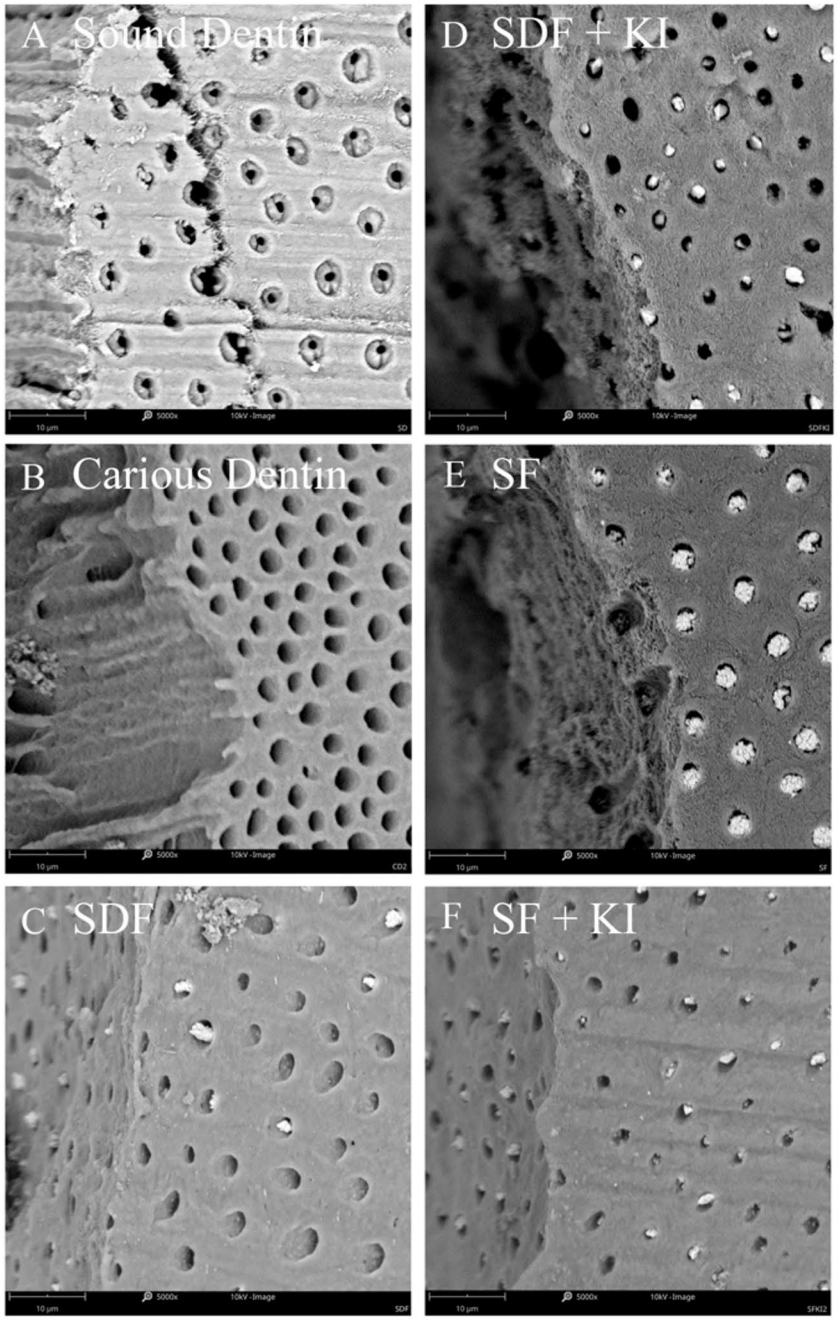

Figure 23. Representative SEM images of the tension side of fractured dentin beams following ammonia- and water-based silver fluoride treatments applied on carious dentin. Sound dentin and untreated carious dentin served as positive and negative control group, respectively. (*From the supplementary data of Study IV*)

6 Discussion

Silver fluoride treatments have been reported to be the most effective in arresting carious lesions at higher concentrations [Contreras et al., 2017], with 38% (w/v) concentration demonstrating superior clinical outcomes compared to 30% and 12% concentrations [Fung et al., 2016; Fung et al., 2018]. Therefore, commercially available 38% ammonia- and water-based silver fluoride (SDF and SF) treatments, with or without the application of potassium iodide (KI), were used in the present thesis. Riva Star and Riva Star Aqua (SDI, Australia) are widely used silver fluoride treatments in Australia, Asia and Europe, including Finland, supporting the clinical relevance of the selected materials. Both products were applied to dentin for 60 s using active application, a protocol that has been shown to be effective in arresting carious lesions [Yan et al., 2025], thereby further justifying the material selection and the application protocol employed in the present thesis.

6.1 Bonding to silver fluoride treatments (Study I)

The use of ammonia- and water-based silver diamine fluoride (SDF and SF) treatments, with or without the application of potassium iodide (KI), has increased considerably in recent years [Jiang et al., 2021]. However, optimal bonding protocols following these treatments remain unclear [Lutgen et al., 2018; Ko et al., 2020]. Depending on the size of the cavity, composite resin restorations are often required after silver fluoride treatments. Commercially available water-based silver fluoride is relatively new on the market, whereas ammonia-based silver fluoride has been available for over a decade and has a much longer history of clinical use. Yet there is still no consensus regarding the appropriate adhesive application mode, whether the treated surface should be rinsed or not, or how long should clinicians wait before placing the composite resin restoration [Fröhlich et al., 2022]. Literature has inconsistent findings, about the choice between the etch-and-rinse and self-etch modes, while some studies emphasize the importance of mode selection [Koizumi et al., 2016; Lutgen et al., 2018; Braz et al., 2020; Cifuentes-Jimenez et al., 2021; Muniz et al., 2024], others report no significant effect [Quock et al., 2012; Firouzmandi et al., 2020; Cardenas et al., 2021]. Even fewer studies have evaluated resin bonding following silver fluoride treatments combined with potassium iodide

(KI) application [Koizumi et al., 2016; Zhao et al., 2019; Van Duker et al., 2019; Fröhlich et al., 2020]. Therefore, it is difficult to translate *in vitro* results into clear clinical recommendations regarding the choice of adhesive application mode.

In Study I, resin-dentin bonding to ammonia-based silver diamine fluoride (SDF), with or without the application of potassium iodide (KI), was evaluated using the micro-tensile bond strength (μTBS) test under both etch-and-rinse and self-etch modes. The effects of water rinsing and airborne particle abrasion after SDF and SDF + KI treatments were examined, along with delayed bonding time points of 7, 15, and 30 days. The μTBS test is considered one of the most reliable in vitro methods for assessing adhesive performance [Armstrong et al., 2017]. The evaluation of water-based silver fluoride (SF), with or without the application of potassium iodide (KI) was not possible because the material was not commercially available at the time the experiments were conducted.

The findings of Study I, were in agreement with the previous reports indicating that resin-dentin bonding effectiveness after SDF and SDF +KI treatments is dependent on adhesive application mode [Koizumi et al., 2016; Lutgen et al., 2018; Cifuentes-Jimenez et al., 2021]. Universal adhesives allow application in both etch-and-rinse and self-etch modes while maintaining similar solvent systems, photoinitiators and functional monomers. For this reason, a mild universal adhesive was selected to minimize the influence of resin chemistry on the bonding outcomes [Breschi, 2025]. By eliminating comparisons between different adhesive systems, the effect of the application mode on bonding performance could be more accurately isolated. In addition, the widespread clinical use of universal adhesives further supports the choice.

Immediate self-etch bonding to SDF- and SDF + KI-treated dentin resulted in drastic reductions in bond strength, with a high frequency of pre-test failures. Bond strengths were similarly compromised for both SDF and SDF + KI groups, indicating that KI application, although intended to reduce staining, did not further impair self-etch bonding. The universal adhesive used in self-etch mode was unable to adequately etch through the silver- and iodine-impregnated smear layer [Van Meerbeek et al., 2011]. In addition, the high alkalinity and pH-buffering capacity of SDF likely neutralized the acidic monomers of the self-etch adhesive, reducing their etching efficiency and weakening monomer-dentin interactions [Cardenas et al., 2021]. Depending on the extent of deposition, SDF and SDF + KI precipitates can act as surface contaminants by occluding dentinal tubules (**Figure 8**), as the deposited silver particles produce physicochemical alterations that interfere with resin bonding [Siqueira et al., 2020].

Immediate water rinsing after SDF and SDF + KI treatment prevented the reduction in self-etch bond strength, likely by removing water-soluble ammoniacal compounds and reducing surface alkalinity. Similarly, delayed self-etch bonding to

both SDF- and SDF + KI-treated dentin restored bond strengths to levels comparable to untreated dentin. During the storage period, artificial saliva likely reduced alkalinity and promoted time-dependent mineral deposition, as indicated by the observed decrease in dentin permeability [Tezvergil-Mutluay et al., 2010; Fröhlich et al., 2022]. Reduced permeability suggests increased mineral precipitation and partial obliteration of dentinal tubules, which may help explain the recovery in bonding performance.

Air-abrasion effectively reduced silver residues on dentin surfaces and significantly improved the immediate self-etch bond strengths of SDF- and SDF + KI-treated dentin. The improvement was likely associated with the combined effect of surface cleaning and subsequent water rinsing, rather than mechanical removal alone [Anja et al., 2015; Lima et al., 2021]. However, the removal of surface silver residues may reduce immediate antibacterial contact at the dentin surface, nevertheless, the long-term clinical relevance of this effect remains unclear, as the antibacterial activity of silver fluoride treatments is not limited to surface deposits and may persist through subsurface silver penetration and sustained silver-ion release. Interestingly, although air-abrasion eliminated differences between self-etch and etch-and-rinse bonding for SDF-treated dentin, SDF + KI-treated dentin still exhibited lower bond strengths in self-etch mode. This may be related to potential chemical interactions between silver iodide and abrasive particles, which could be more effectively removed by phosphoric acid etching.

Etch-and-rinse mode relies on phosphoric acid demineralization to facilitate resin infiltration and micromechanical retention [Pashley et al., 2011]. Phosphoric acid etching effectively removed the SDF- and SDF + KI-impregnated smear layer and residual alkaline compounds, allowing the formation of uniform hybrid layers and resin tags comparable to those observed in untreated dentin (**Figure 7; Figure 8**). Immediate etch-and-rinse bonding eliminated the negative effects of both SDF and SDF + KI treatments, and neither delayed bonding nor airborne particle abrasion provided additional benefit under the etch-and-rinse mode. While immediate etch-and-rinse bonding appears clinically reliable, findings suggest that a short delayed bonding period (< 15 days) may be beneficial following SDF application, indicating time-dependent stabilization of the dentin substrate. Therefore, emerging bonding strategies that preserve SDF within the hybrid layer may enhance the anticariogenic effects and reduce long-term degradation.

6.2 Long-term effect of silver fluoride treatments on dentin collagen matrix (Study II)

Limited number of studies have evaluated the short-term effects of ammonia-based silver fluoride (SDF) on dentin endogenous enzymatic activity, there is not enough

information about the effects of water-based silver fluoride (SF) and their combination with potassium iodide (KI). The long-term influence on dentin endogenous enzymatic activity of SDF and SF treatments, with or without KI application, remains unclear.

In Study II, the effect of ammonia- and water-based silver fluoride (SDF and SF) treatments, with or without potassium iodide (KI) application, on the degradation of the dentin collagen matrix were investigated. Even KI application alone is not used in the clinical practice, KI application alone was also evaluated to determine whether KI independently affects dentin integrity. Demineralized dentin beams were used as the enzyme source to enhance clinical relevance. Zinc- and calcium-containing artificial saliva was used as the incubation medium because MMPs are zinc- and calcium-dependent endopeptidases, capable of degrading both native and denatured collagen [Carrilho et al., 2009; Tezvergil-Mutluay et al., 2010].

Dry dentin mass loss and elastic modulus measured using a three-point bending test were selected to assess collagen degradation and mechanical stability of demineralized dentin matrices [Tjäderhane et al., 2013], respectively. Reductions in dry mass and elastic modulus indicate compromised mechanical properties associated with collagen structural changes [Bedran-Russo et al., 2008]. Dry mass loss and elastic modulus exhibited similar trends, demonstrating that silver fluoride formulation, the use of KI and elapsed time after treatment were critical factors influencing dentin structural integrity and stability. Immediately after treatment, all groups showed an increase in elastic modulus, which correlated with the rapid deposition of silver particles within dentinal tubules. Among the tested materials, ammonia-based SDF and water-based SF demonstrated stable dry mass loss and elastic modulus over time. In contrast, the application of KI as a second-step exacerbated both dry mass loss and the reduction in elastic modulus, indicating increased degradation of the dentin organic matrix. The observed reduction following KI application may be associated with interactions between potassium iodide, silver and the dentin surface, potentially reducing the availability of free silver ions and limiting their interaction with the dentin collagen matrix, including possible collagen-stabilizing effects. The depth of penetration of ammonia- and water-based silver fluoride remains controversial [Sayed et al., 2019; Mulder et al., 2023], however, the poorer long-term performance of KI-treated groups may be attributed to denser material deposition extending into dentinal tubules, potentially interfering with the collagen network. Additionally, KI-treated groups exhibited increased transparency and visible structural degradation, including surface cracks, after one month of incubation. SF + KI showed less severe degradation than SDF + KI, this difference may be related to variations in ammonia and water content between the two formulations.

A generic MMP assay does not differentiate among specific MMP isoforms; however, it provides direct information on overall MMP activation or inhibition

[Tezvergil-Mutluay et al., 2011]. All silver fluoride treatment groups effectively reduced total MMP activity, consistent with previous short-term observations [Mei et al., 2013a; D'Alessandro et al., 2024]. In the short term, ammonia-based silver fluoride, with or without potassium iodide, demonstrated greater MMP inhibition than water-based silver fluoride, with or without KI. These findings were further supported by *in situ* zymography, in which ammonia-based SDF showed lower remaining MMP activity compared to water-based SF. However, KI application reduced the MMP-inactivation capacity of both SDF and SF when compared with their respective treatments alone. The reduced effectiveness of water-based SF may be related to its higher water content. Over long-term incubation, both ammonia- and water-based silver fluoride treatments decreased total enzymatic activity. Unlike other collagen cross-linking approaches that require prolonged application times, silver fluoride treatments offer a clinically practical alternative, as they can be applied within minutes while providing sustained enzymatic inhibition and are already commercially available. However, it remains unclear how long matrix metalloproteinases (MMPs) remain active in dentin following caries progression or restorative procedures, as well as how long the effects of other collagen cross-linking approaches persist. In this context, the use of SDF and SF remains promising.

Collagen degradation was further assessed using enzyme-linked immunosorbent assay (ELISA) and radioimmunoassay (RIA) to quantify enzyme-specific degradation markers for MMPs and cysteine cathepsins (CCs) [Garnero et al., 2003], respectively. KI-applied groups exhibited decreased MMP-mediated ICTP release and increased cathepsin K-mediated CTX release during short-term incubation, revealing an inverse relationship between these degradation pathways. However, the exact mechanisms underlying this shift remain unclear, as dentin proteolysis is not only regulated by MMPs and CCs [Garnero et al., 2003]. It should also be noted that both ICTP and CTX were released only in pg, indicating very small amounts. Therefore, although the data appear to show increased ICTP and CTX release following silver fluoride treatments, the absolute levels were extremely low.

Hydroxyproline analysis revealed higher collagen release in all treatment groups during short-term incubation compared with untreated dentin, with KI-treated groups exhibiting even greater release. These findings indicate that KI contributes to collagen degradation, particularly when applied after SDF and SF. Notably, SF + KI resulted in less collagen loss than SDF + KI, suggesting formulation-dependent interactions. The results of Bradford protein assay supported hydroxyproline analysis.

Application of KI after ammonia- and water-based silver fluoride treatments negatively impacted dentin integrity, as evidenced by increased dry mass loss, reduced elastic modulus, elevated enzymatic degradation and increased collagen and

protein release. These findings align with reports suggesting that KI may reduce the caries-arresting effectiveness of SDF [Zhao et al., 2020].

Although KI application alone has no direct clinical use, its inclusion as a separate group demonstrated that KI independently affects dentin integrity by increasing dry mass loss, protein release and cathepsin K-mediated collagen degradation. To date, no study has evaluated KI alone with respect to dentin collagen matrix degradation. Therefore, further investigation is required to clarify the role of KI in altering dentin composition and structural integrity.

Overall, a material's ability to preserve the dentin organic matrix is indirectly associated with the longevity of restorations. In this context, the improved bonding observed in Study I is consistent with the reduced enzymatic degradation of the dentin collagen matrix in Study II, indicating that rinsing after silver fluoride treatments supports both immediate adhesive performance and the underlying stability of dentin collagen.

6.3 Biocompatibility of silver fluoride treatments (Study III)

Biocompatibility, defined as material's ability to fulfill its intended function without causing adverse local or systemic reactions [Williams, 2008; Rosa et al., 2024] and is an important consideration for ammonia- and water-based silver fluoride treatments (SDF and SF), with or without the application of potassium iodide (KI), particularly in deep carious lesions, where silver particles can diffuse extensively into dentin [Sayed et al., 2019]. Moreover, silver and fluoride ions have been reported to exert cytotoxic effects on human cells even at relatively low concentrations [Greulich et al., 2012].

Most existing in vitro cytotoxicity models expose cells directly to diluted solutions or eluates, therefore, therefore fail to account for the protective function of dentin, which serves as a biological barrier between an applied material and the pulp. While the cytotoxic effects of ammonia-based silver diamine fluoride (SDF) have been evaluated in several studies [Hu et al., 2022; Oropeza et al., 2022; Zaeneldin et al., 2022], only a few have examined its combination with potassium iodide (KI) [García-Bernal et al., 2022; Fernandes et al., 2023] and limited data are available on water-based silver fluoride (SF) with or without KI application [Mulder et al., 2024].

In Study III, the effects of ammonia- and water-based silver fluoride treatments (SDF and SF), with or without potassium iodide (KI), were evaluated using two in vitro ISO-standardized cytotoxicity tests. Trans-dentinal cell viability was assessed by applying the silver fluoride treatments onto a dentin barrier, allowing diffusion toward pulp-derived cells in simulated deep cavities [ISO 7405, 2018] and direct cell

viability was evaluated by exposing cells directly to diluted treatment solutions [ISO 10993-5, 2009].

Trans-dentinal cytotoxicity testing provides greater clinical relevance than direct dilution-based assays, as dentin acts as a biological barrier that significantly modulates material diffusion and toxicity. Although, dilution-based direct cytotoxicity assays are less clinically representative, however, remain useful for comparative evaluation.

According to the findings of Study III, water-based silver fluoride (SF) treatment exhibited lower cytotoxicity than ammonia-based silver fluoride (SDF) in both trans-dentinal and direct cytotoxicity tests. Direct exposure assays revealed dose-dependent cytotoxicity, with all silver fluoride treatments meeting ISO-defined non-cytotoxic thresholds at the lowest dilution, while higher concentrations were cytotoxic. According to ISO criteria for cell damage assessment, SF was classified as moderately cytotoxic, SDF, SDF + KI and SF + KI were classified as severely cytotoxic. The observed differences between ammonia- and water-based formulations are likely related to their chemical composition and pH. Fibroblast viability has been shown to decrease at alkaline pH levels, and the ammonia content of SDF contributes to increased alkalinity, which has been linked with cell damage and reduced proliferation [Kruse et al., 2017]. In contrast, the neutral pH of water-based silver fluoride enables a more regulated diffusion through dentin [Hirose et al., 2016].

The application of potassium iodide (KI) significantly increased cytotoxicity when used as a second step after both ammonia- and water-based silver fluoride. Increased particle accumulation following KI application was observed on dentin surfaces and deeper penetration of treatment-related ions into dentinal tubules has been reported [Sayed et al., 2019]. These findings contrast with previous studies [García-Bernal et al., 2022; Fernandes et al., 2023; López-García et al., 2024] and may be attributed to differences in cell models, dilution protocols or dentin demineralization status. Comprehensive evaluation of material cytotoxicity is crucial to identify clinical limitations, safeguard patient safety and support regulatory approval.

6.4 Fatigue resistance of carious dentin treated with silver fluoride treatments (Study IV)

From a mechanical perspective, teeth are load-bearing structures subjected to complex chemical, mechanical, thermal, and bacterial challenges in the oral environment and fatigue have been identified as a dominant failure mechanism in dental tissues [Arola et al., 2010]. Therefore, fatigue resistance is a key factor in achieving long-term clinical success [Rosentritt et al., 2016]. However, most fatigue

studies have been conducted on sound dentin, which does not adequately represent clinically relevant substrates. Although fatigue testing is technically time-consuming and requires standardized specimen geometry, naturally occurring caries present irregular lesion depths and extensions, making them unsuitable for controlled fatigue evaluation [Kinney et al., 2003]. Furthermore, the lack of consensus on in vitro dentin caries protocols highlights the need for reproducible and clinically relevant models [Maske et al., 2017].

In Study IV, a revised *in vitro* microcosm biofilm protocol to better replicate carious dentin and fatigue resistance of carious dentin treated with ammonia- and water-based silver fluoride (SF and SF), with or without the application of potassium iodide (KI), under four-point quasi-static and cyclic loading were evaluated.

Among existing *in vitro* caries models, microcosm biofilm systems best reflect the complexity of in vivo microbial interactions [McBain, 2009]. In Study IV, a saliva-derived microcosm biofilm model was employed using McBain medium supplemented with 0.2% sucrose. Saliva from multiple donors was collected to enhance biofilm virulence and cariogenic activity. McBain medium was selected due to its salivary components that support bacterial growth and mimic intraoral conditions. Pellicle formation was included to further improve clinical relevance. Among the three incubation periods evaluated, the 2-day model demonstrated adequate bacterial viability, acid production, metabolic activity and dentin demineralization while preserving sufficient structural integrity of the dentin substrate for reliable mechanical testing. The selection of 2-day incubation period was based on both microbiological and mechanical criteria. Pilot experiments using 7-day incubation period resulted in excessive softening of dentin beams, which hindered reliable mechanical testing, particularly under cyclic fatigue loading conditions.

The fatigue resistance of sound dentin aligned with previously reported values, confirming the reliability of the experimental setup. The four-point bending configuration was selected because it provides uniform stress distribution, minimizes stress concentration and increases test sensitivity [ASTM D6272, 2017]. Ammonia- and water-based silver fluoride (SDF and SF) treatments, with or without potassium iodide (KI), did not influence the quasi-static flexural strength of carious dentin. However, both SDF and SF significantly improved fatigue resistance indicating partial recovery of fatigue behavior and enhanced resistance to crack propagation. This suggests improved structural integrity of treated carious dentin, potentially associated with remineralization and/or precipitation of mineral crystals within the dentin matrix. The composition of the silver fluoride formulations played a decisive role, as water-based SF produced a greater improvement in fatigue resistance than ammonia-based SDF. Fatigue life analysis revealed a substantial increase in the endurance limit following SF treatment, whereas SDF did not yield a

meaningful improvement, suggesting limited mechanical reinforcement. While both ammonia- and water-based silver fluoride (SDF and SF) treatments reduced enzymatic activity as shown in Study II, only water-based SF provided measurable collagen reinforcement in Study IV, as a promising agent for immediate mechanical strengthening of carious dentin.

Potassium iodide (KI) application after SF negated the strengthening effect, and after SDF had no influence. Results from Study III of increased cytotoxicity associated with KI and results of reduced mechanical properties from Study IV, further raises concern for the KI use.

6.5 Future directions and further studies

Overall, based on the findings of the present thesis, recently available water-based silver fluoride (SF) treatment appears to be a promising alternative to ammonia-based silver diamine fluoride (SDF) treatment. Additionally, SF offers clinical advantages such as reduced odor, less soft tissue irritation and neutral pH, thereby improving the comfort of both patients and clinicians compared with SDF. Importantly, water-based SF, particularly when applied without the application of potassium iodide (KI), demonstrated improved biocompatibility in Study III and superior fatigue resistance in Study IV.

As mentioned, evaluation of the bonding performance of water-based silver fluoride (SF) was not possible during Study I, due to the material unavailability. However, once the material became accessible, a pilot study was conducted to assess the immediate micro-tensile bond strength of SF and SF + KI. Although the pilot data were not included in the present thesis, no differences were observed between SDF and SF treatments, with or without the application of KI, in terms of resin-dentin micro-tensile bond strength on sound dentin. Nevertheless, further studies are required to confirm the findings and to evaluate long-term bonding performance.

Potassium iodide (KI) application following ammonia- and water-based silver fluoride (SDF and SF) treatments, consistently resulted in inferior mechanical properties, including reduced elastic modulus and dry mass (Study II), increased cytotoxicity (Study III) and decreased fatigue resistance (Study IV) when applied to carious dentin. These findings suggest that although KI may be clinically relevant for esthetic purposes, its use should be approached with caution and avoided when esthetics are not a primary concern. Collectively, the results of the present thesis, support the use of water-based silver fluoride as a viable alternative to ammonia-based and call for careful reconsideration of routine KI application in clinical practice. Alternative strategies to address discoloration, such as zinc-based compounds or nanosilver formulations, should be further investigated

Overall, future research should further elucidate the mechanisms of action of ammonia- and water-based silver fluoride (SDF and SF) treatments, with or without the application of potassium iodide (KI), to enable a more informed evaluation of adjunctive strategies and to support the development of consensus-based clinical guidelines for optimizing treatment protocols.

Future investigations should assess the bonding performance of different ammonia- and water-based silver fluoride formulations from various manufacturers, as direct comparisons among commercially available products remain challenging due to variations in fluoride ion concentration [Patel et al., 2021; Luong et al., 2022] and the continued expansion of the global market. Studies should also incorporate clinically relevant dentin substrates, such as caries-affected and eroded dentin, alongside long-term incubation protocols. Given the demonstrated protective effects of silver fluoride on dentin collagen, long-term *in vitro* and *in vivo* studies should be prioritized. In addition, future research using diverse experimental methodologies, cell types, application protocols and clinically relevant loading conditions is required to fully characterize the biological and mechanical responses to silver fluoride treatments and is essential for translating laboratory findings into reliable clinical applications.

7 Conclusions

Based on the series of studies included in the present thesis, the following conclusions were drawn:

I. Etch-and-rinse mode prevented impairments in resin-dentin bonding, whereas self-etch mode required additional removal of silver deposits from dentin treated with ammonia-based silver fluoride (SDF), with or without the application of potassium iodide (KI). SDF and SDF + KI treatments may promote mineral deposition at the resin-dentin interface following 15 days delayed bonding, contributing to extend service life of composite restorations.

II. Ammonia- and water-based silver fluoride (SDF and SF) treatments can provide long-term protection by preserving mechanical properties and structural integrity of dentin collagen matrix, however, they do not completely inhibit endogenous protease-mediated degradation of demineralized collagen. The use of SDF and SF in combination with potassium iodide (KI) to prevent collagen degradation should be avoided.

III. Ammonia- and water-based silver fluoride (SDF and SF) treatments, with or without the application of potassium iodide (KI), should be applied with caution due to their cytotoxic potential. Water-based SF without the application of KI appears to be the safest choice, especially in cavitated lesions located close to the pulp.

IV. The proposed microcosm biofilm caries model supports its use for standardized *in vitro* simulation of dentin caries in mechanical testing. Water-based silver fluoride (SF) treatment can partially restore the mechanical strength loss of carious dentin, under cyclic mechanical stress. However, the addition of potassium iodide (KI) reduces the strengthening effect and should therefore be reconsidered.

Acknowledgements

This doctoral thesis was conducted at the Department of Cariology and Restorative Dentistry, Institute of Dentistry, Faculty of Medicine, University of Turku, Turku, Finland.

First, I would like to express my deepest gratitude to my supervisors, Prof. Arzu Tezvergil-Mutluay and Prof. Murat Mutluay, for their continuous guidance, support and mentorship throughout my doctoral studies. Their dedication, generosity in sharing their knowledge and experience, and constant encouragement have been invaluable to my academic and personal development. I am truly proud to have been their student.

I would like to sincerely thank my opponent, Prof. Milena Cadenaro, for accepting the role of opponent for this thesis. I greatly look forward to the doctoral defense and to the valuable discussion and insightful questions that will undoubtedly contribute to the quality of this thesis.

My sincere appreciation also goes to Prof. Marja-Liisa Laitala and Associate Prof. Monica Yamauti for carefully reviewing this thesis as pre-examiners and for their invaluable comments and constructive suggestions. I am truly grateful for the time and effort they dedicated.

Years ago, when I was a child, I had the opportunity to visit this beautiful country. At that time, I could not have imagined that I would one day return to Finland to pursue my doctoral studies. I would like to sincerely thank Prof. Pekka Vallittu and Löylymaster Lippo Lassila for showing me the openness, honesty and kindness of Finnish people. Thanks to them, I had the chance to rediscover Finland through cherished childhood memories that have always held a special place for me. I am also grateful for their continued support and the many meaningful conversations we shared throughout my doctoral journey.

Likewise, I would like to express my special thanks to Prof. Ulvi Gürsoy and Docent Mervi Gürsoy, whose kindness and support date back to my childhood. I am deeply grateful for their help, warmth and the many pleasant conversations and memories we have shared over the years.

I would like to thank the Dean of the Institute, Prof. Timo Närhi, for his support throughout my doctoral journey, as well as for his knowledge, kindness and encouragement. He has been a true source of inspiration.

I would also like to thank my follow-up committee member and head of the laboratory, Docent Vuokko Loimaranta, for her support, laboratory assistance and continuous help throughout my doctoral journey.

I would like to acknowledge my co-authors, Associate Prof. Roda Seseogullari-Dirihan and Docent Thiago Stape, for their collaboration and support. Roda, you have always been more than a colleague to me and I truly consider you a sister. I am sincerely grateful for your friendship, guidance and support in both academic and personal matters. I also send my warm regards to Leo and Serdar Dirihan. Thiago, your support and scientific insight have always been invaluable and I am deeply grateful for your help whenever needed.

I would also like to thank Prof. Jukka Matinlinna, Docent Eija Säilynoja, Dr. Jasmina Bijelic-Donova and Roosa Prinssi for their motivation, kindness and positive presence.

I gratefully acknowledge the financial support provided by the Finnish Doctoral Programme in Oral Sciences (FINDOS), EDUFI, University of Turku and the Finnish Cultural Foundation throughout my PhD journey. I also thank the Turku University Foundation, the International Association for Dental, Oral and Craniofacial Research (IADR) and the Scandinavian Division of IADR for the travel grants that enabled me to attend national and international conferences.

I would like to express my gratitude to the FINDOS coordinators Dr. Maiju Kannisto, Sanni Helander, and Nina Blom for their assistance and support throughout my doctoral journey.

I was fortunate to be involved in teaching in the Morphology course together with Docent Merja Laine, Docent Sufyan Garoushi, Tytti Syrjäkari and Marco Stålfors, and in the Cariology course together with Dr. Teemu Tirri, Dr. Carlos Soler Tornero, Dr. Mirja Riippa, Dr. Elisa Lind, Katri Kuismanen, and Katariina Saari. Each morning at the university felt easy and meaningful thanks to your friendship, support and many pleasant conversations we shared.

Conducting research has been truly enjoyable thanks to the excellent technicians at Dentalia (3rd floor), Katja Sampalahti, Oona Hälfors, Tatjana Talja and Aija Koivusaari, as well as at TCBC, Mariia Valkama, Genevieve Alfont (Sevi), and Anna Kostiander. I am grateful for the opportunity to work with you, it has been a pleasure.

I would like to thank our secretary, Sari Heikkilä, for her continuous support and assistance in all matters throughout my doctoral journey.

I would also like to thank my colleagues from our department, whom I am happy to call not only colleagues but also good friends, Dr. Anas Aaqel Salim, Dr. Ikram

Salim, Marcelo Capitanio, Dr. Jaana Sippus, Marilia Canadas, Michel Wendlinger and Dr. Omar Ismail. Special thanks to Damla Erol from the Department of Periodontology for her friendship and support.

My special regards go to visiting researchers and colleagues, including Associate Prof. Ecehan Hazar, Associate Prof. Ahmet Hazar, Dr. Kanae Wada, Dr. Junichiro Wada, Dr. Shoko Miura, Dr. Yiğit Ömür, Dr. Elvin Günel, Dr. Tuğçe Koyu, Associate Prof. Bengisu Yıldırım, Dr. Bestegül Günay, Buse Altay, and Youssef Soliman.

Sports have also played an important role in maintaining my mental well-being during this journey. I would like to thank Taru Montanari for her friendship and support as a sports instructor.

During my stay in Turku, I participated in various friendship programs and I am grateful to Heli Valkama for introducing me to Finnish culture and for her friendship.

Finland has gradually become a home away from home for me. I am deeply grateful to all the wonderful people I met during this doctoral journey and to the friends I made along the way.

Friends are the family we choose and I am incredibly fortunate to have friends who have become my family. I would like to thank my dear friends who visited me in Turku, Finland, Ecem Kumbasar, the Demiryürek family, Merve Demiryürek, Elif Aslan, İrem Ökten, Ceren Öztürk Ulusoy, Mehmet Ege Can Ulusoy, and İrem Özçelik Kul.

I am also grateful to my childhood friends, Müge Oktar Küçükbay, Ada Irmak Özcan, Hazal Ertürk, İlkin Demirci, Itır Aylı, Yaren Doğan, Mert Ustay, Çelik Köseoğlu, Suel İkizer, Ayşe Demir Canbulut, and Naz Bayar for their lifelong friendship and support.

My warmest thanks go to my friends in Finland, who have made life in a new country and language both meaningful and joyful: Sammi Fan, Erika Atencio Herre, Jiri Funda, Elina Tuomikoski, William Eccleshall, Markus Matilainen, Sakari Pöysti, Bianca Zumbo, Simone Pegoraro, Barbara Vähätalo-Ramos, Antti Vähätalo-Ramos, Chandler Ross, Joaquin Valdez Garcia, Claudia Tato Fernandez, Samppa Laine, Paola Moyano-Gomez, Raychel Turola, Santeri Nieminen, Marta Mokrzycka, Magda Niemczura, Juani Villegas Acosta, Petar Kosijer, Marek Janik and Saiganesh Sriraman.

Last but not least, I consider myself incredibly fortunate to have been born into such a loving family. My deepest gratitude goes to my parents, Mine Betül Üçtaşlı and Sadullah Üçtaşlı. Words are not enough to express my love, admiration and appreciation for everything you have done for me. You have always been my greatest role models. I am forever grateful for your unconditional love, support and the opportunities you have provided throughout my life.

I would also like to express my love and gratitude to my extended family, my grandparents, both those who are still with us and those who continue to watch over us, my aunts and uncles, and all my cousins for always making me feel loved, supported and deeply cared for.

Although I am still relatively young, approaching the end of my twenties has led me to realize that growing up surrounded by love and support is one of life's greatest privileges. I am deeply grateful for the memories, experiences and joy I have gained along the way. Thank you all for being part of my journey. I hope to continue sharing life with you in the years to come.

Having completed all my previous education in Ankara, Türkiye, I had the unique opportunity to pursue my doctoral studies abroad. For this opportunity and for the values that made it possible, I dedicate this thesis to the memory of Mustafa Kemal Atatürk, whose vision and reforms made such opportunities attainable.

January 2026
Merve Üçtaşlı

References

Amran T, Esati J, Weiger R, Blatz MB, Eggmann F: Impact of phosphoric acid etching duration on the bonding performance of universal adhesives on enamel: a systematic review of laboratory studies. Journal of Esthetic and Restorative Dentistry 2025; DOI: 10.1111/jerd.70057

Anja B, Walter D, Nicoletta C, Marco F, Pezelj Ribarić S, Ivana M: Influence of air abrasion and sonic technique on microtensile bond strength of one-step self-etch adhesive on human dentin. Sci World J 2015;2015:368745.

Armstrong S, Breschi L, Özcan M, Pfefferkorn F, Ferrari M, Van Meerbeek B: Academy of Dental Materials guidance on in vitro testing of dental composite bonding effectiveness to dentin/enamel using micro-tensile bond strength (μTBS) approach. Dent Mater 2017;33:133–143.

Arola D, Reprogel RK: Tubule orientation and the fatigue strength of human dentin. Biomaterials 2006;27:2131–2140.

Arola D, Bajaj D, Ivancik J, Majd H, Zhang D: Fatigue of biomaterials: Hard tissues. Int J Fatigue 2010;32:1400–1412.

ASTM D6272: Test Method for Flexural Properties of Unreinforced and Reinforced Plastics and Electrical Insulating Materials by Four-Point Bending. ASTM D6272 2017.

Baker JL, Mark Welch JL, Kauffman KM, McLean JS, He X: The oral microbiome: diversity, biogeography and human health. Nat Rev Microbiol 2024;22:89–104.

Baraka M, Tekeya M, Bakry NS, Fontana M: Twelve-month randomized controlled trial of 38% silver diamine fluoride with or without potassium iodide in indirect pulp capping of young permanent molars. J Am Dent Assoc 2022;153:1121-1133.e1.

Bedran-Russo AKB, Pashley DH, Agee K, Drummond JL, Miescke KJ: Changes in stiffness of demineralized dentin following application of collagen crosslinkers. J Biomed Mater Res B Appl Biomater 2008;86:330–334.

Bergmeyer Hans-Uirich: Lactate Dehydrogenase; in : Methods of Enzymatic Analysis. Elsevier, 1974, p 574.

Bradford MM: A rapid and sensitive method for the quantitation of microgram quantities of protein utilizing the principle of protein-dye binding. Anal Biochem 1976;72:248–254.

Braz PVF, Dos Santos AF, Pereira PN, Ribeiro APD: Silver diamine fluoride and cleaning methods effects on dentin bond strength. Am J Dent 2020;33:315–319.

Breschi L, Maravic T, Cunha SR, Comba A, Cadenaro M, Tjäderhane L, et al.: Dentin bonding systems: from dentin collagen structure to bond preservation and clinical applications. Dent Mater 2018;34:78–96.

Breschi L: Buonocore memorial lecture 2023: changing operative mindsets with universal adhesives and cements. Oper Dent 2025;50:12–32.

Buonocore MG: A simple method of increasing the adhesion of acrylic filling materials to enamel surfaces. J Dent Res 1955;34:849–53.

Burke FJT, Mackenzie L: Bonding to dentine: an update on universal adhesives. Dent Update 2021;48:620–631.

Cadenaro M, Antoniolli F, Sauro S, Tay FR, Di Lenarda R, Prati C, et al.: Degree of conversion and permeability of dental adhesives. Eur J Oral Sci 2005;113:525–530.

Cadenaro M, Maravic T, Comba A, Mazzoni A, Fanfoni L, Hilton T, et al.: The role of polymerization in adhesive dentistry. Dental Materials 2019;35:e1–e22.
Cadenaro M, Josic U, Maravić T, Mazzitelli C, Marchesi G, Mancuso E, et al.: Progress in dental adhesive materials. J Dent Res 2023;102:254–262.
Cardenas AFM, Siqueira FSF, Morales LAR, Araujo LCR, Campos VS, Bauer JR, et al.: Influence of silver diamine fluoride on the adhesive properties of interface resin-eroded dentin. Int J Adhes Adhes 2021;106:102813.
Carrilho MR, Tay FR, Donnelly AM, Agee KA, Tjäderhane L, Mazzoni A, et al.: Host-derived loss of dentin matrix stiffness associated with solubilization of collagen. J Biomed Mater Res B Appl Biomater 2009;90:373–380.
Chan AKY, Tamrakar M, Jiang CM, Tsang YC, Leung KCM, Chu CH: Clinical evidence for professionally applied fluoride therapy to prevent and arrest dental caries in older adults: A systematic review. J Dent 2022;125:104273.
Cheng L, Zhang L, Yue L, Ling J, Fan M, Yang D, et al.: Expert consensus on dental caries management. Int J Oral Sci 2022;14:17.
Chu CH, Lo ECM, Lin HC: Effectiveness of silver diamine fluoride and sodium fluoride varnish in arresting dentin caries in chinese pre-school children. J Dent Res 2002;81:767–770.
Chu CH, Lo ECM: Promoting caries arrest in children with silver diamine fluoride: a review. Oral Health Prev Dent 2008;6:315–21.
Chu CH, Mei ML, Lo ECM: Use of fluorides in dental caries management. Gen Dent 2010;58:37–43.
Cifuentes-Jimenez C, Alvarez-Lloret P, Benavides-Reyes C, Gonzalez-Lopez S, Rodriguez-Navarro AB, Bolaños-Carmona MV: Physicochemical and mechanical effects of commercial silver diamine fluoride (SDF) agents on demineralized dentin. J Adhes Dent 2021;23:557–567.
Cifuentes-Jimenez CC, Bolanos-Carmona MV, Enrich-Essvein T, Gonzalez-Lopez S, Álvarez-Lloret P: Evaluation of the remineralizing capacity of silver diamine fluoride on demineralized dentin under pH-cycling conditions. Journal of Applied Oral Science 2023;31:e20220306.
Clarkson BH, Wefel JS, Miller I: A model for producing caries-like lesions in enamel and dentin using oral bacteria in vitro. J Dent Res 1984;63:1186–1189.
Contreras V, Toro MJ, Elías-Boneta AR, Encarnación-Burgos A: Effectiveness of silver diamine fluoride in caries prevention and arrest: a systematic literature review. Gen Dent 2017;65:22–29.
Craig GG, Powell KR, Cooper MH: Caries progression in primary molars: 24-month results from a minimal treatment programme. Community Dent Oral Epidemiol 1981;9:260–265.
Croll TP, Berg J: Delivery methods of silver diammine fluoride to contacting proximal tooth surfaces and history of silver in dentistry. Compend Contin Educ Dent 2020;41:84–89.
Crystal YO, Marghalani AA, Ureles SD, Wright JT, Sulyanto R, Divaris K, et al.: Use of silver diamine fluoride for dental caries management in children and adolescents, including those with special health care needs. Pediatr Dent 2017;39:135–145.
D'Alessandro C, Mancuso E, Mazzitelli C, Maravic T, Josic U, D' Urso D, et al.: Comparisons of ammonia- and water-based silver-containing solutions on dentin bonding and enzymatic activity: 1-yr evaluation. Dent Mater 2024;40:777–788.
Duangthip D, Chu CH, Lo ECM: A randomized clinical trial on arresting dentine caries in preschool children by topical fluorides—18 month results. J Dent 2015;44:57–63.
Exterkate RAM, Crielaard W, Ten Cate JM: Different response to amine fluoride by Streptococcus mutans and polymicrobial biofilms in a novel high-throughput active attachment model. Caries Res 2010;44:372–379.
Fanfoni L, Breschi L, Cadenaro M: Polymerization of universal adhesive: Effect of enamel and curing light. Dental Materials 2017;33:e29.
Featherstone JDB: Prevention and reversal of dental caries: role of low level fluoride. Community Dent Oral Epidemiol 1999;27:31–40.
Featherstone JDB: The science and practice of caries prevention. Journal of the American Dental Association 2000;131:887–899.

Fernandes LO, Mendes Soares IP, Anselmi C, Pires MLBA, Ribeiro RAO, Peruchi V, et al.: Pulp cell response to the application of silver diamine fluoride and potassium iodide on caries-like demineralized dentin. Clin Oral Investig 2023;27:7295–7306.

Ferracane JL: Models of caries formation around dental composite restorations. J Dent Res 2017;96:364–371.

Finland: Act on the Medical Use of Human Organs, Tissues and Cells (101/2001) [Internet]. Helsinki: Ministry of Social Affairs and Health 2001. Available from: https://www.finlex.fi/fi/lainsaadanto/2001/101

Firouzmandi M, Vasei F, Giti R, Sadeghi H: Effect of silver diamine fluoride and proanthocyanidin on resistance of carious dentin to acid challenges. PLoS One 2020;15:e0238590.

Fröhlich TT, Rocha R de O, Botton G: Does previous application of silver diammine fluoride influence the bond strength of glass ionomer cement and adhesive systems to dentin? systematic review and meta-analysis. Int J Paediatr Dent 2020;30:85–95.

Fröhlich TT, Botton G, Rocha R de O: Bonding of glass-ionomer cement and adhesives to silver diamine fluoride-treated dentin: an updated systematic review and meta-analysis. J Adhes Dent 2022;24:29–38.

Fronza BM, Braga RR, Cadenaro M: Dental adhesives—surface modifications of dentin structure for stable bonding. Dent Clin North Am 2022;66:503–515.

Fung MHT, Duangthip D, Wong MCM, Lo ECM, Chu CH: Arresting dentine caries with different concentration and periodicity of silver diamine fluoride. JDR Clin Trans Res 2016;1:143–152.

Fung MHT, Duangthip D, Wong MCM, Lo ECM, Chu CH: Randomized clinical trial of 12% and 38% silver diamine fluoride treatment. J Dent Res 2018;97:171–178.

Galis ZS, Sukhova GK, Lark MW, Libby P: Increased expression of matrix metalloproteinases and matrix degrading activity in vulnerable regions of human atherosclerotic plaques. J Clin Invest 1994;94:2493–2503.

Gao SS, Amarquaye G, Arrow P, Bansal K, Bedi R, Campus G, et al.: Global oral health policies and guidelines: using silver diamine fluoride for caries control. Front Oral Health 2021;2:1–12.

García-Bernal D, Pecci-Lloret MP, López-García S: The cytocompatibility of silver diamine fluoride on mesenchymal stromal cells from human exfoliated deciduous teeth: an in vitro study. Materials 2022;15:2104.

Garnero P, Ferreras M, Karsdal M, Nicamhlaoibh R, Risteli J, Borel O, et al.: The type I collagen fragments ICTP and CTX reveal distinct enzymatic pathways of bone collagen degradation. J Bone Miner Res 2003;18:859–867.

Germann HP, Heidemann E: A synthetic model of collagen: An experimental investigation of the triple-helix stability. Biopolymers 1988;27:157–163.

Greenwall-Cohen J, Greenwall L, Barry S: Silver diamine fluoride - an overview of the literature and current clinical techniques. Br Dent J 2020;228:831–838.

Greulich C, Braun D, Peetsch A, Diendorf J, Siebers B, Epple M, et al.: The toxic effect of silver ions and silver nanoparticles towards bacteria and human cells occurs in the same concentration range. RSC Adv 2012;2:6981–6987.

Hamdi K, Hamama HH, Motawea A, Fawzy A, Mahmoud SH: Long-term evaluation of early-enamel lesions treated with novel experimental tricalcium silicate paste: A 2-year randomized clinical trial. J Esthet Restor Dent 2022;34:1113–1121.

Hayes M, Brady P, Burke FM, Allen PF: Failure rates of class V restorations in the management of root caries in adults-a systematic review. Gerodontology 2016;33:299–307.

Hirose Y, Yamaguchi M, Kawabata S, Murakami M, Nakashima M, Gotoh M, et al.: Effects of extracellular pH on dental pulp cells in vitro. J Endod 2016;42:735–741.

Hu S, Muniraj G, Mishra A, Hong K, Lum JL, Hong CHL, et al.: Characterization of silver diamine fluoride cytotoxicity using microfluidic tooth-on-a-chip and gingival equivalents. Dent Mater 2022;38:1385–1394.

Ionescu AC, Brambilla E: Bioreactors: How to Study Biofilms In Vitro; in : Oral Biofilms and Modern Dental Materials. Cham, Springer International Publishing, 2021, pp 37–54.

ISO 7405: International Organization for Standartization. ISO 7405:2018, dentistry — evaluation of biocompatibility of medical devices used in dentistry. Geneva: International Organization for Standardization; 2018.

ISO 10993-5: International Organization for Standartization. ISO 10993-5, biological evaluation of medical devices — Part 5: tests for in vitro cytotoxicity. Geneva: International Organization for Standardization; 2009.

Jamal D, AlMushayt A, Abujamel T, Bamashmous S, Bamashmous N, Alamoudi N: Silver diamine fluoride: the science behind the action – a narrative review. BMC Oral Health 2025;25:1195.

Jiang CM, Duangthip D, Chan AKY, Tamrakar M, Lo ECM, Chu CH: Global research interest regarding silver diamine fluoride in dentistry: A bibliometric analysis. J Dent 2021;113:103778.

Kinney JH, Marshall SJ, Marshall GW: The mechanical properties of human dentin: A critical review and re-evaluation of the dental literature. Crit Rev Oral Biol Med 2003;14:13–29.

Knight GM, McIntyre JM, Craig GG, Mulyani, Zilm PS, Gully NJ: An in vitro model to measure the effect of a silver fluoride and potassium iodide treatment on the permeability of demineralized dentine to Streptococcus mutans. Aust Dent J 2005;50:242–245.

Knight GM, McIntyre JM, Mulyani: The effect of silver fluoride and potassium iodide on the bond strength of auto cure glass ionomer cement to dentine. Aust Dent J 2006;51:42–45.

Ko AK, Matsui N, Nakamoto A, Ikeda M, Nikaido T, Burrow MF, et al.: Effect of silver diammine fluoride application on dentin bonding performance. Dent Mater J 2020;39:407–414.

Koizumi H, Hamama HH, Burrow MF: Effect of a silver diamine fluoride and potassium iodide-based desensitizing and cavity cleaning agent on bond strength to dentine. Int J Adhes Adhes 2016;68:54–61.

Kreth J, Ferracane JL, Pfeifer CS, Khajotia S, Merritt J: At the interface of materials and microbiology: a call for the development of dtandardized approaches to assay biomaterial-biofilm interactions. J Dent Res 2019;98:850–852.

Kruse CR, Singh M, Targosinski S, Sinha I, Sørensen JA, Eriksson E, et al.: The effect of pH on cell viability, cell migration, cell proliferation, wound closure, and wound reepithelialization: In vitro and in vivo study. Wound Repair Regen 2017;25:260–269.

Li F, Weir MD, Fouad AF, Xu HHK: Effect of salivary pellicle on antibacterial activity of novel antibacterial dental adhesives using a dental plaque microcosm biofilm model. Dent Mater 2014a;30:182–191.

Li X, Wang J, Joiner A, Chang J: The remineralisation of enamel: a review of the literature. J Dent 2014b;42:S12–S20.

Li R, Lo ECM, Liu BY, Wong MCM, Chu CH: Randomized clinical trial on arresting dental root caries through silver diammine fluoride applications in community-dwelling elders. J Dent 2016;51:15–20.

Lima V, Soares K, Caldeira V, Faria-e-Silva A, Loomans B, Moraes R: Airborne-particle abrasion and dentin bonding: systematic review and meta-analysis. Oper Dent 2021;46:E21–E33.

López-García S, Sanz JL, Oñate-Sánchez RE, Forner L, García-Bernal D, Murcia L, et al.: In vitro biocompatibility of ammonia-free silver fluoride products on human dental pulp stem cells. Tissue Cell 2024;86:102283.

Luong M, Sadr A, Chan D: Dentin discoloration and pulpal ion concentrations following silver diamine fluoride and potassium iodide treatment. Oper Dent 2022;47:640–647.

Lutgen P, Chan D, Sadr A: Effects of silver diammine fluoride on bond strength of adhesives to sound dentin. Dent Mater J 2018;37:1003–1009.

MacHiulskiene V, Campus G, Carvalho JC, Dige I, Ekstrand KR, Jablonski-Momeni A, et al.: Terminology of dental caries and dental caries management: Consensus report of a workshop organized by ORCA and cariology research group of IADR. Caries Res 2020;54:7–14.

Mann AB, Dickinson ME: Nanomechanics, Chemistry and Structure at the Enamel Surface; in : The Teeth and Their Environment Physical, Chemical and Biochemical Influences. 2005, pp 105–131.
Marchesi G, Frassetto A, Visintini E, Diolosà M, Turco G, Salgarello S, et al.: Influence of ageing on self-etch adhesives: One-step vs. two-step systems. Eur J Oral Sci 2013;121:43–49.
Maske TT, van de Sande FH, Arthur RA, Huysmans MCDNJM, Cenci MS: In vitro biofilm models to study dental caries: a systematic review. Biofouling 2017;33:661–675.
Mazzoni A, Breschi L, Carrilho M, Nascimento FD, Orsini G, Ruggeri A, et al.: A review of the nature, role, and function of dentin non-collagenous proteins. Part II: enzymes, serum proteins, and growth factors. Endod Topics 2009;21:19–40.
Mazzoni A, Nascimento FD, Carrilho M, Tersariol I, Papa V, Tjäderhane L, et al.: MMP activity in the hybrid layer detected with in situ zymography. J Dent Res 2012;91:467–472.
Mazzoni A, Apolonio FM, Saboia VPA, Santi S, Angeloni V, Checchi V, et al.: Carbodiimide inactivation of MMPs and effect on dentin bonding. J Dent Res 2014;93:263–268.
Mazzoni A, Tjäderhane L, Checchi V, Di Lenarda R, Salo T, Tay FR, et al.: Role of dentin MMPs in caries progression and bond stability. J Dent Res 2015;94:241–251.
McBain AJ, Sissons C, Ledder RG, Sreenivasan PK, De Vizio W, Gilbert P: Development and characterization of a simple perfused oral microcosm. J Appl Microbiol 2005;98:624–634.
McBain AJ: In vitro biofilm models: an overview. Adv Appl Microbiol 2009;69:99–132.
Mei ML, Li QL, Chu CH, Yiu CKY, Lo ECM: The inhibitory effects of silver diamine fluoride at different concentrations on matrix metalloproteinases. Dent Mater 2012;28:903–908.
Mei ML, Ito L, Cao Y, Li QLL, Lo ECM, Chu CHH: Inhibitory effect of silver diamine fluoride on dentine demineralisation and collagen degradation. J Dent 2013a;41:809–817.
Mei ML, Li Q, Chu C-H, Lo EC-M, Samaranayake LP: Antibacterial effects of silver diamine fluoride on multi-species cariogenic biofilm on caries. Ann Clin Microbiol Antimicrob 2013b;12:4.
Mei ML, Ito L, Cao Y, Li QL, Chu CH, Lo ECM: The inhibitory effects of silver diamine fluorides on cysteine cathepsins. J Dent 2014;42:329–335.
Mei ML, Nudelman F, Marzec B, Walker JM, Lo ECM, Walls AW, et al.: Formation of fluorohydroxyapatite with silver diamine fluoride. J Dent Res 2017;96:1122–1128.
Mei ML, Lo ECM, Chu CH: Arresting dentine caries with silver diamine fluoride: what's behind it? J Dent Res 2018;97:751–758.
Melaiye A, Youngs WJ: Silver and its application as an antimicrobial agent. Expert Opin Ther Pat 2005;15:125–130.
Mulder R, Potgieter N, Noordien N: Penetration of SDF and AgF from the infected dentine towards the unaffected tooth structure. Frontiers in Oral Health 2023;4:1298211.
Mulder R, Noordien N, Potgieter N: Comparing cytocompatibility of two fluoride-containing solutions and two resin-based restorative materials—a pilot study. Front Oral Health 2024;5:1330944.
Mungur A, Chen H, Shahid S, Baysan A: A systematic review on the effect of silver diamine fluoride for management of dental caries in permanent teeth. Clin Exp Dent Res 2023;9:375–387.
Muniz L, Wendlinger M, Cochinski G, Moreira P, Cardenas A, Carvalho T, et al.: Effect of silver diamine fluoride on the longevity of the bonding properties to caries-affected dentine. J Dent 2024;143:104897.
Mutluay MM, Zhang K, Ryou H, Yahyazadehfar M, Majd H, Xu HHK, et al.: On the fatigue behavior of resin–dentin bonds after degradation by biofilm. J Mech Behav Biomed Mater 2013;18:219–231.
Nagarkar S, Theis-Mahon N, Perdigão J: Universal dental adhesives: Current status, laboratory testing, and clinical performance. J Biomed Mater Res B Appl Biomater 2019;107:2121–2131.
Nascimento FD, Minciotti CL, Geraldeli S, Carrilho MR, Pashley DH, Tay FR, et al.: Cysteine cathepsins in human carious dentin. J Dent Res 2011;90:506–511.
Nishino M: Studies on the topical application of ammoniacal silver fluoride for the arrest of dental caries. Osaka Daigaku Shigaku Zasshi 1969;14:1–14.

O´Brien WJ: Surface Phenomena and Adhesion to Tooth Structure; in : Dental Materials and Their Selection Fourth Edition. Quintessence Publishing Co Inc, 2008, pp 62–75.

Oho T, Yamashita Y, Shimazaki Y, Kushiyama M, Koga T: Simple and rapid detection of Streptococcus mutans and Streptococcus sobrinus in human saliva by polymerase chain reaction. Oral Microbiol Immunol 2000;15:258–262.

Oliveira BH, Cunha-Cruz J, Rajendra A, Niederman R: Controlling caries in exposed root surfaces with silver diamine fluoride: A systematic review with meta-analysis. J Am Dent Assoc 2018;149:671–679.

Opdam N, Montagner A, Cenci M: Buonocore memorial lecture 2023: Longevity of dental restorations or longevity of teeth: What matters? Oper Dent 2024;49:655–664.

Oropeza R, de Souza LC, Quock RL, Chiquet BT, Barros JA: Cytotoxicity analysis of human dental pulp stem cells after silver diamine fluoride application. Pediatr Dent 2022;44:440–444.

Paris S, Banerjee A, Bottenberg P, Breschi L, Campus G, Doméjean S, et al.: How to Intervene in the Caries Process in Older Adults: A Joint ORCA and EFCD Expert Delphi Consensus Statement. Caries Res 2020;54:459–465.

Pashley DH, Andringa HJ, Derkson GD, Derkson ME, Kalathoor SR: Regional variability in the permeability of human dentine. Arch Oral Biol 1987;32:519–523.

Pashley DH, Tay FR, Yiu C, Hashimoto M, Breschi L, Carvalho RM, et al.: Collagen degradation by host-derived enzymes during aging. J Dent Res 2004;83:216–221.

Pashley DH, Tay FR, Breschi L, Tjäderhane L, Carvalho RM, Carrilho M, et al.: State of the art etch-and-rinse adhesives. Dental Materials 2011;27:1–16.

Patel J, Foster D, Smirk M, Turton B, Anthonappa R: Acidity, fluoride and silver ion concentrations in silver diamine fluoride solutions: a pilot study. Aust Dent J 2021;66:188–193.

Perdigao J, Lambrechts P, Van Meerbeek B, Vanherle G, Lopes ALB: Field emission SEM comparison of four postfixation drying techniques for human dentin. J Biomed Mater Res 1995;29:1111–1120.

Perdigão J, Walter R, Miguez PA, Swift EJ: Fundamental Concepts of Enamel and Dentin Adhesion; in : Sturdevant's Art and Science of Operative Dentistry. Elsevier, 2019, pp 136–169.

Perdigão J: Current perspectives on dental adhesion: (1) Dentin adhesion - not there yet. Jpn Dent Sci Rev 2020;56:190–207.

Pitts N, Ekstrand K, ICDAS Foundation: International Caries Detection and Assessment System (ICDAS) and its International Caries Classification and Management System (ICCMS) – methods for staging of the caries process and enabling dentists to manage caries. Community Dent Oral Epidemiol 2013;41:e41–e52.

Pitts NB, Zero DT, Marsh PD, Ekstrand K, Weintraub JA, Ramos-Gomez F, et al.: Dental caries. Nat Rev Dis Primers 2017;3:17030.

Primus C: Potassium iodide. The solution to silver diamine fluoride discoloration? Adv Dent Oral Health 2017;5:1–6.

Pugach MK, Strother J, Darling CL, Fried D, Gansky SA, Marshall SJ, et al.: Dentin caries zones: mineral, structure, and properties. J Dent Res 2009;88:71–76.

Quock RL, Barros JA, Yang SW, Patel SA: Effect of silver diamine fluoride on microtensile bond strength to dentin. Oper Dent 2012;37:610–616.

Reddy GK, Enwemeka CS: A simplified method for the analysis of hydroxyproline in biological tissues. Clin Biochem 1996;29:225–229.

Ricketts D, Lamont T, Innes NP, Kidd E, Clarkson JE: Operative caries management in adults and children. Cochrane Database of Systematic Reviews 2013;CD003808.

Roberts A, Bradley J, Merkley S, Pachal T, Gopal J, Sharma D: Does potassium iodide application following silver diamine fluoride reduce staining of tooth? A systematic review. Aust Dent J 2020;65:109–117.

Rosa V, Silikas N, Yu B, Dubey N, Gopu S, Zinelis S, et al.: Guidance on the assessment of biocompatibility of biomaterials: Fundamentals and testing considerations. Dent Mater 2024;40:1773–1785.

Rosenblatt A, Stamford TCM, Niederman R: Silver diamine fluoride: A caries “silver-fluoride bullet.” J Dent Res 2009;88:116–125.

Rosentritt M, Behr M, Preis V: A critical evaluation of fatigue studies for restorative materials in dentistry. Curr Oral Health Rep 2016;3:221–228.

Salim Al-Ani AAS, Salim IA, Seseogullari-Dirihan R, Mutluay M, Tjäderhane L, Tezvergil-Mutluay A: Incorporation of dimethyl sulfoxide into experimental hydrophilic and hydrophobic adhesive resins: evaluation of cytotoxic activities. Eur J Oral Sci 2021;129:e12756.

Sapp JP, Eversole LR, Wysocki GP: Infections of Teeth and Bone; in : Contemporary Oral and Maxillofacial Pathology. Elsevier, 2004, pp 70–93.

Sayed M, Matsui N, Uo M, Nikaido T, Oikawa M, Burrow MF, et al.: Morphological and elemental analysis of silver penetration into sound/demineralized dentin after SDF application. Dent Mater 2019;35:1718–1727.

Schwendicke F, Al-Abdi A, Pascual Moscardó A, Ferrando Cascales A, Sauro S: Remineralization effects of conventional and experimental ion-releasing materials in chemically or bacterially-induced dentin caries lesions. Dent Mater 2019;35:772–779.

Schwendicke F, Walsh T, Lamont T, Al-yaseen W, Bjørndal L, Clarkson JE, et al.: Interventions for treating cavitated or dentine carious lesions. Cochrane Database Syst Rev 2021;7:cd013039.

Selwitz RH, Ismail AI, Pitts NB: Dental caries. Lancet 2007;369:51–59.

Seseogullari-Dirihan R, Apollonio F, Mazzoni A, Tjaderhane L, Pashley D, Breschi L, et al.: Use of crosslinkers to inactivate dentin MMPs. Dent Mater 2016;32:423–432.

Sheridan A, Mei ML, Cooper PR, Milne T, Friedlander LT: Silver diamine fluoride treatment for the management of deep caries: A scoping review. J Dent 2025;161:105946.

Sissons CH, Anderson SA, Wong L, Coleman MJ, White DC: Microbiota of plaque microcosm biofilms: effect of three times daily sucrose pulses in different simulated oral environments. Caries Res 2007;41:413–422.

Siqueira FSF, Angheloris Rivadeneira Morales L, Cecilia Perez Granja M, de Oliveira de Melo B, Monteiro-Neto V, Reis A, et al.: Effect of silver diamine fluoride on the bonding properties to caries-affected dentin. J Adhes Dent 2020;22:161–172.

Slayton RL, Urquhart O, Araujo MWB, Fontana M, Guzmán-Armstrong S, Nascimento MM, et al.: Evidence-based clinical practice guideline on nonrestorative treatments for carious lesions. J Am Dent Assoc 2018;149:837–849.

Stape THS, Tulkki O, Salim IA, Jamal KN, Mutluay MM, Tezvergil-Mutluay A: Composite repair: On the fatigue strength of universal adhesives. Dent Mater 2022;38:231–241.

Suomalainen Lääkäriseura Duodecim Finnish Dental Society Appollonia: Karies (hallinta). Current Care Guidelines [Internet]. Helsinki: The Finnish Medical Society Duodecim 2023. Available from: https://www.kaypahoito.fi/hoi50127#s13

Tassery H, Miletic I, Turkun LS, Sauro S, Gurgan S, Banerjee A, et al.: Preventive management of carious lesions: from non-invasive to micro-invasive operative interventions. British Dental Journal 2024 236:8 2024;236:603–610.

Tezvergil-Mutluay A, Agee KA, Hoshika T, Carrilho M, Breschi L, Tjäderhane L, et al.: The requirement of zinc and calcium ions for functional MMP activity in demineralized dentin matrices. Dent Mater 2010;26:1059–1067.

Tezvergil-Mutluay A, Agee KA, Hoshika T, Uchiyama T, Tjäderhane L, Breschi L, et al.: Inhibition of MMPs by alcohols. Dent Mater 2011;27:926–933.

Tezvergil-Mutluay A, Mutluay MM, Agee KA, Seseogullari-Dirihan R, Hoshika T, Cadenaro M, et al.: Carbodiimide cross-linking inactivates soluble and matrix-bound MMPs, in vitro. J Dent Res 2012;91:192–196.

Tezvergil-Mutluay A, Agee KA, Mazzoni A, Carvalho RM, Carrilho M, Tersariol IL, et al.: Can quaternary ammonium methacrylates inhibit matrix MMPs and cathepsins? Dent Mater 2015a;31:e25–e32.

Tezvergil-Mutluay A, Pashley D, Mutluay MM: Long-term durability of dental adhesives. Curr Oral Health Rep 2015b;2:174–181.

Thonemann B, Schmalz G: Immortalization of bovine dental papilla cells with simian virus 40 large t antigen. Arch Oral Biol 2000;45:857–869.

Tjäderhane L, Larjava H, Sorsa T, Uitto VJ, Larmas M, Salo T: The activation and function of host matrix metalloproteinases in dentin matrix breakdown in caries lesions. J Dent Res 1998;77:1622–1629.

Tjäderhane L, Carrilho MR, Breschi L, Tay FR, Pashley DH: Dentin basic structure and composition—an overview. Endod Topics 2009;20:3–29.

Tjäderhane L, Haapasalo M: The dentin–pulp border: a dynamic interface between hard and soft tissues. Endod Topics 2009;20:52–84.

Tjäderhane L, Nascimento FD, Breschi L, Mazzoni A, Tersariol ILS, Geraldeli S, et al.: Optimizing dentin bond durability: Control of collagen degradation by matrix metalloproteinases and cysteine cathepsins. Dent Mater 2013;29:116–135.

Tjäderhane L: Dentin bonding: Can we make it last? Oper Dent 2015;40:4–18.

Turco G, Cadenaro M, Maravić T, Frassetto A, Marsich E, Mazzoni A, et al.: Release of ICTP and CTX telopeptides from demineralized dentin matrices: Effect of time, mass and surface area. Dental Materials 2018;34:452–459.

Turk V, Stoka V, Vasiljeva O, Renko M, Sun T, Turk B, et al.: Cysteine cathepsins: From structure, function and regulation to new frontiers. Biochim Biophys Acta Proteins Proteom 2011;1824:68–88.

Turton B, Horn R, Durward C: Caries arrest and lesion appearance using two different silver fluoride therapies on primary teeth with and without potassium iodide: 12-month results. Clin Exp Dent Res 2021;7:609–619.

Van Duker M, Hayashi J, Chan DC, Tagami J, Sadr A: Effect of silver diamine fluoride and potassium iodide on bonding to demineralized dentin. Am J Dent 2019;32:143–146.

Van Meerbeek B, De Munck J, Yoshida Y, Inoue S, Vargas M, Vijay P, et al.: Buonocore memorial lecture. Adhesion to enamel and dentin: current status and future challenges. Oper Dent 2003;28:215–235.

Van Meerbeek B, Yoshihara K, Yoshida Y, Mine A, De Munck J, Van Landuyt K: State of the art of self-etch adhesives. Dent Mater 2011;27:17–28.

Van Meerbeek B, Yoshihara K, Van Landuyt K, Yoshida Y, Peumans M: From Buonocore's pioneering acid-etch technique to self-adhering restoratives. A status perspective of rapidly advancing dental adhesive technology. J Adhes Dent 2020;22:7–34.

Vargas-Ferreira F, Salas MMS, Nascimento GG, Tarquinio SBC, Faggion CM, Peres MA, et al.: Association between developmental defects of enamel and dental caries: A systematic review and meta-analysis. J Dent 2015;43:619–628.

Wen PYF, Chen MX, Zhong YJ, Dong QQ, Wong HM: Global burden and inequality of dental caries, 1990 to 2019. J Dent Res 2022;101:392–399.

Wierichs RJJ, Meyer-Lueckel H: Systematic review on noninvasive treatment of root caries lesions. J Dent Res 2015;94:261–271.

Williams DF: On the mechanisms of biocompatibility. Biomaterials 2008;29:2941–2953.

World Health Organization (WHO): Global strategy and action plan on oral health 2023–2030. 2022;1–104.

Yan IG, Zheng FM, Sun IG, Lo ECM, Duangthip D, Chu CH: A Randomized Controlled Trial of Silver Diamine Fluoride Application Time. J Dent Res 2025;104:1453–1461.

Yamaga R: The inventory of saforide according to the combination of eastern and western medicine. Japanese J Clin Dent Child 2003;8:79–91.

Yee R, Holmgren C, Mulder J, Lama D, Walker D, Helderman WVP: Efficacy of silver diamine fluoride for arresting caries treatment. J Dent Res 2009;88:644–647.

Yu OY, Zhao IS, Mei ML, Lo ECM, Chu CH: Caries-arresting effects of silver diamine fluoride and sodium fluoride on dentine caries lesions. J Dent 2018;78:65–71.
Zaeneldin A, Yu OY, Chu C-H: Effect of silver diamine fluoride on vital dental pulp: A systematic review. J Dent 2022;119:104066.
Zhang J, Sardana D, Wong MCM, Leung KCM, Lo ECM: Factors associated with dental root caries: a systematic review. JDR Clin Trans Res 2020;5:13–29.
Zhang L, Sun H, Yu J, Yang H, Song F, Huang C: Application of electrophoretic deposition to occlude dentinal tubules in vitro. J Dent 2018;71:43–48.
Zhao IS, Gao SS, Hiraishi N, Burrow MF, Duangthip D, Mei ML, et al.: Mechanisms of silver diamine fluoride on arresting caries: a literature review. Int Dent J 2018;68:67–76.
Zhao IS, Chu S, Yu OY, Mei ML, Chu CH, Lo ECM: Effect of silver diamine fluoride and potassium iodide on shear bond strength of glass ionomer cements to caries-affected dentine. Int Dent J 2019;69:341–347.
Zhao IS, Yin IX, Mei ML, Lo ECM, Tang J, Li Q, et al.: Remineralising dentine caries using sodium fluoride with silver nanoparticles: an in vitro study. Int J Nanomedicine 2020;15:2829–2839.
Zheng FM, Yan IG, Duangthip D, Gao SS, Lo ECM, Chu CH: Silver diamine fluoride therapy for dental care. Jpn Dent Sci Rev 2022;58:249–257.
Zhi QH, Lo ECM, Lin HC: Randomized clinical trial on effectiveness of silver diamine fluoride and glass ionomer in arresting dentine caries in preschool children. J Dent 2012;40:962–967.

List of Tables and Figures

Tables

Figures

TURUN
YLIOPISTO
UNIVERSITY
OF TURKU

Painosalama, Turku, Finland 2026

ISBN 978-952-02-0656-7 (PRINT)
ISBN 978-952-02-0657-4 (PDF)
ISSN 0355-9483 (Print)
ISSN 2343-3213 (Online)